Virginia Commonwealth University
VCU Scholars Compass

Theses and Dissertations

Graduate School

2012

Sorafenib enhances pemetrexed-induced cytotoxicity through and autophagy-dependent mechanism in cancer cells

Bareford Mary
Virginia Commonwealth University

Follow this and additional works at: https://scholarscompass.vcu.edu/etd

Part of the Biochemistry, Biophysics, and Structural Biology Commons

© The Author

Downloaded from
https://scholarscompass.vcu.edu/etd/2870

This Dissertation is brought to you for free and open access by the Graduate School at VCU Scholars Compass. It has been accepted for inclusion in Theses and Dissertations by an authorized administrator of VCU Scholars Compass. For more information, please contact libcompass@vcu.edu.

© Mary Danielle Bareford 2012

All Rights Reserved

SORAFENIB ENHANCES PEMETREXED CYTOTOXICITY THROUGH AN AUTOPHAGY-DEPENDENT MECHANISM IN CANCER CELLS

A dissertation submitted in partial fulfillment of the requirements for the degree of Doctor of
Philosophy of Biochemistry and Molecular Biology at
Virginia Commonwealth University.

by

MARY DANIELLE BAREFORD
B.S. Forensic Science-Biology, Virginia Commonwealth University, 2004

Director: Dr. Paul Dent
Vice Chair of Research, Department of Neurosurgery

Virginia Commonwealth University
Richmond, Virginia
July, 2012

Acknowledgments

I would like to dedicate this dissertation to my grandmother, Dorothy Bareford, who is the reason why I chose to pursue cancer research as a field of study.

I would like to thank several people for their contributions to this dissertation. I would first like to offer a special thank you to Dr. Paul Dent for the opportunity to complete my Ph.D. work in his laboratory. I am very grateful for your invitation into the laboratory as a senior graduate student, as well as the opportunity to be mentored by you. The studies I preformed in your laboratory fulfilled my expectations of the research I hoped to pursue as a graduate student, especially by allowing me to focus on breast cancer. Thank you to all past and current Dent Lab members for your support and advice over the years. I consider you all family.

I would also like to thank my committee members for their guidance, patience, and flexibility. I could not have chosen a better group of people to serve on my committee. Thank you to Dr. Spiegel and the Department of Biochemistry and Molecular Biology for providing me with the training and resources necessary to become to a successful scientist. Previous lab members I owe thanks to are Tom Seegar and Muna Suliman for their advice and encouraging support. Additionally, I would like to offer my appreciation to Dr. Bill Barton for his mentoring and contributions to advancement of my technical skills.

Thank you to all of my friends whom offered patience and positive encouragement throughout all of years of my graduate studies. This journey would have been far more difficult without each of you. Last but not least, I would like to thank my parents and sister for their continued support and encouragement throughout this experience. Your love, undeniable support, and belief in my success served as the foundation for my completion of this dissertation.

TABLE OF CONTENTS

Acknowledgements …………………..………………………………………………...….. ii

List of Tables ………………………………………………………………….…………. viii

List of Figures ……………………………………………………………………..…. ix

List of Abbreviations ……………………………………………………………..…. xii

Abstract …………………………………………………………………………..……… xxii

Chapter 1- Introduction on cancer cell signaling ……………………………………...……… 1

1.1 Cancer Cell Signaling ……………………………………………………..… 1

1.1.1 MAPK Signaling …………………………………………………………... 2

1.1.2 PI3K/Akt Signaling ………………………………………………………... 9

1.1.3 Akt/ LKB1/mTOR Signaling …….………………………………………......15

1.2 Mechanisms of cell death ……………………………………………..………. 19

1.2.1 Apoptosis ……………………………………………………………..……….. 19

1.2.2 Formation of the autophagosome …………………………………………….... 22

1.2.3 Regulation of autophagy …..…………………………………………….…… 26

1.3 Lipid signaling in cancer …………………………………………………….….. 28

1.3.1 Sphingomyelin hydrolysis ……………………………………………..…… 29

1.3.2 The *de novo* ceramide synthesis pathway ……………………………..………. 30

1.3.3 The lipid salvage pathway ……………………………………………...…..…. 31

Chapter 2- Introduction to chemotherapeutic agents ……………………………………... 34

2.1 Combination drug therapy for treatment of cancer …………………………..….. 34

2.2 Pemetrexed …………………………………………………………………..…... 35

2.2.1 Antifolates as chemotherapeutic agents ……….…………………………..….. 35

2.2.2 Thymidylate synthetase (TS) is a primary target for pemetrexed ……………..…. 37

2.2.3 AICART is a secondary target for pemetrexed …………………………….…. 38

2.2.4 Other known targets of pemetrexed ……………………………………….... 38

2.2.5 Clinical relevance of pemetrexed ……………………………….……….. 40

2.3 Sorafenib ………………………………………………………………….... 41

2.3.1 Sorafenib for the treatment of multiple tumor types ……………………….... 41

2.3.2 Sorafenib targets …………………………………………………………..... 42

2.3.3 Clinical relevance of sorafenib ………………………………………………... 45

2.3.4 The aims of our studies using pemetrexed and sorafenib in combination ……..… 46

Chapter 3- Methods and Methodology ……………………………………….…….. 48

3.1 Materials ……………………………………………………………………..... 48

3.1.1 Cell Culture ………………………………………………………………..... 48

3.1.2 Cancer cell lines ..……………………………………………..……….. 48

3.1.3 siRNA …………………………………………………………………..…... 48

3.1.4 DNA constructs ……………..…………………………………......…….. 49

3.1.5 DNA propogation in bacteria …………………….………………………..…... 49

3.1.6 Chemotherapeutic drugs ……………………………………………..….. 50

3.1.7 SDS-PAGE ………………………………………………………………..…... 50

3.1.8 Western blotting/ Immunohistochemistry ...……………………………………... 50

3.1.9 Fluorescence-based technology ………………………………………..…... 51

3.1.10 *In vivo* studies 51

3.1.11 General supplies 51

3.1.12 Instrumentation 52

3.2 Methodology 52

3.2.1 Cell Culture 52

3.2.2 DNA propogation in bacteria 53

3.2.3 Agarose gel electrophoresis 53

3.2.4 DNA transfection/ protein overexpression 54

3.2.5 siRNA transfection/ protein knockdown 54

3.2.6 Validation of dialyzed fetal bovine serum 55

3.2.7 SDS-PAGE 56

3.2.8 Western blotting/ Immunohistochemistry 57

3.2.9 Normalization of protein levels by densitometry 58

3.2.10 Cell death analysis 58

3.2.11 Quantification of GFP-LC3 incorporation into early autophagic vesicles 59

3.2.12 Lysotracker Red staining for visualization of acidification of late endosomes 59

3.2.13 Analysis of PP2A activity 60

3.2.14 Quantification of ceramide and dihydroceramide levels 61

3.2.15 *In vivo* studies 62

Chapter 4: Results- Sorafenib enhances pemetrexed cytotoxicity through an autophagy-dependent mechanism in cancer cells 64

4.1 Pemetrexed treatment causes a dose dependent activation of autophagy and cell death in multiple cancer cell types 64

4.2 Sorafenib interacts with pemetrexed to enhance pemetrexed toxicity and induce autophagy in multiple tumor types 68

4.3 Pemetrexed/ sorafenib combination therapy is an effective therapeutic for triple negative breast cancer ……………………………………………………..…….. 71

4.4 MCF7F cells express higher levels of autophagy-related proteins and are more sensitive to pemetrexed/ sorafenib treatment than their estrogen-dependent counterparts ……………………………………...…………………..…..…. 75

4.5 Pemetrexed and sorafenib interact to promote cell death *in vivo* ……………..…… 84

Chapter 5: Results- Sorafenib and pemetrexed toxicity in cancer cells is mediated via Src-Erk signaling ………………………………..………………………………..……. 86

5.1 Pemetrexed induces a cytotoxic form of autophagy in Her2+ and triple negative breast cancer cells ……………………………………………………………..…. 86

5.2 Pemetrexed/ sorafenib cytotoxicity is dependent upon the generation of ROS …... 88

5.3 Pemetrexed/ sorafenib cytotoxicity is regulated by Src ………………………….... 89

5.4 Pemetrexed/ sorafenib toxicity is mediated by the MEK/ Erk pathway ………….... 91

5.5 Protein phosphatase PP2A is involved in the cytotoxic response of parental and Fulvestrant-resistant MCF7 cells to pemetrexed/ sorafenib treatment …………..…. 95

5.6 Pemetrexed/ sorafenib interactions in breast cancer cells are ceramide-dependent .. 99

Chapter 6- Discussion ……………………………………………………………………… 103

Literature Cited …………………………………………………………………………..…. 118

Curriculum vitae …...……………..………..…………………………………..……... 148

List of Tables

Table 1: siRNA Constructs …………………………………………………………………..… 49

List of Figures

Figure 1-1: MAP kinase signaling pathways ………………………………………………… 3

Figure 1-2: A general overview of the MEK/Erk signaling pathway …………………………... 6

Figure 1-3: A general overview of PI3K/ Akt pathway signaling ……………………….…. 11

Figure 1-4: Akt regulation of mTOR, a component of TORC1 and TORC2 complexes …..…. 14

Figure 1-5: The AMPK signaling pathway ……………………………………………..….... 18

Figure 1-6: The extrinsic and intrinsic apoptotic pathways …………………………….….. 21

Figure 1-7: Formation of the autophagosome by autophagy-related proteins ………………… 25

Figure 1-8: Activation of autophagy via intracellular stress signaling ……………………..…. 28

Figure 1-9: The ceramide synthesis pathways ……………………………………..…….. 33

Figure 2-1: Mechanisms of pemetrexed toxicity in NSCLC cells ……………………..…… 40

Figure 2-2: Overview of known sorafenib targets ……………………………………..…… 45

Figure 3-1: Validation of dialyzed fetal bovine serum in CEM lymphoma cells ……….……. 56

Figure 4-1: Pemetrexed induces autophagy and cell death in H460 NSCLC cells that is suppressed by treatment with 3-MA or knockdown of Beclin1 ………………..… 66

Figure 4-2: Treatment with pemetrexed causes an increase in autophagic vesicle formation in mammary and hepatic carcinoma cells ……………………………………... 67

Figure 4-3: Pemetrexed lethality is autophagy-dependent in multiple tumor types ………..…. 68

Figure 4-4: Cotreatment with pemetrexed and sorafenib enhanced toxicity in H460 NSCLC cells …………………………………………………………………......… 69

Figure 4-5: Pemetrexed interacts with sorafenib to enhance cell death that is suppressed by knockdown of Beclin1 in multiple tumor types …………………………………...... 70

Figure 4-6: Pemetrexed interacts with sorafenib to enhance autophagy that is suppressed by knockdown of Beclin1 in multiple tumor types …………………………………...... 71

Figure 4-7: Pemetrexed and sorafenib interact in a dose-dependent manner to cause cell death in Her2+ and triple negative breast cancer cells ………………………...…. 73

Figure 4-8: Cotreatment with pemetrexed and sorafenib cause a dose-dependent increase in cell death in parental and Fulvestrant-resistant MCF7 cells ……………………..…. 75

Figure 4-9: Fulvestrant-resistant MCF7F cells express higher basal levels of autophagy-related proteins than do their estrogen-dependent counterparts …………………..… 77

Figure 4-10: Toxicity resultant of combination treatment with pemetrexed and sorafenib follows an intrinsic, rather than extrinsic, death signaling mechanism ……......… 78

Figure 4-11: Pemetrexed/ sorafenib cotreatment alters signaling through mTOR and MAPK pathways ……………………………………………………………..……... 80

Figure 4-12: MCF7F cells are more sensitive to pemetrexed treatment than the estrogen-dependent parental strain and pemetrexed-induced toxicity can be enhanced by knockdown of PDGFRβ ………………………………………………..…... 81

Figure 4-13: mTOR and p70 S6 kinase pathways play an important role in pemetrexed/ sorafenib lethality ……………………………………………………...……. 82

Figure 4-14: Constitutive activation of mTOR and p70 S6 kinase pathways desensitizes MCF7 cells to pemetrexed/ sorafenib cotherapy ………………………………...…. 83

Figure 4-15: Pemetrexed and sorafenib interact to reduce tumor growth in a breast cancer-induced mouse model ……………………………………………………...….. 85

Figure 5-1: Pemetrexed- induced autophagy and tumor cell killing is suppressed by knockdown of Beclin1 ………………………………………………...….… 87

Figure 5-2: Pemetrexed interacts with sorafenib in a time-dependent fashion to increase autophagy which is suppressed by knockdown of Beclin1 …………….……...… 88

Figure 5-3: Inhibition of autophagy at the mitochondrial level abolishes drug combination-induced cell death ……………………………………………………...… 89

Figure 5-4: Src is an important player in the mechanistic means by which pemetrexed and sorafenib enhance cell death ………………………………………...……… 91

Figure 5-5: Src regulates an Erk1/2-mediated response to pemetrexed/ sorafenib in mammary carcinoma cell lines ……………………………………….…………………..… 92

Figure 5-6: Overexpression of a non-functional form of MEK1 attenuates activation of autophagy in pemetrexed/ sorafenib-treated cells ………………………….…...... 93

Figure 5-7: Overexpression of dnMEK1 suppresses drug combination-induced acidic lysosome formation ……………….……………………………………………….... 94

Figure 5-8: PP2A is activated in response to pemetrexed/ sorafenib cotreatment in MCF7F cells ………….……………………………………………………………….... 97

Figure 5-9: Overexpression of I2PP2A suppresses drug-induced autophagy and toxicity in MCF7F cells …………………………………………………………..……. 98

Figure 5-10: Knockdown of LASS6 abolishes drug combination-induced activation of PP2A in breast cancer cells …….………………………………………………………… 100

Figure 5-11: The *de novo* ceramide synthesis pathway plays a role in the toxic interaction of pemetrexed and sorafenib in BT474 cells ……………………….……………… 101

Figure 6-1: A working model of the mechanisms which promote cytotoxicity as a result of cotreatment of breast cancer cells with pemetrexed and sorafenib …..………… 116

List of Abbreviations

3-MA - 3-methyladenine

4EBP1 - translation initiation factor 4E binding protein 1

ACC1/2 - acetyl CoA carboxylases 1 and 2

AICAR - 5-aminoimidazole-3-carboxamide-1-β-D-ribofuranoside

AICART - 5’ aminoamidazole- carboximide ribonucleotide formyl transferase

AIF - apoptosis inducing factor

Akt1/2/3 - protein kinase B isoforms α/β/γ

ALL - acute lymphoblastic leukemia

AML - acute myeloid leukemia

Aminopterin - 4-amino-folic acid

AMP - adenosine monophosphate

AMPK - AMP-activated protein kinase

ASK1 - apoptosis signal-regulating kinase 1

Atg3-10,13-17 - autophagy-related genes 3,4,5,6,7,8,9,10,13,14,15,16, and 17

ATP - adenosine triphosphate

BAD - Bcl-2-associated death promoter

BAX - Bcl-1-associated X protein

Bcl-2 - B cell lymphoma 2

Bcl-XL - Bcl-2 like protein 1

BCRP - breast cancer resistance protein

Beclin1 - Bcl-2-interacting myosin like coiled-coil protein 1

BID - BH3-interacting death domain agonist

BIM - Bcl-2-like protein 11

BH 1-4 - Bcl-2 homology domains 1, 2, 3, and 4

BME - β-mercaptoethanol

C16 - 16 carbon

C22 - 22 carbon

C24 - 24 carbon

c-FLIP-1 - cellular FLICE-like inhibitory protein 1

c-FLIP-s - cellular FLICE-like inhibitory protein s

c-Kit - mast/stem cell growth factor receptor

caAkt - constitutively active Akt

camTOR - constitutively active mTOR

cap70 - constitutively active p70 S6 kinase

CaMKKβ - calmodulin-dependent kinase kinase β

CD95 - cell death receptor 95

CDK - cyclin-dependent kinase

CERT - ceramide transfer protein

CMA - chaperone-mediated autophagy

CMV - cytomegalo virus vector control virus

CNK - connector enhancer of kinase suppressor of Raf-1

Cox-2 - cyclooxegenase-2

DISC - death-inducing signaling complex

DFF40 - DNA fragmentation factor-40

DFF45 - DNA fragmentation factor-45

DHFR - dihydrofolate reductase

DMSO - dimethyl sulfoxide

DNA - deoxyribonucleic acid

dnAkt - dominant negative Akt

dncaspase-9 - dominant negative caspase-9

dnMEK1 - dominant negative MEK1

dnSrc - dominant negative Src

dTMP - deoxythymidine monophosphate

dUMP - deoxyuridine monophosphate

dTTP - deoxythymidine 5’ triphosphate

dUMPase - deoxyuridine monophosphatase

dUTP - deoxyuridine 5’ triphosphate

eEF2 - eukaryotic elongation factor 2

EGF - epidermal growth factor

EGFR - epidermal growth factor receptor

eIF2α - eukaryotic initiation factor 2 alpha

eIF4E - eukaryotic translation initiation factor 4E

eNOS - endothelial nitric oxide synthase

EPC - endothelial progenitor cells

Erk1/2 - extracellular signal-regulated kinases 1 and 2

Erk5 - extracellular signal-regulated kinase 5

Erk6 - extracellular signal-regulated kinase 6

FADD - Fas-associated protein with death domain

FBS - fetal bovine serum

FDA - Food and Drug Administration

FGAR - formylglycinamide ribonucleotide

FGFR - fibroblast growth factor receptor

FLIP - FADD-like apoptosis regulator

FLT3 - macrophage colony-stimulating factor-related tyrosine kinase 3

FLT3-ITD - FLT3 internal tandem duplication

FoxO - forkhead box O

FoxO3a - forkhead box O 3a

GAPDH - glyceraldehydes-3-phosphate dehydrogenase

GART - phosphoribosylglycinamide formyltransferase

GDP - guanosine diphosphate

GLUT4 - insulin-regulated glucose transporter 4

GPCR - G-protein coupled receptor

GSK-3 - glycogen synthase kinase 3

GFP - green fluorescent protein

GTP - guanosine triphosphate

GTPase - guanosine triphosphatase

H_2O_2 - hydrogen peroxide

HDAC - histone deacetylase

HMGR - HMG CoA reductase

HNSCC - head and neck squamous cell carcinoma

Hsp90 - heat shock protein 90

I2PP2A – inhibitory protein 2 of protein phosphatase 2A

IGF - insulin like growth factor

IgG - immunoglobulin G

IκB - I kappa B

IKK - IκB kinase

IL-1β - interleukin 1β

IRF-1 - interferon regulatory factor 1

IRS - insulin receptor substrate protein

IRS1 - insulin receptor substrate protein 1

JNK1/2/3 - c-Jun N-terminal kinases 1, 2, and 3

Kb – Kilobase

L - liter

LASS6 - ceramide synthase 6

LB - Luria-Bertani

LC3 - microtubule-associated protein 1 light-chain 3

LKB1 - tumor suppressor liver kinase B1

LPA - lysophosphatidic acid

M - molar

μg – microgram

μL – microliter

μM – micromolar

MAPK - mitogen-activated protein kinase

MAP2K- mitogen-activated protein kinase kinase

MAP3K - mitogen-activated protein kinase kinase kinase

MAPK - mitogen-activated protein kinase

MAPK8/9/10/11/12/13/14 - mitogen-activated protein kinases 8,9,10,11,12,13, and 14

MCF7F - Fulvestrant-resistant MCF7 cells

Mcl-1 - myeloid leukemia cell differentiation protein 1

mdm2 - mouse double minute-2

MEK1/2 - mammalian homologue of STE11 proteins 1 and 2

MEKK1/2/3 - mammalian homologue of STE11 kinases 1, 2, and 3

MKK3/4/6/7 - mitogen-activated kinase kinases 3, 4, 6, and 7

mg – milligram

mL - milliliter

mm - millimeter

mm^3 - cubic millimeter

mM - millimolar

mLST8 - mTOR-associated protein LST8 homolog

MLK1/2/4 - mixed lineage kinases 1, 2 and 4

mTOR - mammalian target of rapamycin

Nbr1 - breast cancer type 1 susceptibility gene protein 1

NF-κB - nuclear factor kappa-light-chain-enhancer of B

NH_4Cl - ammonium chloride

nM - nanomolar

nm - nanometer

NOXA - adult T cell leukemia derived PMA-responsive protein

NSCLC - non-small cell lung carcinoma

$p21^{WAF1/CIP1}$ - cyclin-dependent kinase inhibitor 21

$p27^{KIP1}$ - cyclin dependent kinase inhibitor 27

p-Erk - phosphorylated Erk

p-mTOR - phosphorylated mTOR

p-p70 - phosphorylated p70 S6K

PAK1 - p21-activating kinase 1

PBS - phosphate buffered saline

PDGFRα/β - platelet-derived growth factors alpha and beta

PDK1 - phosphoinositide-dependent kinase-1

PE – phosphotidylethanolamine

PERK – protein kinase RNA-like endoplasmic reticulum kinase

PFK-2 - 6-phosphofructokinase 2

pg - picogram

PH- pleckstrin homology

PHLPP - PH domain leucine-rich repeat protein phosphatase

phospho-Erk - phosphorylated Erk

phospho-mTOR - phosphorylated mTOR

phospho-p70 - phosphorylated p70 S6K

PI - propidium iodide

PI3K- phosphoinositide 3 kinase

PI(4)P - phosphoinositol-4-phosphate

PI(3,4)P2 - phosphoinositol-3,4-diphosphate

PI(3,4,5)P3 - phosphoinositol-3,4,5-triphosphate

PI(4,5)P2 - phosphoinositol-4,5-diphosphate

pmol – picomolar

PP1 - protein phosphatase 1

PP2A- protein phosphatase 2A

PRB1 - proteinase B1

Pralatrexate - 10-proargyl-10-deazaminopterin

PROTOR1/2 - protein-associated with Rictor 1 and 2

PTEN - phosphotase and tension homology

PTP1B - protein tyrosine phosphatase 1B

PTX - pemetrexed

PUMA - p53 upregulated modulator of apoptosis

Raptor - regulatory associated protein of mTOR

RCC - renal cell carcinoma

Rictor - rapamycin insensitive companion of mTOR

RKIP - Raf kinase-inhibitory protein

RNA - ribonucleic acid

ROS - reactive oxygen species

rpm. - rotations per minute

RTK - receptror tyrosine kinase

S6K1 - S6 kinase-1

SAPK - stress-activated protein kinase

SDS - sodium dodecyl sulfate

SDS-PAGE - sodium dodecyl sulfate polyacrylamide gel electrophoresis

SEM - standard error of measurement

Ser - serine

SH2 - Src homology 2

si - short interfering

Sin1 - stress-associated protein kinase interacting protein 1

SMase – sphingomyelinase

SNARE - soluble n-ethylmaleimide sensitive fusion attachment protein

SOR - sorafenib

SRCAP- Snf-2 related CREB binding protein-activation protein

SREBP-1 - sterol regulatory element-binding protein 1

STRAD - STE20-like pseudokinas

Tak1 - transforming growth factor β-activated kinase-1

tBID - truncated BID

THF - 10-formyl tetrahydrofolate

Thr - threonine

Tie2 - endothelium-specific receptor tyrosine kinase 2

TNF-α - tumor necrosis factor-α

TORC1 - target of rapamycin complex 1

TORC2 - target of rapamycin complex 2

TNFα - tumor necrosis factor α

TP53 - tumor protein 53

TRAIL - TNF-related apoptosis-inducing ligand receptor I

TS - thymidylate synthase

TSC-1/2 - tuberous sclerosis-1 and 2

Tyr - tyrosine

UVRAG - ultraviolet-irradiation resistance-associated gene

VE - vascular endothelial

VEGF - vascular endothelial growth factor

VEGFR1/2/3 - vascular endothelial growth factor receptors 1, 2, and 3

Vps34 - class III PI3K protein 34

WT - wild-type

ZMP - AICAR monophophate

Abstract

SORAFENIB ENHANCES PEMETREXED CYTOTOXICITY THROUGH AN AUTOPHAGY-DEPENDENT MECHANISM IN CANCER CELLS

By Mary Danielle Bareford, Ph.D.

A dissertation submitted in partial fulfillment of the requirements for the degree of Doctor of Philosophy, Biochemistry and Molecular Biology at Virginia Commonwealth University.

Virginia Commonwealth University, 2012

Major Director: Dr. Paul Dent, Vice Chair of Research, Department of Neurosurgery

Acquired cellular resistance to traditional chemotherapeutics is a common obstacle in the treatment of most cancer cell types. This resistance occurs as a result of changes in the underlying molecular mechanisms of disease progression. The development of novel chemotherapeutic approaches designed to enhance the efficacy of protypical anti-cancer drugs is important in order to overcome this issue. Such approaches will aid in understanding the biomolecular phenomena responsible for drug resistance and disease progression. Combining signaling pathway inhibitors has become an effective strategy for enhancing tumor cell death by targeting multiple pathways known to regulate cell survival. Pemetrexed, an FDA-approved anti-folate drug, targets thymidylate synthase (TS) and a secondary folate-dependent enzyme, 5' aminoimidazole-carboximide ribonucleotide formyltransferase (AICART); both important for DNA synthesis. Studies performed by our collaborator demonstrated that TS inhibition causes intracellular accumulation of ZMP^+ and activation of AMPK which is known to induce autophagy in mammalian cells. Previous studies from our lab and others showed that sorafenib, a multi-kinase inhibitor of Raf-1 and class III receptor tyrosine kinases, was able to induce a cytotoxic form of autophagy in a variety of tumor cell types. Combination treatment using pemetrexed and sorafenib in these cancer cells resulted in an enhancement of autophagy and cell lethality beyond that of individual drugs alone. Inhibition of autophagy suppressed the toxic interactions of these drugs in all cell types examined. Pemetrexed/sorafenib cotherapy also proved to be an effective treatment for triple negative breast cancer cells having advanced to a stage of estrogen independence. Fulvestrant-resistant MCF7 cells were more sensitive to the drug combination than parental, estrogen-dependent MCF7 cells. Breast cancer cells cotreated with pemetrexed and sorafenib exhibited enhanced MEK/ERK signaling, Src activation that was dependent on platelet-derived growth factor β (PDGFRβ) downregulation, elevated protein phosphatase 2A (PP2A) activity, and increased *de novo* ceramide synthesis. Studies using a mouse model of experimentally-induced breast cancer validated drug combination effectiveness through inhibition of tumor growth, while no deleterious effects on normal tissues were observed. The data presented demonstrates that pemetrexed/sorafenib cotreatment augments chemosensitivity in both *in vitro* and *in vivo* systems. Based upon these findings, a Phase I clinical trial involving pemetrexed and sorafenib in breast cancer patients with solid, recurrent tumors was begun in 2011. In conclusion, this work strongly supports a promising therapeutic utility for the pemetrexed/sorafenib combination in treatment of various cancer cell types.

Chapter 1: Introduction on cancer cell signaling

1.1 Cancer Cell Signaling

The development of cancer is a concern for persons of all races and among all demographics. The 5 year survival rate for patients diagnosed with cancer as an average for all cancer cell types spanning the years 1999-2005 was 68%, up from 50% between the years of 1975-1977 (1). The increase in survival rate is attributed to early diagnostic measures, as well as more efficient treatment regimens. Breast cancer is the least discriminatory form of cancer, as it will affect 1 in 8 women in every country in the world (2). Indeed, breast cancer is the second leading cause of cancer deaths in women, following lung cancer. The 5 year survival rate for women with breast cancer has increased from 63% in the 1960s to 90% today (1). The development of novel breast cancer treatments, in addition to the enhancement of current standards of treatment, has improved the outcome and extended survival rate for the ~200,000 patients diagnosed with breast cancer each year (1). Characterization of cellular signaling pathways involved in carcinogenesis has encouraged the development of target-specific chemotherapeutic drugs and treatment strategies aimed towards counteracting disadvantageous alterations seen in tumor cells.

From studies pertaining to the specific signaling mechanisms involved in the deregulation of cellular growth pathways, as well as studies involving loss of function of proteins triggering cell death; an understanding of cellular signaling networks yields a wealth of information concerning the development, progression, and treatment of all cancer cell types. Both genetic and environmental factors promote the development of cancer. Progression of cancer can be a result of epigenetic alterations in one or many of the signaling cascades that our cells rely upon. These alterations provide cells with a means of bypassing signals that result in cell death, as well as exploiting those that promote cell survival. Due to the inter-connectedness of cellular signaling networks, subsequent alterations in signal transduction pathways will occur as a compensatory mechanism to accommodate and stabilize these changes.

1.1.1- MAPK signaling

Mitogen-activated protein kinase (MAPK) signaling involves four separate, yet inter-connected pathways including extracellular-signal regulated kinases 1 and 2 (ERK1/2), extracellular-signal regulated kinase 5 (ERK5), c-Jun N-terminal kinase (JNK/ stress-activated protein kinase/SAPK), and p38 (Figure 1-1) (3-13). Activation of these kinases induces a variety of cellular events such as cell survival, cell death, regulation of gene expression, metabolism, and changes in cell morphology. Transmission of signal through any of the MAPK pathways is initiated by stimulation of upstream cellular membrane receptors, resulting in formation of specific adaptor protein complexes. These signals are then transmitted through a sequential, 3-tiered MAP kinase cascade involving MAP kinase kinase kinase (MAP3K), MAP kinase kinase (MAP2K), and MAPK proteins (Figure 1-1). Signaling through Erk1/2 is generally thought to produce a proliferative signal, but on occasion can promote cell death. The Erk5 pathway promotes cell growth (14-15). The JNK and p38 MAPK pathways are typically activated in response to cellular stress or pro-inflammatory cytokines such as tumor necrosis factor-α (TNFα) and interleukin 1β (IL-1β), and most often promote apoptosis (3,6,8,13). All four MAPK pathways have been shown to be activated in response to radiation and chemotherapy-based treatments (16). In the case of Erk1/2, growth signals such as those from the epidermal growth factor (EGF) receptor lead to activation of Raf family proteins (A-Raf, B-Raf, C-Raf/Raf-1), which serve as the MAP3K component of this cascade. Ras proteins are usually activated prior to stimulation of Raf family protein members (17). Regarding signals transmitted through activation of Ras, a guanosine triphosphatase (GTPase) bound to guanosine diphosphate (GDP) in its inactive form, GDP is exchanged for guanosine triphosphate (GTP) in response to growth promoting stimuli (7,18). The complete mechanism by which Raf becomes activated by Ras is not fully understood (19).

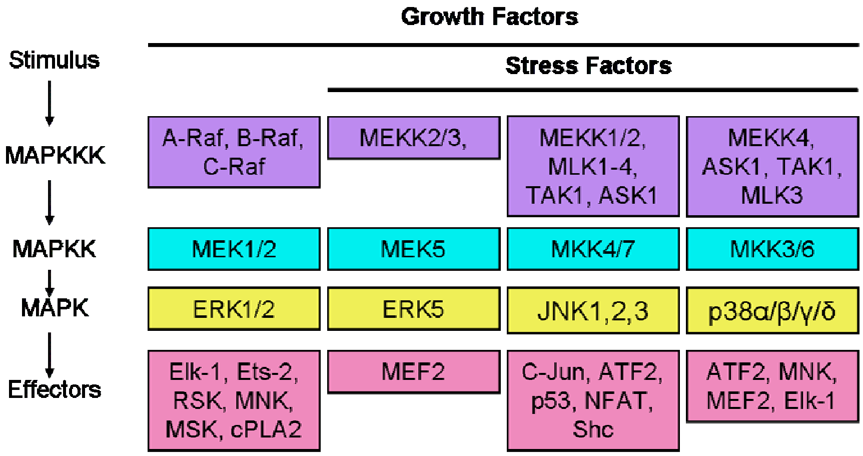
Growth Factors
Stress Factors
Stimulus
MAPKKK
MAPKK
MAPK
Effectors
A-Raf, B-Raf, C-Raf
MEKK2/3,
MEKK1/2, MLK1-4, TAK1, ASK1
MEKK4, ASK1, TAK1, MLK3
MEK1/2
MEK5
MKK4/7
MKK3/6
ERK1/2
ERK5
JNK1,2,3
p38α/β/γ/δ
Elk-1, Ets-2, RSK, MNK, MSK, cPLA2
MEF2
C-Jun, ATF2, p53, NFAT, Shc
ATF2, MNK, MEF2, Elk-1

Figure 1-1: MAP kinase signaling pathways. Upon stimulation by a diverse array of extracellular and intracellular signals, pathways promoting both cell survival and cell death activate specific signaling through one of the four MAP kinase pathways. These pathways involve a sequential, 3-tier kinase cascade through MAPKKK (MAP3K), MAPKK (MAP2K), and finally one of the four MAPK proteins. Erk1/2, Erk5, JNK, and p38 MAP kinase pathways transduce signal to promote responses such as cell proliferation, cell differentiation, migration, apoptosis, and inflammation.

Raf protein kinases serve as the MAP3K component of the Erk1/2 MAP kinase signaling cascade (7-8,20). B-Raf is the substrate with the greatest affinity for Ras, therefore making it more efficiently activated than the other Raf protein kinases (20). For this reason it is understandable that B-Raf mutations, predominantly the activating V600E mutation, have the highest level of incidence in cancer amongst the Raf protein family members (21). In recent years, Raf kinases were shown to have the ability to form homo and heterodimers, as well as be controlled by their association with inhibitory proteins such as Raf kinase-inhibitory protein (RKIP), 14-3-3, and connector enhancer of kinase suppressor of Raf-1 (CNK) (22). MAPK signaling is mediated by adaptor protein complexes which enable its specific localization within the cell for precise communication of function to downstream targets. Raf can also be regulated by protein phosphatase 2A (PP2A), which dephosphorylates the Ser259 residue of Raf, leading to its activation. Signal transduction through Raf is relayed to mammalian homologue of STE11 kinases 1 and 2 (MEK1/2) through phosphorylation of two serine residues (Ser218 and Ser222) in the activation loop of the protein (23). Full activation of MEK1/2 is achieved only when acted upon by both Raf1 and p21-activating kinase 1 (PAK1) (24-25). Active MEK1/2 binds to inactive Erk1/2 resulting in phosphorylation of threonine and serine residues within their phosphorylation loop. Once activated, Erk1/2 is released from its association with MEK1/2 enabling dimerization and translocation to the nucleus where it phosphorylates transcription factors and other kinases (26). Erk1/2 also has additional targets in the cytoplasm including other kinases and cytoskeletal proteins (27-28). In total, Erk1/2 is thought to have over 100 potential substrates which provide for a diverse variety of cellular functions (Figure 1-2). While it is generally accepted to be a transducer of proliferative signals, evidence also suggests that it is upregulated upon treatment with various chemotherapeutic drug regimens (29-31). Protein phosphatase PP2A is also known to regulate MEK1/2 and Erk1/2 function by inactivating these enzymes when targeted, thus indicating a complex role for PP2A in this signaling pathway.

Ras/Raf/MEK/Erk is the most commonly dysregulated MAP kinase pathway identified in cancer. In fact, Raf-1 was the first serine/threonine kinase to be identified as oncogenic (32). A multitude of Raf-related signaling events which promote cancer development and progression have been reported in the literature. K-Ras and Raf activation has been shown to induce expression of mouse double minute-2 (mdm2), an inhibitor of tumor suppressor protein p53 (TP53), resulting in enhancement of cell growth (33). Upregulation of nuclear factor-kappa B (NF-κB) or cyclooxegenase-2 (Cox-2) expression mediated by Raf-1 provides growth survival advantages to tumor cells (34-35). Oncogenic forms of Raf demonstrate resistance to radiotherapy and chemotherapy in some tumor types, thus protecting the cells from a common means of treatment for these diseases (36-38). In some tumors, the B-Raf V600E mutant disrupts Erk-mediated activation of tumor suppressor liver kinase B1 (LKB1) by AMP-activated protein kinase (AMPK) preventing its restrictive limitations on protein translation (39). On the other hand, Erk1/2 can also act as an antagonizing factor for cancer growth. In human hepatoma cell lines, HepG2 and Huh7, doxorubicin or cisplatin treatment leads to Erk1/2 activation and cell death (40). Activation of Erk1/2 following cisplatin treatment has also been shown to play a role in drug-induced apoptosis in HeLa human cervical carcinoma cells (41). Additionally, in MCF-7 breast cancer cells, tamoxifen treatment induced sustained activation of Erk1/2 and drug-induced cell death (42). These specific examples are but a few of the many ways that signaling through the Ras/Raf/MEK/Erk pathway regulates cancer pathogenesis, as well as cancer treatment. For these reasons, the Erk1/2 pathway is of major interest in cancer studies.

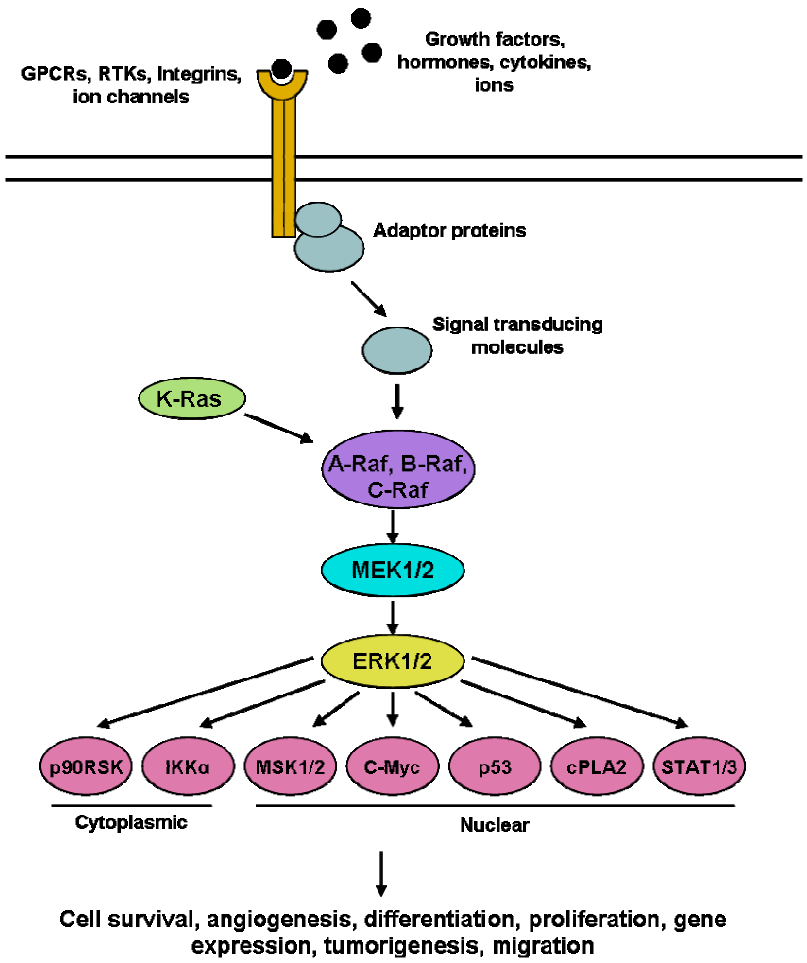
GPCRs, RTKs, Integrins, ion channels
Growth factors, hormones, cytokines, ions
Adaptor proteins
Signal transducing molecules
K-Ras
A-Raf, B-Raf, C-Raf
MEK1/2
ERK1/2
p90RSK
IKKα
MSK1/2
C-Myc
p53
cPLA2
STAT1/3
Cytoplasmic
Nuclear
Cell survival, angiogenesis, differentiation, proliferation, gene expression, tumorigenesis, migration

Figure 1-2: A general overview of the MEK/Erk signaling pathway. The ERK1/2 signaling pathway is initiated through activation of G-protein coupled receptors (GPCRs), receptor tyrosine kinases (RTKs), integrin receptors, and ion channels by their respective ligands. Activation of these pathways leads to recruitment of adaptor protein complexes which transduce signal to the MEK/Erk MAP kinase cascade via a variety of proteins. This figure illustrates a general scheme by which these events occur, as there are many different mechanisms and signaling proteins identified to be involved. In some cases, the GTPase K-Ras may be stimulated to serve as an upstream activator of the MAP3K component of this pathway (Raf family members). Raf proteins phosphorylate and activate MEK1/2 (MAP2K) for subsequent activation of Erk1/2 (MAPK). Erk1/2 phosphorylates over a hundred documented downstream targets, located in both the cytoplasm and the nucleus, to promote cell survival, proliferation, translation, differentiation, tumorigenesis, and migration.

The Erk5 MAPK is stimulated by cytokines and proliferative mitogenic signals such as EGF, lysophosphatidic acid (LPA), neurotrophins, and phorbol ester; while some evidence suggests that it can also become activated in response to stress signaling molecules such as hydrogen peroxide (H_2O_2), sorbitol, and ultraviolet irradiation (4,10,43). MEKK2 or MEKK3 (MAP3K) phosphorylate MEK5 (MAP2K) for subsequent activation of Erk5 (MAPK). Downstream targets of Erk5 include forkhead box O 3a (FoxO3a) and B cell lymphoma 2 (Bcl-2)-associated death promoter (BAD) proteins. Activation of these proteins by Erk5 causes them to be sequestered in the cytoplasm, preventing their translocation into the nucleus and mitochondrial membrane, which promotes anti-apoptotic events (43).

The p38 and JNK MAP kinases are the last of the family of MAPK proteins which are generally thought to be activated in response to stress stimuli. Signaling through p38 and JNK pathways is stimulated by growth factors, environmental stresses, and inflammatory cytokines (44). The JNK and p38 pathways have been shown to play a role in immune response, tissue homeostasis, cell death, cell migration, cell survival, and cell differentiation (45-47). p38 kinases constitute a group of MAPK proteins including p38α (MAPK14), p38β (MAPK11), p38γ (SAPK3/Erk6/MAPK12), and p38δ (SAPK4/MAPK13) (48-52). Each is encoded from a unique gene transcript and family members share 60% homology to one another, although they are thought to have different tissue-type specific expression patterns (53). Likewise, JNK proteins constitute a group of three distinct MAP kinases termed JNK1 (MAPK8), JNK2 (MAPK9), and JNK3 (MAPK10). JNK family protein members arise from spliced variations of the same gene transcript. JNK1 and JNK2 are expressed in almost all cells, while JNK3 is primarily expressed in the brain (44,47). p38 and JNK are activated by numerous kinases and are involved in a variety of cellular functions (44,47-48). For both the p38 and JNK pathways, transmission of signal from upstream events leads to the activation of their MAP3K kinases including apoptosis signal-regulating kinase 1 (ASK1), MEKK1, MEKK2, MLK1, MLK2, and MLK4 (44,48).

MKK7 and MKK4 (JNK) or MKK3 and MKK6 (p38) serve as the MAP2K components of these pathways. MKK4 can also serve as an activating kinase for p38α by way of association with alternative signaling complexes (47,54). p38 and JNK signal to cytoplasmic and nuclear downstream effectors which stimulate events associated with immunity, growth, differentiation, migration, and apoptosis (45-47) (Figure 1-1). p38 activates multiple transcription factors, as well as numerous proteins kinases (55-56). JNK was found to phosphorylate several targets promoting apoptosis such as 14-3-3, (Bcl-2-associated X protein) BAX, (Bcl-2-associated death promoter) BAD, caspase-8 and (Fas-associated protein with death domain) FADD-like apoptosis regulator (FLIP). JNK can also promote caspase-8 independent cleavage of BH3-interacting domain death agonist (BID) (57-61).

Both p38 and JNK pathways have been implicated in development of cancer. The most well documented correlation to this disease is a loss-of-function mutation in MKK4 (44). MKK4 is a putative tumor suppressor protein and loss-of-function mutations are found in 5% of pancreatic, lung, colon, breast, and prostate tumors (57). p38 induced activation of Snf-2 related CREB-binding protein-activator protein (SRCAP) promotes p53-dependent transcription of DNA damage proteins, indicating a tumor suppressive function for p38 (54). JNK was shown to negatively regulate tumor suppressor p53, thus promoting cell growth. Constitutively active forms of JNK1 also promote cell growth *in vivo* (61). JNK and p38 proteins regulate the activity of proteases involved in inflammation and pro-inflammatory cytokine production, suggesting possible roles for these proteins in cancer, as chronic inflammation is a well-documented cause of cancer development (62). Signaling through these pathways is very complex due to multiple factors by which these pathways can communicate. For each, pro-survival and pro-death responses can occur, dependent on the specific interactions of the signaling proteins involved.

1.1.2 PI3K/Akt signaling

Signals transduced through receptor tyrosine kinases (RTKs), integrins, and G-protein-coupled receptors (GPCRs) can lead to activation of the phosphoinositide 3-kinase (PI3K) pathway (63-67). The PI3K pathway is most commonly noted for promoting pro-growth/survival responses and it is one of the best studied pathways in the cell. PI3K/ protein kinase B (Akt/PKB) signaling is involved in a vast array of cellular events including maintenance of homeostasis, glucose and lipid metabolism, cell growth, cell death, autophagy, neuronal function, structural organization, proliferation, angiogenesis, and migration (68) (Figure 1-3). PI3K is a heterodimer compromising a catalytic subunit (p110) and a docking subunit (p85). Upon stimulation of the upstream activating kinases, the enzymes associate with the p85 subunit of PI3K through the recruitment of adaptor proteins coordinated by their Src homology 2 (SH2) domains. Phospholipids located within lipid rafts on the plasma cell membrane are recruited to this complex and serve as targets for PI3K phosphorylation. Phospholipid substrates for PI3K include phosphoinositide phosphate {PI(4)P} and phosphoinositide diphosphate {PI(4,5)P2} (69-71). The phospholipid products of these PI3K events include {PI(3,4)P2} and {PI(3,4,5)P3}, respectively (69-72). PI3K activity can be counteracted by phosphatase and tension homolog (PTEN), which catalyzes the removal of a phosphate group from the 3 position of the phospholipids; therefore making PTEN a negative regulator of PI3K. PI(3,4,5)P3 recruits downstream targets for PI3K such as phosphoinositide-dependent kinase-1 (PDK1), and Akt via their pleckstrin homology (PH) domains (63,69-70).

Akt is a multi-domain protein composed of 3 conserved domains: an amino-terminal PH domain, a central kinase domain, and a carboxyl-terminal regulatory domain for mediating its interactions with other proteins. Akt exists as three isoforms Akt1 (PKBα), Akt2 (PKBβ), and Akt3 (PKBγ). Almost all cell types express at least one isoform, while AKT2 and AKT3 are generally thought to be expressed in a tissue type-specific manner (73-74). The association of PI(3,4,5)P3 and its PTEN breakdown product PI(4,5)P2 with Akt enables localization of PDK1 to the plasma membrane for activation of Akt by phosphorylation of Thr308 (75). Akt activity is also modulated by phosphorylation at Ser473. PDK1 is the primary activating kinase for Akt Thr308; however phosphorylation of Ser473 is necessary for its full activity (69). Several kinases have been reported to phosphorylate Ser473 including mammalian target of rapamycin (mTOR) (when bound in the mammalian target of rapamycin complex 2/ TORC2 complex/ TORC2), PDK1, integrin-linked kinase (ILK), DNA-dependent kinase, and Akt itself (70-74). The action of phosphatases is one of the many means by which Akt is regulated. A phosphatase known to regulate Akt activity is PH domain leucine-rich repeat protein phosphatase (PHLPP), which exists as two isoforms that both specifically attenuate Akt activity through dephosphorylation of Ser473 (74,81). Additionally, the serine/threonine phosphatase PP2A dephosphorylates Akt residue Thr308 (74). Much like the MAPK/Erk signaling network, the PI3K/Akt pathway possesses over 100 known targets exhibiting a variety of cellular outcomes (82) (Figure 1-3).

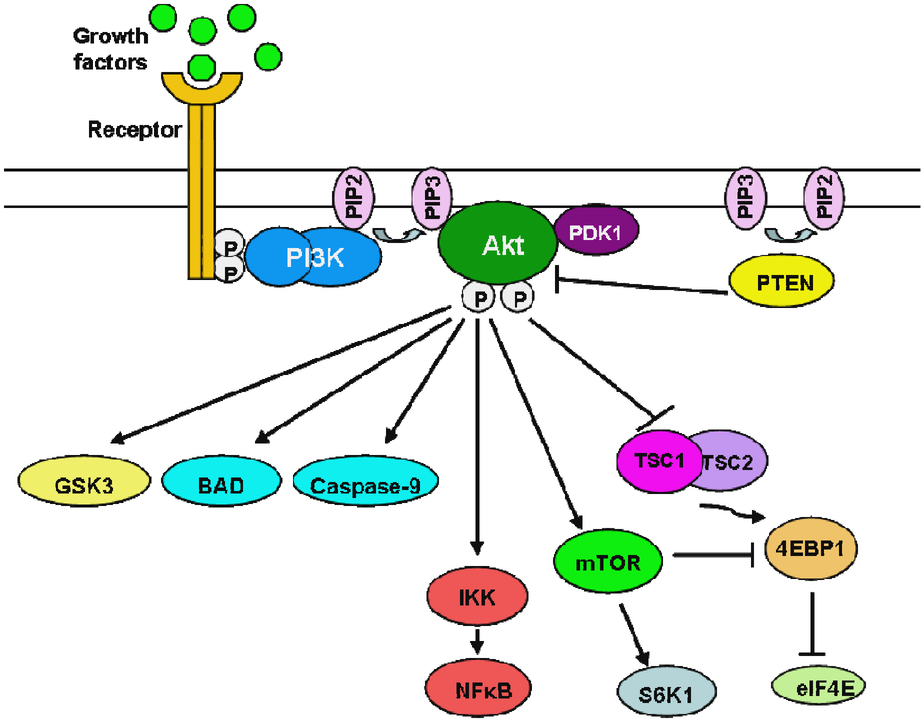

Figure 1-3: A general overview of PI3K/Akt pathway signaling. AKT is activated by growth factors, cytokines, mitogens, and hormones. Receptor activation leads to the recruitment and activation of PI3K to promote generation of PI(3,4,5)P3 on the plasma membrane. PI(3,4,5)P3 (PIP3 as illustrated in this figure) forms a complex with PDK1 and AKT via interactions with their PH domains resulting in activation of AKT Thr308. Full activation of Akt also requires phosphorylation at Ser473. PTEN serves as a negative regulator of PI3K activity by dephosphorylating PIP3 to generate PI(4,5)P2 (PIP2 as illustrated in this figure). Akt is also known to have over a hundred downstream effector proteins found within the cytoplasm. Akt serves as a critical regulator of many cellular functions including metabolism, translation, proliferation, survival, and angiogenesis.

One critical function of Akt signaling is regulation of glucose uptake in insulin-responsive cells. Akt enhancement of glucose transport into the cell is a result of translocation of insulin-regulated glucose transporter 4 (GLUT4) to the plasma membrane. Expression of constitutively active Akt (caAkt) enables translocation of GLUT4 to the plasma membrane in the absence of insulin, while overexpression of dominant negative Akt (dnAkt) demonstrated a reduction in insulin-stimulated glucose uptake in these cells (74). In addition, Akt can activate a positive feedback mechanism by phosphorylation and inactivation of protein tyrosine phosphatase 1B (PTP1B), a negative regulator of the insulin receptor (IR) (83). Akt signaling also mediates glucose metabolism by phosphorylating glycogen synthase kinase 3 (GSK-3) at Ser21, preventing its inhibitory effects on glycogen synthase. This event enables the conversion of glucose into glycogen for cellular storage (84).

Akt acts as a positive mediator of angiogenesis by promoting both direct and indirect activation of pro-angiogenic events. Direct activation of endothelial nitric oxide synthase (eNOS) at Ser1777 by Akt was found to promote migration of endothelial progenitor cells (EPCs) from the bone marrow to the vascular endothelium *in vivo* (85). Akt activity was found to correlate with the activities of vascular endothelial growth factor (VEGF), vascular endothelial (VE)-cadherin, and endothelium-specific receptor tyrosine kinase 2 (Tie2) receptors *in vivo* (86). Little is known about the mechanisms by which Akt indirectly stimulates pro-angiogenic events.

Cell growth and survival are considered to be the major cellular outcomes of Akt signaling. Downstream effectors for Akt known to promote these events include IκB kinase (IKK), mTOR, cyclin-dependent kinase inhibitors ($p21^{WAF1/CIP1}$, $p27^{KIP1}$), BAD, ASK1, and forkhead box O (FoxO) subfamily transcription factors (87-92). When active, IKK phosphorylates IκB leading to activation of nuclear factor kappa-light-chain-enhancer of B (NFκB), a transcription factor promoting expression of numerous pro-survival proteins. Phosphorylation of BAD, a pro-apoptotic Bcl-2 family member, results in the release of BAD from its inhibitory association with anti-apoptotic Bcl-2 family members which bind 14-3-3 proteins to promote cell survival (93-94). Akt signaling promotes phosphorylation of several cell cycle inhibitors to prevent them from restricting cell growth.

mTOR is the best-studied substrate for AKT phosphorylation. Akt activates mTOR through direct phosphorylation of Ser2448, as well as through phosphorylation and inactivation of tuberous sclerosis-2 (TSC2). Inactivated TSC2 allows the GTPase Rheb to remain in its GTP-bound state making mTOR available for activation (95). mTOR may be associated with 2 different signaling complexes: TORC1, through association with regulatory associated protein of mTOR (Raptor) and mLST8; or TORC2, through association with rapamycin insensitive companion of mTOR (Rictor), stress-associated protein kinase interacting protein 1 (Sin1), mTOR-associated protein LST8 homolog (mLST8), and protein-associated with Rictor 1 and 2 (PROTOR1/2) (Figure 1-4) (95). Phosphorylation of insulin receptor substrate protein 1 (IRS1) by insulin and insulin-like growth factors (IGFs) leads to IRS-1 association with PI3K, promoting PDK1 activation of Akt and cell growth (96). Bound within the (TORC1) complex, mTOR activates S6 kinase-1 (S6K1) leading to activation of ribosomal protein S6 and increased protein translation. Another means by which activated mTOR (TORC1) can enhance protein translation is through activation of eukaryotic translation initiation factor 4E binding protein 1 (4EBP-1) which then recruits eukaryotic translation initiation factor 4E (eIF-4E) (97-98). Active mTORC1 and S6K can target insulin receptor substrate 1 (IRS-1) to provide a negative feedback mechanism for these events (68,73). Additional signaling involving mTOR will be detailed further in later sections as mTOR plays a critical role in the studies to be discussed.

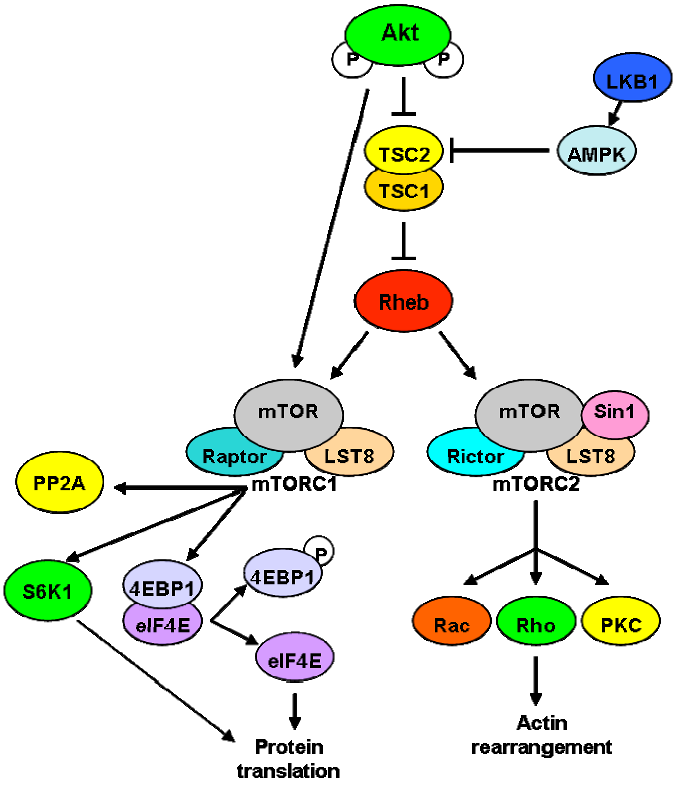
Akt
P
P
LKB1
AMPK
TSC2
TSC1
Rheb
mTOR
Raptor
LST8
mTORC1
mTOR
Sin1
Rictor
LST8
mTORC2
PP2A
S6K1
4EBP1
eIF4E
P
4EBP1
eIF4E
Protein translation
Rac
Rho
PKC
Actin rearrangement

Figure 1-4: Akt regulation of mTOR, a component of TORC1 and TORC2 complexes. Akt is a direct and indirect regulator of mTOR. Akt indirectly regulates mTORC1 through phosphorylation of TSC2, dissociating it from TSC1, enabling GTP hydrolysis of Rheb for subsequent activation of mTOR. mTORC1 can activate multiple downstream effectors, most notably S6 kinase (S6K1) and 4EBP-1 to promote protein translation. mTORC1 also targets PP2A which aids in the regulation of 4EBP-1. Akt activation of mTOR bound within the mTORC2 complex leads to the activation of Rac, Rho, and PKC to stimulate cytoskeletal rearrangement.

The PI3K/Akt pathway contributes to cell growth, cell survival, cell migration, and angiogenesis; therefore it should come as no surprise that alterations in this pathway contribute significantly to the development and progression of cancer. Typically, signaling within the PI3K/ Akt pathway is highly active in tumor cells, yielding cells a growth and survival advantage. This pathway is also a factor in cellular resistance to chemotherapy and radiotherapy (98). A point mutation within the p110 kinase domain of PI3K is the most common Akt pathway-associated dysregulatory event found in cancer (98-100). This mutation occurs frequently in Her2+ breast cancers, while they have also been noted in bowel, ovarian, head and neck squamous, cervical squamous, gastric, lung, brain, and medulloblastoma cancers (98-106). mTOR, a major target of Akt, is commonly activated in transformed cells. Inhibitors of mTOR have been approved for treatment of renal cell carcinoma, while clinical trials are in progress for treatment of glioblastoma and metastatic breast cancer cells (107-109). PTEN loss of function is another common factor in tumor cell pathogenesis and is most prevalent in brain, breast, thyroid, prostate, and endometrial carcinomas (98,110-112). Amplifications or mutations within Akt have low prevalence in cancer, some rare sporadic cases have been reported for gastric, pancreatic, breast, and colorectal cancers (98,113-114). PDK1 mutations are also rare, while some cases have been documented in colorectal cancer patients (98).

1.1.3 AMPK/ LKB1/ mTOR signaling

AMP-activated protein kinase (AMPK) is a major regulator of cellular homeostasis by stimulating events related to cellular metabolism and adenosine triphosphate (ATP) production. This pathway is activated in response to several stimuli including low intracellular ATP levels, low intracellular Ca^{2+} levels, hypoxia, ischemia, and heat shock (115). The AMPK protein complex consists of 3 subunits: a catalytic subunit (α), a glycogen-sensing subunit (β), and a regulatory subunit (γ) containing 2 allosteric adenosine monophosphate (AMP) binding sites (115-117). AMPK is activated by phosphorylation on its Thr172 residue which is located within the β subunit. There are multiple sites shown to be phosphorylated within its activation loop, while the mechanisms by which these residues become phosphorylated are currently poorly understood (116). Three upstream kinases have been reported to phosphorylate AMPK Thr172: liver kinase B1 (LKB1), calmodulin-dependent kinase kinase β (CaMKKβ) and transforming growth factor β-activated kinase-1 (Tak1) (118-121). Tumor suppressor LKB1 is considered to be the major activating kinase for AMPK Thr172 (122-123). LKB1 can be activated by AMPK kinases STE20-like pseudokinase (STRAD) and a homologue of mouse protein 25 (MO25) (124). The AMPK pathway activates several downstream targets in an effort to restore intracellular energy and nutrient levels. Some of the targets for AMPK include glycogen synthase, acetyl CoA carboxylases 1 and 2 (ACC1/2), HMG CoA reductase (HMGR), 6-phosphofructokinase 2 (PFK-2), eukaryotic elongation factor 2 (eEF2), TSC2, Raptor, mTOR, interferon regulatory factor 1 (IRF-1), and sterol regulatory element-binding protein 1 (SREBP-1) (Figure 1-5) (116,125-128). Signaling through these targets promotes ATP-generation, while inhibiting ATP-requiring mechanisms in order to restore optimal energy and nutrient levels (116,125-128).

AMPK maintains energy levels primarily through regulation of glycogen and lipid metabolism (116,122-130). AMPK negatively regulates proteins involved in glucose and lipid biosynthesis, as these are ATP-consuming events. Proteins negatively regulated by AMPK include glycogen synthase, SREBP-1, TSC2, and TORC2 (131). In cases where glucose levels within the cell are low, 5-aminoimidazole-3-carboxamide-1-β-D-ribofuranoside (AICAR) is converted into ZMP leading to activation of AMPK and translocation of tissue-specific GLUT receptors to the plasma membrane to enhance glucose uptake (128-130,132). Lipid metabolism is another means by which the cell restores energy levels. Allosteric activation of AMPK by AMP negatively regulates lipid synthesis. In energy-depleted cells with an elevated AMP:ATP ratio, AMPK signaling promotes lipid breakdown (Figure 1-5). Lipid metabolism and biosynthesis occur throughout the cell and produce a variety of lipid molecules which have demonstrated importance in nearly every cellular outcome (133). These events will be discussed in further detail in a later section (Section 1.3).

AMPK is also an important regulator of autophagy. It coordinates autophagy through direct phosphorylation of multiple components within the mTORC1 pathway. One such event involves the phosphorylation of Raptor on residues Ser722 and Ser792 which inhibits activity of this complex. Evidence suggests that AMPK directly phosphorylates tumor suppressor TSC2 in nutrient-depleted conditions thus inactivating Rheb and preventing mTORC1 activation. Activation of AMPK by AICART can also lead to inhibition of mTORC1 activity (ref 134-135).

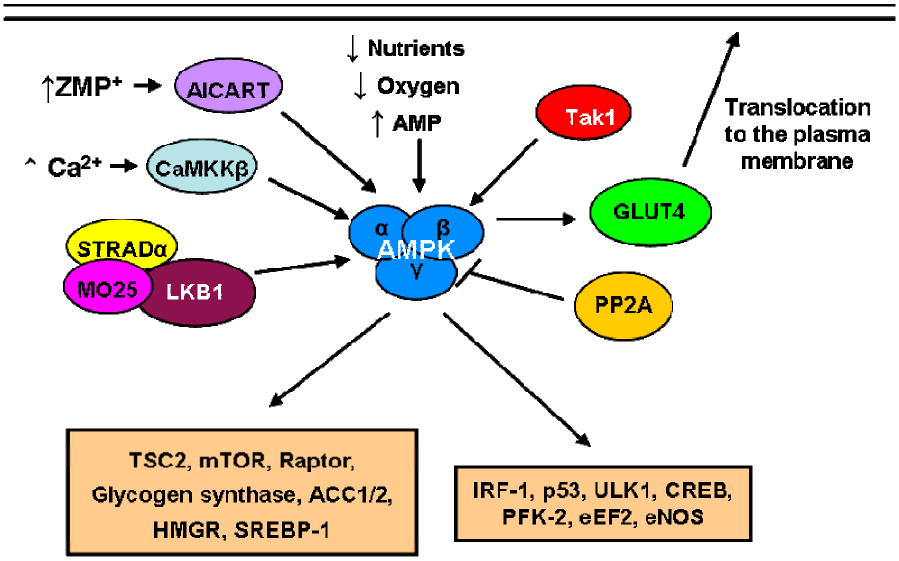
↑ZMP+
AICART
^ Ca2+
CaMKKβ
STRADα
MO25
LKB1
↓ Nutrients
↓ Oxygen
↑ AMP
Tak1
Translocation to the plasma membrane
GLUT4
α
β
AMPK
γ
PP2A
TSC2, mTOR, Raptor, Glycogen synthase, ACC1/2, HMGR, SREBP-1
IRF-1, p53, ULK1, CREB, PFK-2, eEF2, eNOS

Figure 1-5: The AMPK signaling pathway. The AMPK pathway is the major pathway for maintaining cellular homeostasis. AMPK signaling is stimulated by various cellular stress signals including low glucose, low oxygen, high AMP$^+$, and high ZMP$^+$ levels. Low glucose results in the conversion of AICAR to ZMP$^+$ for activation of AMPK. Upstream activating kinases for AMPK include LKB1, CaMKKβ, and Tak1. Active AMPK targets multiple downstream effector proteins. ATP-requiring targets are negatively regulated by the actions of AMPK and these include TSC2, Raptor, mTOR, glycogen synthase, HMG CoA reductase, acetyl CoA carboxylase 1/2 (ACC1/2), and SREBP-1. Proteins activated by AMPK which stimulate ATP-generating events include IRF-1, eNOS, ULK1, p53, CREB, PFK2, and eEF2.

The AMPK pathway is targeted for treatment of diseases such as obesity, type II diabetes mellitus, and multiple types of cancer (136). Studies have shown that the AMPK pathway is dysregulated in breast cancers through a variety of molecular mechanisms causing down regulation of AMPK (137-138). The AMPK pathway has also been implicated in malignant melanoma studies. In these cells, the V600E B-Raf mutation enables hyperactivation of the MEK/Erk pathway and significant downregulation of AMPK signaling through inactivation of LKB1 promoting cell growth (139). In lung cancer cells, attenuation of LKB1 activity enhances cell proliferation and metastasis in cells harboring mutant K-Ras (140). AICAR activation of

AMPK was shown to exhibit anti-proliferative effects in malignant melanomas, while in lung cancer cells harboring wild-type LKB1, AICAR-activated AMPK promoted cell growth (141-142). AMPK activators have been suggested for treatment of ovarian cancers because these compounds sensitize these cells to glucose-deprived activation of AMPK (143). The AMPK pathway acts to suppress cell growth and proliferation in energy-starved conditions which are common in tumor cells, making this pathway important in the treatment of multiple cancer types.

1.2 Mechanisms of Cell Death

1.2.1 Apoptosis

There are two types of programmed cell death: Type I, apoptosis; and Type II, cytotoxic autophagy. Type I, apoptosis, involves an energy dependent process that is controlled by the transcription and translation of proteins involved in DNA repair and regulation of cellular homeostasis. Propagation of this response can occur via the extrinsic or intrinsic pathways (Figures 1-6, 1-7). The extrinsic cellular death pathway involves activation of receptors belonging to the death receptor subclass of the TNF receptor family such as CD95 (cell death receptor 95/APO-1/ Fas) and TNF-related apoptosis-inducing ligand receptor I (TRAIL/ DR4) (144). These receptors are pre-associated homotrimers located within lipid rafts on the plasma cell membrane and, upon binding of their respective ligands, undergo a conformational change enabling binding of death domain adaptor proteins to form the death-inducing signaling complex (DISC) (Figure 1-6). The DISC complex is composed of the activated receptor bound to its respective ligand and the corresponding death domain-associated adaptor proteins, such FADD; which recruits and specifically binds to the effector caspase, procaspase-8 (145). Upon its recruitment, procaspase-8 undergoes self-cleavage into its active form, caspase-8. Caspase-8 activation is suppressed by expression of cellular FLICE-like inhibitory protein 1 (c-FLIP-1) and cellular FLICE-like inhibitory protein s (c-FLIP-s) (146). Activated caspase-8 then can either: cleave BID to truncated-BID (tBID), which by way of the mitochondrial pathway leads to cell death; or directly lead to the cleavage and activation of caspase-3, promoting cell death. Caspase-3 may then translocate to the nucleus and deactivate DNA fragmentation factor-45 (DFF45) through cleavage of the protein, disabling it from binding to and inhibiting the DNA fragmentation factor-40 (DFF40) enzyme. DFF40, otherwise referred to as caspase-activated DNase, is then able to perform its enzymatic duty of DNA fragmentation, thus leading to a cell's demise (147).

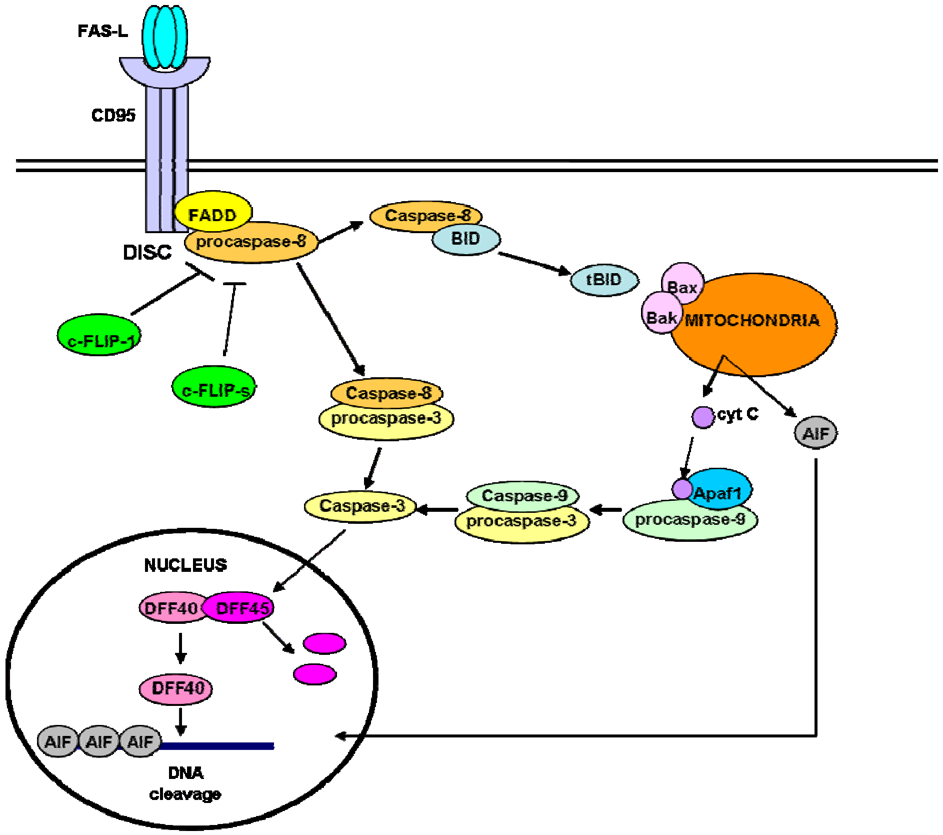
FAS-L
CD95
FADD
procaspase-8
DISC
Caspase-8
BID
tBID
Bax
Bak
MITOCHONDRIA
c-FLIP-1
c-FLIP-s
Caspase-8
procaspase-3
cyt C
AIF
Apaf1
procaspase-9
Caspase-9
procaspase-3
Caspase-3
NUCLEUS
DFF40
DFF45
DFF40
AIF
AIF
AIF
DNA
cleavage

Figure 1-6: The extrinsic and intrinsic apoptotic pathways. Extrinsic apoptosis: In the case of the CD95 death receptor, a pre-associated homotrimeric CD95 complex binds extracellularly to its ligand (Fas-L) to promote and activating conformational change. This change enables binding of its death domain adaptor protein (FADD) and formation of the death-inducing signaling complex (DISC) on the plasma cell membrane. Procaspase-8 is recruited to this complex where is undergoes self-cleavage into its active form caspase-8. Activation of caspase-8 is inhibited by c-FLIP-1 and c-FLIP-s proteins. Activated caspase-8 cleaves and activates caspase-3, enabling its translocation to the nucleus for dissociation of the DFF40 nuclease from its inhibitor, DFF45, resulting in DNA fragmentation and cellular death. Intrinsic apoptosis: Activated caspase-8 can also cleave BID into its active form tBID. Once activated, tBID translocates to the mitochondria to associate with other pro-apoptotic Bcl-2 family member proteins (Bax, Bak) to promote mitochondrial membrane permeabilization and the release of factors AIF and cytochrome c. Cytochrome C forms a complex with Apaf-1 and procaspase-9 to promote activation of caspase-9. Caspase-9 then activates caspase-3 for translocation to the nucleus for promotion of DNA fragmentation and eventual cell death.

The intrinsic apoptosis pathway involves intracellular insults which promote activation of pro-apoptotic Bcl-2 family member proteins (Figure 1-6) (148). The mitochondrial component of the extrinsic pathway is termed the intrinsic apoptosis pathway. Extrinsic apoptotic pathway events leading to the cleavage of BID into its active form, tBID, by caspase-8 enables its translocation to the mitochondrial membrane. tBID associates with anti-apoptotic Bcl-2 family member proteins, causing their release from association on the outer mitochondrial membrane with Bax and Bak. Bax and Bak then undergo conformational changes which enable permeabilization of the mitochondrial membrane and the release of factors, in particular cytochrome c, cytochrome c interacts with Apaf-1 and together, this complex causes activation of procaspase-9. Active caspase-9 induces cleavage and activation of caspase-3 and eventual cell death (further described in Section 1.2.3) (145). Inhibition of the intrinsic apoptosis pathway has previously been shown to suppress the cyto-toxicity of several thymidylate synthase (TS) inhibitors, including pemetrexed (149-150). The intrinsic apoptotic events occurring at the mitochondrial membrane resemble the signaling events that take place in the case of autophagy-induced cellular death, Type II.

1.2.2 Formation of the autophagosome

Autophagy is a naturally occurring event which takes place in normal quiescent cells as a means of defense for clearing pathogens, as well as a mechanism by which the cell restores and maintains homeostasis (151-152). Autophagy involves lysosomal degradation of non-vital cellular proteins and organelles, in order to recycle proteins back into their amino acid building block forms. This process is activated by extracellular and intracellular insults resulting in elevated levels of reactive oxygen species (ROS), increases in intracellular Ca^{2+} levels, AICAR monophosphate (ZMP) accumulation, or energy and nutrient starvation (115-116). Activation of autophagy occurs as a protective effort to restore energy and nutrient levels in an effort to restore homeostasis within the cell and promote survival (cytostatic autophagy). Prolonged activation of this signal, without restoration of the cell to an unstressed and unstarved state, can lead to induction of a cytotoxic form of autophagy. Treatment of cells with anti-cancer drugs can cause prolonged cellular stress leading to the cytotoxic form of autophagy resultant of degradation of vital cellular contents (153-156). Autophagic events are subdivided into 3 categories: micro-autophagy, macro-autophagy, and chaperone-mediated autophagy (CMA) (153,156). CMA involves the translocation of unfolded proteins directly through the lysosomal membrane for proteolytic degradation. Direct engulfment of cytosolic proteins and organelles into the lysosome is described as micro-autophagy. Once contained within the lysosome, proteins and organelles are degraded and recycled for the purpose of minimizing energy expenditure of non-vital cellular components, as well as releasing nutrients back into the cell that are required for survival. Macro-autophagy describes events where cellular components are first incorporated into the autophagosome prior to fusion with the endocytic lysosome (153-155,157-162). This process is thought to be responsible for a majority of protein degradation occurring within the cell. Macro-autophagy (hereafter referred to as autophagy) is mediated by two ubiquitin-like conjugation systems, autophagy-related genes 5-12 (Atg5-Atg12) and microtubule-associated protein 1 light-chain 3 (LC3/ATG8)- phosphotidylethanolamine (PE) (159-162). Green fluorescent protein (GFP)-conjugated LC3, therefore serves as a useful tool for evaluating autophagosome formation in our tumor cell models. The events responsible for formation of the autophagosome are important for the studies to be discussed in this dissertation because the data demonstrated significant enhancement of autophagosome formation, as judged by GFP-LC3+ vesicle formation.

Autophagy encompasses a series of events involving initiation of autophagosome formation, engulfment of non-vital cellular components, vesicle nucleation, vesicle expansion, Atg protein recycling, autophagosome fusion with the lysosome, and autolysosomal digestion of its contents to provide nutrients and amino acids for the cell (Figure 1-7) (160-162). Two important proteins which regulate autophagy are mTOR and Bcl-2-interacting myosin like coiled-coil protein (Beclin1/Atg6) (153-154,161-162). Beclin1 is the key initiator of autophagy in mammalian cells, while there is also some evidence to suggest that autophagy may be activated through Beclin1-independent events (163). When stimulated, Beclin1 is released from its association with anti-apoptotic Bcl-2 family members Bcl-2, Bcl-2 protein 1 (Bcl-XL), and myeloid leukemia cell differentiation protein 1 (Mcl-1) to carry out its positive regulatory role in autophagy. mTOR activation by PI3K/Akt serves as a negative mediator of these events by stimulating transcription and translation of anti-autophagic proteins, as well as directly binding to and inhibiting phosphorylated Atg proteins (164-165). The core components of the autophagosome will be detailed in this section, while the specific molecular events that trigger an autophagic cellular response will be discussed in the next section (Section 1.2.3).

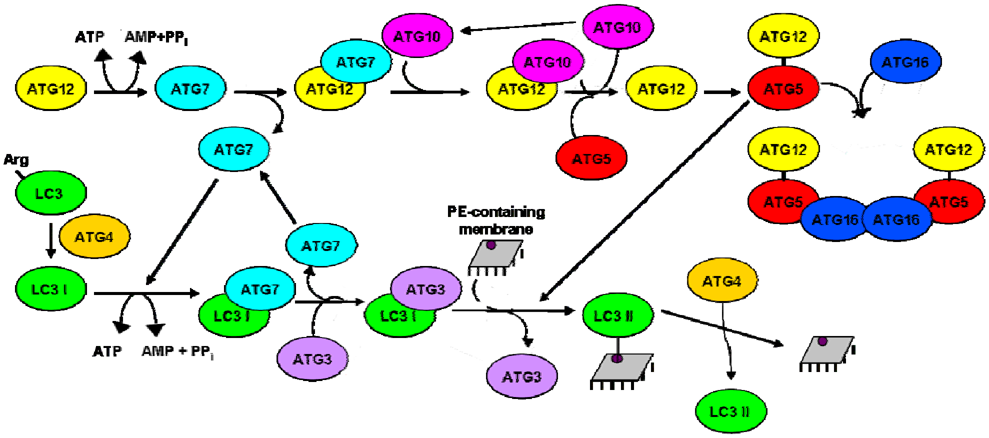
ATP
AMP+PPi
ATG12
ATG7
ATG7
ATG12
ATG10
ATG10
ATG10
ATG12
ATG12
ATG12
ATG5
ATG16
ATG5
ATG7
Arg
LC3
ATG4
LC3 I
ATG12
ATG12
ATG5
ATG16
ATG16
ATG5
PE-containing membrane
ATG7
ATG7
LC3 I
ATG3
LC3 I
LC3 II
ATG4
ATP
AMP + PPi
ATG3
ATG3
LC3 II

Figure 1-7: Formation of the autophagosome by autophagy-related proteins. Reduced PI3K signaling stimulates a sequence of events which results in formation of the autophagosome. There are two ubiquitin-like protease conjugation systems necessary for autophagosome formation to occur, the ATG5-12 (top half) and ATG8 (LC3)-phosphotidylethanolamine (PE) (bottom half) systems. The ATG5-12 conjugation system involves a sequence of ubiquitin ligase events (E1- ATG7 and E2- ATG10) resulting in formation of a ATG5-12-16 trimer. The trimer dimerizes to perform its function as the site of LC3 lipidation for membrane biogenesis. The ATG8/ LC3-PE conjugation system begins with ATG4 cleavage of LC3 to expose a glycine residue where conjugation occurs. ATG7 also serves as the E1 ubiquitin ligase for LC3 conjugation, while the E2 ligase is ATG3. After the E2 ligase step LC3 has affinity for PE on the plasma membrane, to which it binds. Together, these events promote autophagy through initial formation of the autophagosome.

Autophagic vesicle formation begins with the formation of the pre-autophagosome. Atg17 recruits Atg13 and Atg9 to activate a class III PI3K complex which includes class III PI3K protein 34 (Vps34), the p150 PI3K regulatory subunit, Atg14, Beclin1/Atg6, and ultraviolet-irradiation resistance-associated gene (UVRAG). Wortmannin, LY294002, and 3-methyladenine (3-MA) are small molecule inhibitors of the class III PI3K Vps67 and can be used to block induction of autophagy (166). Events associated with this complex drive pre-autophagosome membrane nucleation by promoting the association of initial protein components (163). Elongation of the pre-autophagosome occurs by way of Atg5-Atg12 and LC3II-PE ubiquitin-like conjugation systems which are both localized to the PI3K complex. Atg7 and Atg10 mediate the covalent association of Atg5 with Atg12 (Atg5-Atg12), which interacts with Atg16 to promote elongation of the developing membrane. This complex is later released and does not serve as a component of the mature autophagosome. The LC3 (ATG8)-PE conjugation system associates with the pre-autophagosome and does serve as a component of the mature autophagosome. LC3 is cleaved to LC3-I by ATG4, then conjugated to phosphotidylethanolamine (PE) to generate LC-II through ATG3/ATG7-dependent events (154). Once lipidated, LC3-II associates with Beclin1/ATG6 on the vesicle membrane and provides a means for recruitment of the cargo to be recycled. Cargo adaptor proteins such as p62, next to breast cancer type 1 susceptibility gene protein 1 (Nbr1), and the proapoptotic Bcl-2 related protein Nix, mediate delivery of specific cargo to the autophagosome through direct and tight interactions with LC3-II. Ubiquitination domains are located on cargo adaptor proteins and associate with ubiquitinated cargo for incorporation into the autophagosome. Fusion of the mature autophagosome with acidic lysosomes is regulated by soluble n-ethylmaleimide sensitive fusion attachment protein (SNARE) proteins. Proteinase B-1 (PRB1) and Atg15 lipase function to break down the autophagosomal vesicle leading to fusion with the lysome and formation of the autophagolysosome where degradation of cargo takes place (154).

1.2.3 Regulation of Autophagy

Type II cell death, a cytotoxic form of autophagy, involves downregulation of anti-apoptotic Bcl-2 family member proteins Mcl-1 and Bcl-XL. Deactivation is a result of disassociation with pro-apoptotic members of the same family through interactions between their Bcl-2 homology 3 (BH3) domains (Figure 1-8) (167-169). Bcl-2 family members possess one to four Bcl-2 homology domains (BH1-BH4) that mediate their interactions with other Bcl-2 homology domain containing proteins for regulation of specific downstream signaling events. All Bcl-2 family members contain a BH3 domain (167). Bcl-XL and Mcl-1 may bind to Beclin1 or BH3-only proteins such as BID, Bcl-2-like protein 11 (BIM), BAD, p53 upregulated modulator of apoptosis (PUMA), and adult T cell leukemia derived PMA-responsive protein (NOXA). These BH3-only proteins are sequestered by Mcl-1 and Bcl-XL away from the mitochondrial membrane (167,170). Release of Beclin1 allows it to perform its function as an inducer of autophagy as described in the previous section. Upon disassociation from Bcl-XL and Mcl-1, Bax and Bak undergo an activating conformational change and homodimerize to form pores with the mitochondrial membrane. Pore formation allows for the release of pro-apoptotic signals from the mitochondrial inter-membrane space into the cytosol (171). These signaling molecules include cytochrome c and apoptosis-inducing factor (AIF) which perform separate functions within the cytosol of the cell (Figure 1-9) (172-173). AIF released into the cytosol can translocate to the nucleus to promote chromatin condensation and DNA fragmentation (174). When released, cytochrome c binds to Apaf-1, disassociating Apaf-1 from pro-caspase 9, enabling its self-cleavage and activation. Activated caspase 9 may then cleave and activate caspase 3 (as mentioned in Section 1.2.1). Caspase-3 then translocates to the nucleus for deactivation of DFF45 and release of the DFF40 DNase promoting DNA fragmentation and eventual cell death (175).

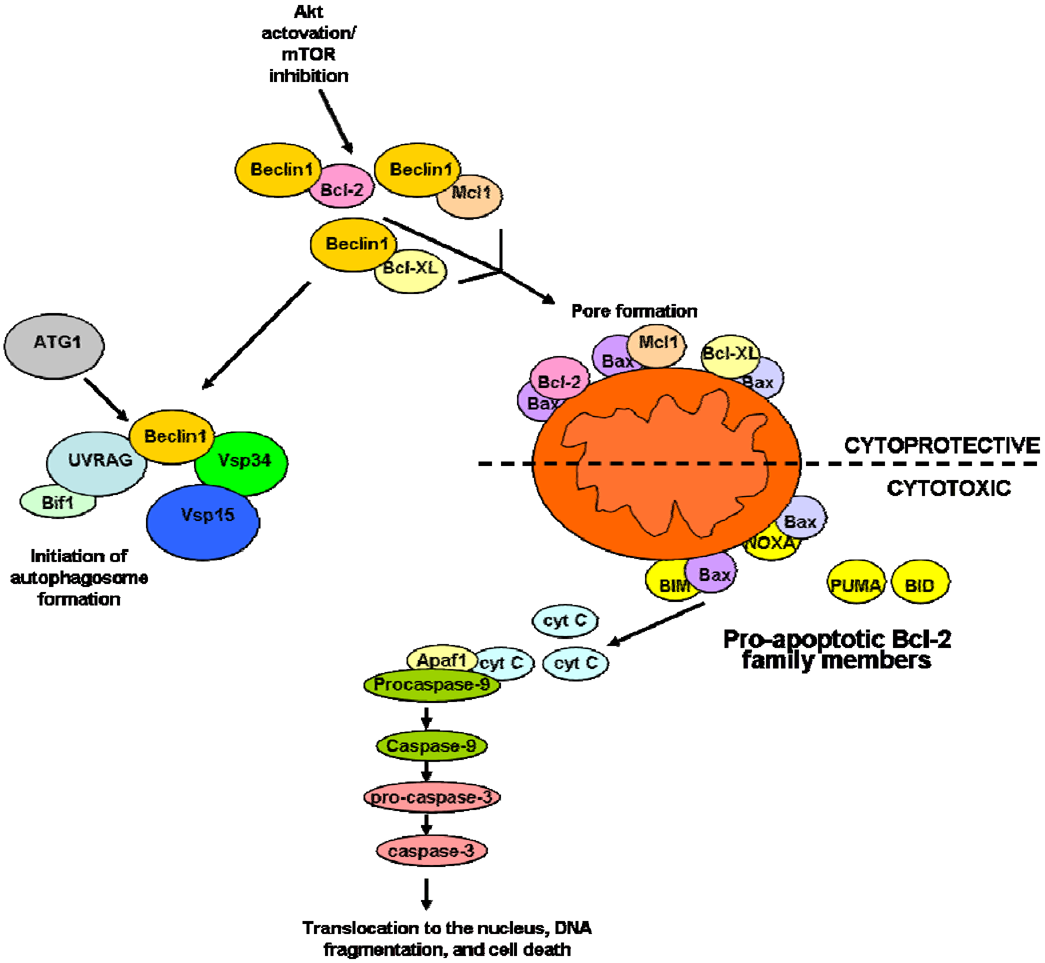
Akt
actovation/
mTOR
inhibition
Beclin1
Bcl-2
Beclin1
Mcl1
Beclin1
Bcl-XL
Pore formation
ATG1
Beclin1
UVRAG
Vsp34
Bif1
Vsp15
Initiation of
autophagosome
formation
Mcl1
Bax
Bcl-XL
Bcl-2
Bax
Bax
CYTOPROTECTIVE
CYTOTOXIC
Bax
NOXA
BIM
Bax
PUMA
BID
cyt C
Apaf1
cyt C
cyt C
Procaspase-9
Pro-apoptotic Bcl-2
family members
Caspase-9
pro-caspase-3
caspase-3
Translocation to the nucleus, DNA
fragmentation, and cell death

Figure 1-8: Activation of autophagy via intracellular stress signaling. Initiation of autophagy occurs as a response to cell stress and is regulated by a variety of factors. Anti-apoptotic Bcl-2 family member proteins (Bcl-XL and Mcl-1) interact with BH3-domain containing proteins (Bax and Bak). Bax and Bak homodimerize to form pores on the mitochondrial membrane enabling the release of cytochrome C from the inner mitochondrial membrane space. Cytochrome C binds to the Apaf1/procaspase-9 complex to promote cleavage of procaspase-9 for generation of active caspase-9. Active caspase-9 cleaves and activates caspase-3 to promote cell death.

1.3 Lipid Signaling in Cancer

Lipids, while important for cellular membrane structure and integrity, have received an increasing amount of attention over the last two decades with regards to their roles in cellular signaling. A majority of the signaling events found to be regulated by lipid molecules involve sphingolipids. Sphingolipids are ubiquitinously expressed in the membranes of mammalian cells and their metabolites possess potent biological activity. Bioactive sphingolipid metabolites include sphingosine, ceramide, sphingosine-1-phosphate, and ceramide-1-phosphate (176). These molecules have been shown to play a role in numerous cellular processes including apoptosis, growth arrest, differentiation, inflammation, angiogenesis, intracellular trafficking, cell migration, and cell adhesion (177). The enzymes responsible for sphingolipid biosynthesis and function are regulated by a complex set of cellular events, the specific mechanisms that control these enzymes remain to be elucidated (178). Dysregulation of sphingolipid levels has implications in neurodegenerative disorders, metabolic diseases, and multiple cancer types. Enhanced lipid biosynthesis is an event commonly associated with cancer. These phenomena are likely due to an enhanced need for lipids during cell membrane production, as well as an alternative means of energy production through β-oxidation and lipid modification of proteins (179). For this reason, enzymes involved in the synthesis of sphingolipid molecules are of interest in development of novel chemotherapeutic drugs. Generation of sphingolipids occurs through three primary mechanisms: sphingomyelin hydrolysis, the *de novo* ceramide synthesis pathway, and the salvage pathway. Each mechanism involves sequential actions of multiple enzymes to generate each of the unique lipid moieties.

1.3.1- Sphingomyelin hydrolysis

Sphingomyelin hydrolysis involves the breakdown of lipid metabolites into ceramide. Biosynthesis of sphingomyelin is catalyzed by sphingomyelin synthase and involves the transfer of phosphocholine from phosphatidylcholine to ceramide, which occurs in the pre-Golgi membranes (180). Sphingomyelin is then transported to the plasma membrane by vesicular means to become an abundant outer lipid bilayer component. During times of cellular stress often associated with tumor necrosis factor α (TNFα) stimulation, hypoxia, and chemotherapeutic drug exposure; sphingomyelinase enzymes (SMase) are activated to produce ceramide, a second messenger for apoptosis alongside receptor-mediated mechanisms. This event occurs at the plasma membrane where sphingomyelin is abundant and is the primary means by which intracellular ceramide is produced (180). Plasma membrane-associated SMase (neutral SMase) carries out the hydrolysis of sphingomyelin to form phosphocholine and ceramide. Alkaline and acidic SMases are also present in cells. However, these enzymes are cell type-specific or compartmentalized to specific subcellular locations where they carry out similar functions. Ceramide is then available for promoting an apoptotic response or may be acted on by other enzymes involved in lipid biosynthesis to generate other sphingolipid derivatives.

1.3.2- The de novo ceramide synthesis pathway

The *de novo* ceramide synthesis pathway is more highly activated in cancer cells to accommodate the needs of rapidly proliferating tumor cells. The *de novo* fatty-acid synthesis pathway takes place in the ER and is utilized to generate ceramide. This process begins with the condensation of palmitate and serine to form 3-ketodihydrosphingosine which is catalyzed by serine-palmitoyl transferase. 3-ketodihydrosphingosine is then reduced to dihydrosphingosine by 3-ketoreductase. At this point, dihydrosphingosine is acylated by dihydroceramide synthase to produce dihydroceramide (176-178,181-193). Introduction of a 4,5 double bond in the sphingoid base of dihydroceramide by a specific dehydrogenase enzyme yields ceramide. Ceramide is then transported to the Golgi apparatus via the ATP-dependent ceramide transfer protein (CERT) (194). Once ceramide reaches the Golgi it is converted to sphingomyelin by SMase to become one of the major components of the outer bilayer of the plasma membrane (177,180,188-193,195). Ceramide produced at the ER can also be acted upon by ceramidase to produce sphingosine, which may be converted into sphingosine-1-phosphate by sphingosine kinase. In some cases, sphingosine-1-phosphate is further broken down into phosphatidylethanolamine and fatty aldehydes by a specific lyase enzyme (176,178,182,196-197). The *de novo* ceramide synthesis pathway has been implicated in induction of apoptosis upon treatment with numerous chemotherapeutic drugs in multiple tumor types including: glioblastoma, head and neck squamous cell carcinoma (HNSCC), renal cell carcinoma (RCC) and non-small cell lung carcinoma (NSCLC), chronic myeloid leukemia, neuroblastoma, gastrointestinal, breast, ovarian, and colon cancer cells (180-183,185-186,190-194,198-207). In recent years, ceramide-activated serine/threonine protein phosphatases PP1 and PP2A, as well as inhibitory protein 2 of PP2A (I2PP2A/SET) were found to directly bind ceramides. In the case of I2PP2A, ceramide binding prevents its inhibitory association with PP2A, thus activating the enzyme. These serine/threonine phosphatase regulatory events were found to occur in multiple tumor types and promoted a tumor suppressive role for PP2A (177,194,208-210). Recent studies have demonstrated activating roles for these synthetic sphingolipid molecules towards ceramide-activated protein phosphatases and the onset of apoptosis (181,186,205,211).

1.3.3- The lipid salvage pathway

The salvage pathway takes place within the acidic late endosomes and lysosomes and accounts for 50%-90% of sphingolipid biosynthesis in the cell (178,184,187). Production of sphingosine itself only occurs by way of the salvage pathway (187). Acidic sphingomyelinase converts sphingomyelin into ceramide, which can be further hydrolyzed into sphingosine and a long-chain free fatty acid. Sphingosine and free fatty acids are then released from the lysosome, whereas ceramide is not. The salvage pathway is typically thought of as the mechanism by which sphingosine is recycled and is often referred to as the recycling pathway. Once sphingosine is released from the lysosome it can be converted into ceramide by the action of ceramide synthase, similar to the *de novo* ceramide synthesis pathway (178,184,187).

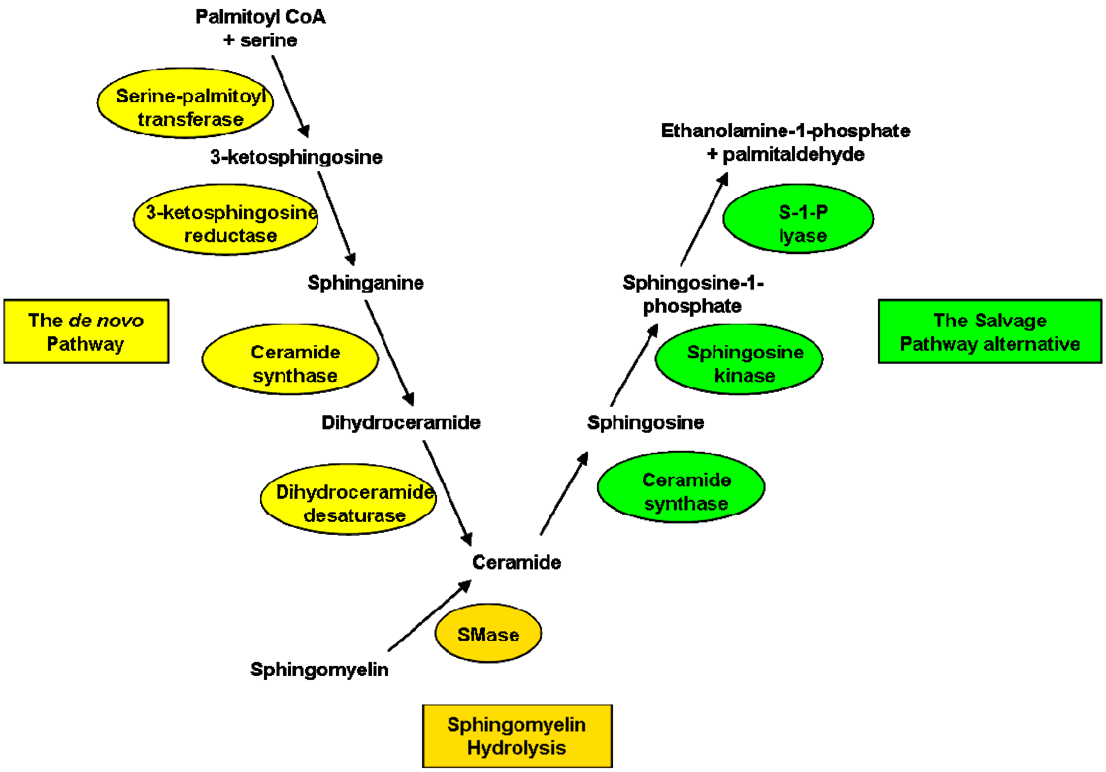
Palmitoyl CoA
+ serine
Serine-palmitoyl transferase
3-ketosphingosine
3-ketosphingosine reductase
Sphinganine
The *de novo* Pathway
Ceramide synthase
Dihydroceramide
Dihydroceramide desaturase
Ceramide
SMase
Sphingomyelin
Sphingomyelin Hydrolysis
Ethanolamine-1-phosphate
+ palmitaldehyde
S-1-P lyase
Sphingosine-1-phosphate
Sphingosine kinase
The Salvage Pathway alternative
Sphingosine
Ceramide synthase

Figure 1-9: The ceramide synthesis pathways. The first step in this pathway involves the rate-limiting condensation of palmitate and serine to form 3-ketodihydrosphingosine, catalyzed by serine-palmitoyl transferase. 3-ketoreductase then reduces 3-ketodihydrosphingosine to dihydrosphingosine. Dihydrosphingosine is acylated by dihydroceramide synthase to produce dihydroceramide. Dihydroceramide desaturase introduces a 4,5 double bond in the sphingoid base of dihydroceramide to yield ceramide. Ceramide is then transported to the Golgi apparatus for enzymatic conversion to sphingomyelin to become one of the major components of the outer bilayer of the plasma membrane. Ceramide produced at the ER can also be acted on by ceramidase to produce sphingosine, which may be converted into sphingosine-1-phosphate by sphingosine kinase. In some cases, sphingosine-1-phosphate is further broken down into phosphatidylethanolamine and fatty aldehydes by a specific lyase enzyme.

Chapter 2- Introduction on Chemotherapeutic Agents

2.1 Combinatorial drug therapy for treatment of cancer

Chemotherapeutic targeting of individual cellular signaling pathways is a highly effective method of treatment for cancer, yet there are many obstacles surrounding this approach. One major example, resulting from prolonged administration of many of the Food and Drug Administration (FDA)-approved chemotherapeutic drugs is acquired drug resistance. In cancer, resistance to anticancer drugs manifests through a variety of factors related to an individual's genetics, as well as, intrinsic alterations in cellular signaling pathways which enable alternative mechanisms for bypassing drug toxicity (212). One means of circumventing this obstacle is through use of a combination of chemotherapeutic agents chosen to specifically target two pathways simultaneously. Molecular targeted combination drug therapies are designed to inhibit cell survival pathways, as well as stimulate cellular death signals/signaling. A clinically relevant theory pertaining to treatment of tumor cells with multiple agents encompasses the thought that intended concentrations for each drug can be minimized to concentrations below that of clinically relevance, as a result of achieving a novel lethal effect. Minimizing the concentrations of each drug should in turn minimize the levels of normal tissue toxicity.

There are many combination drug therapies currently approved for treatment of a wide variety of cancer cell types. There is also a growing number of targeted cotherapy trials reaching the clinic.

For example, a current Phase III trial for NSCLC patients involves ganetespib, a heat shock protein 90 (Hsp90) inhibitor, combined with docetaxol, paclitaxel, or another microtubule targeting agent. And recently, a Phase III trial involving lapatinib and herceptin in early-stage breast cancer patients achieved a 51.3% pathological complete response, as compared to lapatinib (23.4%) and herceptin (21.1%) agents alone (213). The combination of sorafenib, a class III receptor tyrosine kinase inhibitor, with Docetaxol and/or Letrozole is currently in Phase III clinical trials as an initial line of treatment for recurrent Her2-neu negative breast cancer patients (214). With respect to pre-clinical studies, our lab and others have shown that sorafenib combined with histone deacetylase (HDAC) inhibitors causes synergistic cell killing in hepatoma, cholangiocarcinoma, and leukemia cells (215). HDAC inhibitors also synergize with the cyclin-dependent kinase (CDK) inhibitor flavopiridol *in vitro* to synergistically kill human leukemia cells through a mechanism involving suppression of the NF-κB pathway (216). We have also shown that flavopiridol and vorinostat causes enhanced cell death in breast cancer cells, providing another promising clinical treatment option for these patients (217).

2.2 Pemetrexed

2.2.1- Anti-folates as chemotherapeutic agents

Anti-folate compounds compromise a category of chemotherapeutic agents designed to suppress DNA and RNA synthesis. Anti-folates have been utilized in the clinic for several decades with methotrexate being the most common. Methotrexate was first identified as an analog of aminopterin (4-amino-folic acid) to more effectively inhibit DNA and RNA synthesis (218). Methotrexate was later found to specifically target dihydrofolate reductase (DHFR) (219). The drug was FDA-approved for multi-drug treatment of acute lymphoblastic leukemia (ALL); as well as the standard of treatment for rheumatoid arthritis (220-221). In addition to these diseases, it has shown utility in the treatment of choriocarcinoma, osteosarcoma, non-Hodgkin lymphoma, head and neck, breast, and lung cancers (222). In an effort to identify methotrexate analogs with greater affinity for DHFR that are less specific for normal tissue cells, studies identified pralatrexate (10-proargyl-10-deazaminopterin, Folotyn®), which was since approved for the treatment of relapsed peripheral T-cell lymphoma in 2009 (223). In a unique effort to inhibit DNA synthesis, later studies were conducted to identify novel anti-folate compounds primarily targeting the thymidine and purine biosynthetic machinery, as opposed to DHFR. Several of these compounds were initially identified (CB37175, Lometrexol), unfortunately, these drugs met with little success in the clinic (224-225). Subsequent studies aimed towards synthetic analogs of Lometrexol, led to the discovery of Pemetrexed (PTX/ ALIMTA®) (226).

Pemetrexed is a second generation anti-folate drug identified as targeting *de* novo thymidine and purine bio-synthetic enzymes. In February 2004, pemetrexed was FDA-approved for treatment of malignant pleural mesothelioma (MPM) in combination with cisplatin for patients whom surgical resection is not an option (227-232). In August of the same year, pemetrexed was approved as a single agent second-line therapy for locally advanced or metastatic non-squamous NSCLC. It was approved for combination therapy with cisplatin as an initial line of treatment for the same disease in 2008. The following year, it received approval as a single agent therapeutic route in non-squamous NSCLC after 4 rounds of treatment with platinum-based compounds (cisplatin, carboplatin, oxaliplatin) (229,233). Pemetrexed has also entered the clinical setting for trials in a variety of other tumor types, including small cell lung carcinoma, breast, pancreatic, colorectal, esophageal, gastric, renal, head and neck, bladder, cervical, and ovarian cancers (234-239).

Pemetrexed is transported into the cell by the reduced folate carrier and protein-coupled folate transport systems. Once transported into the cell, pemetrexed is polyglutamated by folylpolyglutamate synthetase enabling its retention in the cell for subsequent inhibition of its intracellular target(s). Pemetrexed was originally developed as an inhibitor of thymidylate synthase (TS), but has subsequently been shown to target multiple enzymes involved in folate metabolism and purine and pyrimidine biosynthesis.

2.2.2- Thymidylate Synthase (TS) as a primary target for Pemetrexed

Pemetrexed was initially found to be an inhibitor of thymidylate synthetase (TS). TS catalyzes the reductive methylation of deoxyuridine monophosphate (dUMP) into deoxythymidine monophosphate (dTMP) using N5,N10-methylene tetrahydrofolate as a co-factor which gets oxidized to yield the secondary product dihydrofolate. Through successive phosphorylation events involving nucleoside monophosphate kinase and nucleoside diphosphate kinase, dTMP is converted into deoxythymidine-5'-triphosphate (dTTP or TTP) for use in DNA synthesis (240) (Figure 2-1). TS is the rate-limiting enzyme in *de novo* thymidine synthesis. Pemetrexed binds in the active site of TS to form an inhibitory complex preventing consequent steps which form dTTP (238,241). Inhibition of TS causes a dramatic reduction in cell proliferation resultant of reduced DNA synthesis and cell death. Inhibition of TS also causes an accumulation of dUMP because dUMP is a substrate for the TS reaction. dUMP is then converted into deoxyuridine 5' triphosphate (dUTP) by dUMP phosphatases (dUMPases) naturally present in the cell. DNA polyermase allows for misincorporation of dUTP in sites where dTTP should be incorporated during DNA synthesis causing cell stress and eventual cell death; thus providing a secondary means of negative regulation by pemetrexed on cell proliferation and survival (242). Patients with NSCLC who are non-responsive to pemetrexed were found to have elevated levels of TS, indicating that TS is a potential predictive biomarker of drug effectiveness (238,242). Based on the continued anti-proliferative effect upon cells *in vitro* in the presence of exogenous thymidine to prevent the cytotoxic effects of TS inhibition, it became apparent that pemetrexed has at least one secondary target (243-246).

2.2.3- AICART is a secondary target for Pemetrexed

In an effort to define additional targets of pemetrexed, our collaborators identified the folate-dependent enzyme, aminoimidazole-carboxamide ribonucleotide formyl-transferase (AICART), as a secondary drug target (243-244). AICART is the second folate-dependent enzyme in *de novo* purine biosynthesis (244) (Figure 2-1). AICART catalyzes the reaction of 10-formyl-tetrahydrofolate (THF) and 5-aminoimidazole-4-carboximide-1-β-D-ribofuranoside (AICAR) to formyl THF and formyl-AICAR. This reaction follows the first step in *de novo* purine synthesis, which is catalyzed by phosphoribosylglycinamide formyltransferase (GART). Both are essential steps in purine biosynthesis for cells not exposed to exogenous purines (247). Supplementation of cells with a precursor of the product of the GART reaction, aminoamidazole carboxamide (AICAR), suggested AICART as a secondary target of pemetrexed. The kinetic inhibitory rates of pemetrexed for AICART were later determined (244). Inhibition of AICART results in elevated levels of 5-aminoimidazole-4-carboxamide ribonucleotide (ZMP), a substrate for AICART, to cause ER stress resulting in induction of autophagy. Pemetrexed inhibition of AICART in NSCLC resulted in an intracellular accumulation of ZMP promoting activation of AMPK and downstream inhibition of mTOR (Figure 2-1) (243-244). Suppression of mTOR promotes activation of autophagy by enabling the association of ATG proteins which is required to initiate formation of the autophagosome (248-249).

2.2.4- Other known targets of pemetrexed

In addition to TS and AICART, several other secondary targets have been identified for pemetrexed. AICART was identified more recently, while GART and DHFR were identified early in validation of the drug. These enzymes are involved in *de novo* purine synthesis and pyrimidine metabolism (Figure 2-1). Inhibition of DHFR by pemetrexed was shown to reduce the turnover of THF, a co-factor for the TS reaction, to further promote its growth inhibitory effects (237). Pemetrexed binds to TS 60 times more tightly than to DHFR, making the effects of DHFR inhibition on TS activity nearly irrelevant (247). GART, the primary target of 6R-DDATHF, was originally identified as a secondary target of pemetrexed action. However, studies aimed at determining the effects downstream of GART, led to the identification of AICART as the major enzyme within the *de novo* purine synthesis pathway targeted by pemetrexed (244). The studies within this dissertation assume that the major toxic effect achieved by pemetrexed is that of TS and AICART inhibition. For that reason, media for cell culture experiments is supplemented with dialyzed serum which does not contain exogenous thymidine for the purposes of mimicking the environment in humans/ patients, as well as elucidating the effect of TS inhibition.

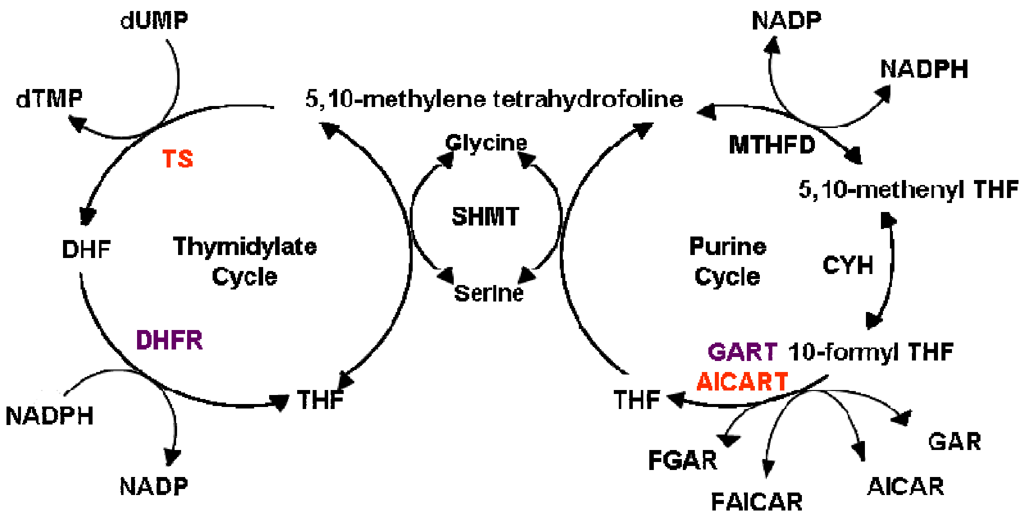
dUMP
dTMP
TS
5,10-methylene tetrahydrofoline
DHF
Thymidylate Cycle
DHFR
NADPH
NADP
THF
Glycine
SHMT
Serine
NADP
NADPH
MTHFD
5,10-methenyl THF
Purine Cycle
CYH
GART
10-formyl THF
AICART
THF
FGAR
FAICAR
AICAR
GAR

Figure 2-1: Mechanisms of pemetrexed toxicity in NSCLC cells. Thymidylate synthase (TS) (red) is the primary target of pemetrexed (red). Inhibition of TS prevents the production of dTMP from dUMP, therefore preventing the natural synthesis of thymidine for use in DNA synthesis. AICART (red) was identified by our collaborators as a secondary target for pemetrexed, inhibiting the generation of formyl-AICAR from AICAR, thus inhibiting purine synthesis. GART and DHFR (purple) have also been identified as secondary targets of pemetrexed, while inhibition of these targets requires significantly high concentrations of the drug to inhibit much lower levels of enzyme molecules per cell, as compared to TS and AICART. All other enzymes involved in thymidylate and purine synthesis (blue) have not been shown to be targeted by pemetrexed.

2.2.5- Clinical relevance of Pemetrexed

In addition to being approved for the treatment of non-squamous NSCLC and malignant pleural mesothelioma, pemetrexed has shown much success in clinic trials. Pemetrexed in combination with other approved drugs compromise over 100 studies currently in clinical trials for various types of cancer; including advanced mammary carcinoma, metastatic colorectal carcinoma, squamous cell carcinoma of the head and neck, advanced urothelial carcinoma, and small and non-small cell lung carcinomas (250). The drug is only issued to adults and its pharmacokinetics do not differ based on gender or race. It is primarily excreted by the kidney and eliminated in the urine due to a low extent of metabolism based according to studies examining patients with normal renal function (245). The side effects seen in patients exposed to the drug can be severe. However, folate, vitamin B12, and sometimes corticosteroid supplements may be given to eliminate the toxic side effects of pemetrexed (227). Pemetrexed has also proven successful when combined with radiation in treatment of pleural mesothelioma and NSCLC (246). Due to the number of promising pemetrexed co-therapy treatment regimens in clinical trials, in addition to its success as a single agent, pemetrexed is a relatively safe and attractive option for development of novel chemotherapeutic strategies for the treatment of multiple types of cancer.

2.3 Sorafenib

2.3.1- Sorafenib for the treatment of multiple cancer cell types

Sorafenib (Bay 43-9006, Nexavar®; a Raf family kinase inhibitor) is a dual-action drug developed for targeting Raf-1, an upstream activator of the MEK/Erk pathway. Sorafenib was later shown to be a promiscuous inhibitor for multiple class III tyrosine kinase receptors (255-263). These growth factor receptor pathways, in addition to the Erk1/2 pathway, are responsible for cellular events including survival, proliferation, migration, differentiation, and angiogenesis. Many, but not all, studies have validated the effects of sorafenib on Raf-1 by illustrating suppression of Erk1/2 activation which correlated with reduced cell proliferation and angiogenesis. These findings were demonstrated in several different cancer cell types including NSCLC, hepatoma, renal carcinoma, melanoma, colon, ovarian, and breast carcinoma cells (264-269). Sorafenib was FDA-approved for advanced renal cell carcinoma (RCC) in 2005 and then for inoperable, advanced hepatocellular carcinoma in 2007 (255). There are numerous studies underway involving this drug as a single agent or in combination with another approved drug to treat soft tissue sarcomas, recurrent glioblastomas, NSCLC, colorectal, pancreatic, thyroid, ovarian, and breast carcinomas (255).

2.3.2- Sorafenib targets

Sorafenib was originally developed as an inhibitor of Raf family kinases, primarily B-Raf and Raf-1, while the drug has a greater affinity for Raf-1. Raf-1 serves as the MAP3K component of MEK/Erk1/2 pathway signaling, which is typically associated with pro-survival events. Down regulation of the Erk1/2 pathway is considered to be one mode of cell killing for the drug, due to Raf-1 inhibition. In several tumor types, baseline Erk1/2 phosphorylation levels were shown to be a good predictive marker of sorafenib sensitivity, where higher basal levels of p-Erk1/2 is indicative of enhanced drug resistance (270). In recent years, sorafenib-induced Raf-1 inhibition was demonstrated to also promote cell death in a MEK/Erk1/2-*independent* manner, possibly due to direct effects on apoptosis-regulating proteins or the combined effects of inhibition of alternative drug targets such as growth factor receptors (271-274). In pancreatic carcinoma cells, sorafenib induced apoptosis occurred in MEK/Erk1/2-dependent and independent manners depending on the specific cell line being tested. Treatment of skin, kidney, and liver carcinoma cells with sorafenib was shown to paradoxically activate ERK1/2 in tumors harboring wild-type BRAF (275-277). These effects were shown to occur using low concentrations of sorafenib and were suggested to occur as a result of inhibition of a single Raf bound within a dimer, enabling transactivation of the adjacent Raf. While the exact mechanism by which sorafenib carries out its toxic effects is based on the specific signaling pathway components present in each cell type, it is generally accepted that drug treatment results in inhibition of eukaryotic initiation factor 4E (eIF-4E) and downregulation of Mcl-1 (252,259,278-279). Previous studies in our laboratory and others have shown that sorafenib is toxic at concentrations well below the maximal achievable dose (~15 μM) using a mechanism involving down-regulation of Mcl-1. This mechanism was shown to occur as a result of ER stress followed by activation of a cytotoxic form of autophagy (280-283).

In addition to Raf family kinase members, sorafenib also targets multiple class III RTKs such as platelet-derived growth factor receptor α/β (PDGFRα/β), vascular endothelial growth factor receptors 1, 2 and 3 (VEGFR1, VEGFR2, VEGFR3), fibroblast growth factor receptor (FGFR), mast/stem cell growth factor receptor (c-Kit/ proto-oncogene c-Kit/ SGFR), and macrophage colony-stimulating factor-related tyrosine kinase 3 (FLT3/ FMS-related tyrosine kinase 3) (250-257) (Figure 2-2). Inhibition of the receptors mentioned above leads to suppression of angiogenesis at the tumor site, decreased cell proliferation, and reduced cell migration. VEGFR signaling is one of the major means by which the cell mediates blood vessel maintenance and new vessel formation. Thus, alterations in VEGF receptors signaling can promote growth of solid tumors which depend on angiogenesis to thrive, whereas untransformed cells remain in a state of vascular endothelial cell maintenance. Sorafenib mediated inhibition of VEGFR2, which is the major VEGFR on the endothelial cell membrane, resulted in increased caspase-3 cleavage leading to apoptosis in RCC. When sorafenib was combined with a murine double minute 2 (mdm2) uncoupling agent (nutlin-3), the drug combination produced a synergistic cell killing characterized by reduced phosphorylation of VEGFR2 and Erk1/2, increased phosphorylation of tumor suppressor p53, and a decrease in levels of anti-apoptotic Bcl2 family members (284).

The PDGFRα/β surface receptors also play an important role in angiogenesis. Inhibition of both PDGFRβ and VEGFR2 in RCC resulted in enhanced suppression of tumor angiogenesis when compared to inhibition of individual receptors (285). Our laboratory has also shown that sorafenib-mediated inhibition of PDGFRβ plays a key role in the ability of this agent to promote autophagy in gastrointestinal tumor cells (286). FLT-3 is a RTK cytokine receptor expressed on the surface of hematopoietic progenitor cells and is important for lymphocyte development (287). Mutations in FLT-3, typically internal tandem duplication (FLT3-ITD) and D835 point mutations, render the enzyme an onco-protein that is found in 20-30% of acute myeloid leukemia (AML) cases and correlates with a poor prognosis (288-289). Lack of response to FLT3-targetting drugs is a common occurrence in AML patients who express the FLT3-ITD and FLT3 D835 mutations. Interestingly, at concentrations much lower than the typical clinical dose, sorafenib more effectively induced cell growth arrest and apoptosis in AML cells expressing the FLT3-ITD and D835 mutants, than those harboring wild-type (WT) FLT3 on the order of 1000 to 3000-fold (290).

Sorafenib has entered into clinical trials for multiple forms of cancer both as a single agent and in combination with other approved chemotherapeutic drugs. For example, sorafenib interacted with epidermal growth factor receptor (EGFR) inhibitors (erlotinib and cetuximab) in a pronounced synergistic fashion to reduce tumor cell migration and significantly delay tumor growth in NSCLC and colorectal carcinoma animal models (291). Sorafenib in combination with the MEK inhibitor U0126 prevented the epithelial mesenchymal transition in hepatocellular carcinoma cells and reduced cellular migration as a result of downregulation of E-cadherin. E-cadherin is a calcium-dependent cell adhesion molecule known to play a role in tumor invasiveness and metastasis (292).

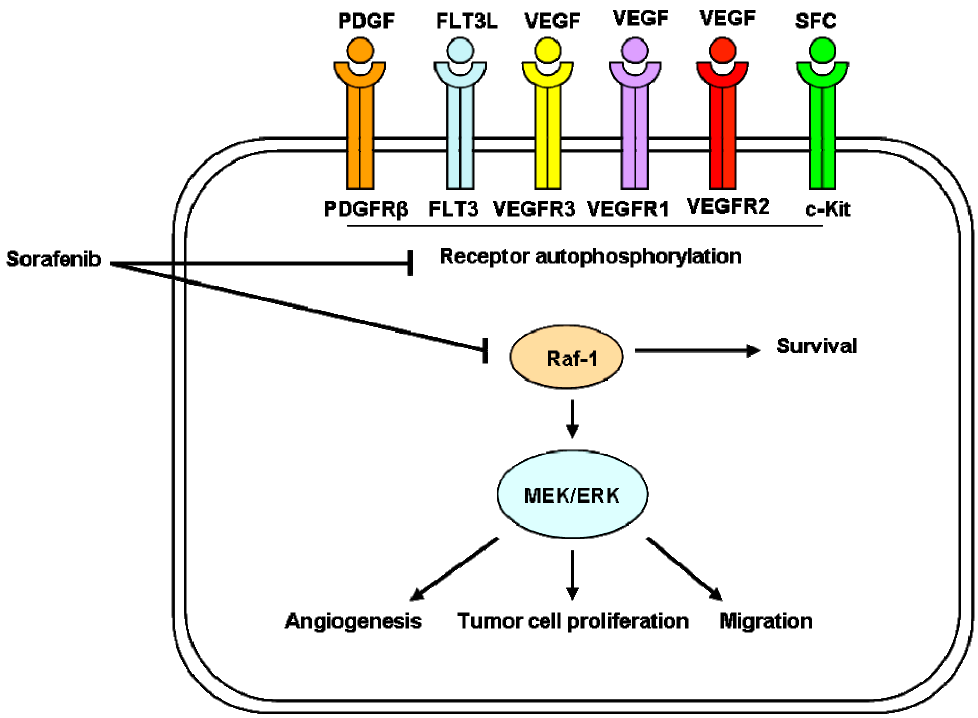
PDGF
FLT3L
VEGF
VEGF
VEGF
SFC
PDGFRβ
FLT3
VEGFR3
VEGFR1
VEGFR2
c-Kit
Sorafenib
Receptor autophosphorylation
Raf-1
Survival
MEK/ERK
Angiogenesis
Tumor cell proliferation
Migration

Figure 2-2: Overview of known sorafenib targets. Sorafenib is a promiscuous tyrosine kinase inhibitor developed to inhibit Raf-1, an upstream activator of the MEK/ERK pathway. Inhibition of Raf-1 in theory should reduce angiogenesis, proliferation, and migration of tumor cells. Sorafenib was also reported to inhibit several members of the class III tyrosine kinase receptor family including VEGFR1, VEGFR2, VEGFR3, PDGFRβ, c-Kit, and FLT3. When inhibited, pathways involved in angiogenesis, proliferation, differentiation, and metastasis are downregulated to promote cell death.

2.3.3- Clinical relevance of Sorafenib

Sorafenib is an orally-administered bi-aryl drug given at an optimal 400 mg b.i.d. in solid refractory tumors. Sorafenib is metabolized primarily in the liver by oxidative metabolism, as well as glucoronidation. Its primary metabolite found circulating in the plasma, pyridine N-oxide, was found to be of potency comparable to that of the parent drug *in vitro* (293). Sorafenib is approved for the treatment of two angiogenesis-driven cancers, renal and hepatic cell carcinoma. Its anti-tumor activity in renal and hepatic cell cancers has been attributed to anti-angiogenic effects caused by inhibition of specific growth factor receptor targets (254-258). In tumor cells, the activities of sorafenib have been strongly correlated with down regulation of anti-apoptotic Bcl-2 family member protein Mcl-1, which was the result of a translational control mediated via induction of ER stress.

2.3.4- The aims of our studies using pemetrexed and sorafenib in combination

Pemetrexed kills a wide variety of cancer cell types. Hypothetically this could occur as a result of AMPK-induced activation of autophagy. Activated AMPK leads to inhibition of mTOR, a major regulator of the autophagic response, which enables formation of the autophagosome. Initially, investigations were performed to determine whether pemetrexed as a single agent promotes a cytotoxic form of autophagy in a variety of cancer cell lines. An autophagic response may occur as a result of inhibition of its secondary target (AICART) causing elevations in ZMP^+ which result in activation of AMPK. This response has already been established in a pemetrexed dose-dependent manner in NSCLC and we wished to determine if a similar response would occur in other tumor cell types. Those cell models sensitive to pemetrexed were assessed to determine whether sorafenib could enhance pemetrexed-induced cytotoxic autophagy (Chapter 4 Results). Both Her2+ and triple negative breast cancer cell phenotypes were tested. Additional studies were conducted to elucidate the signaling mechanisms by which these drugs interact to promote cytotoxic autophagy in our tumor models. Earlier studies performed in our laboratory identified Src as a key mediator of cell death in HCC resultant of sorafenib-induced PDGFRβ down regulation. As a result, studies were performed to determine whether Src was involved in regulation of Erk1/2 and cell lethality in drug combination-treated breast cancer cells. In addition, an evaluation of the role of protein phosphatases in this response was assessed, since these enzymes are known to be important for regulating the Erk1/2 pathway. Alterations seen in protein phosphatase activity may indicate the validity of further investigation into the effects of pemetrexed/ sorafenib treatment on the *de novo* ceramide synthesis pathway, which has been shown to regulate these proteins and has been implicated in the development and progression of multiple cancer cell types (294). The ultimate goal of all combination therapy studies is to pre-clinically validate the pemetrexed/ sorafenib combination therapy in treatment of multiple tumor types.

Chapter 3: Materials and Methods

3.1- Materials

3.1.1- Cell Culture: Invitrogen reagents: RPMI 1640, DMEM, Penicillin-streptomycin, PBS, 0.25% Trypsin-EDTA, Opti-MEM, Lipofectamine 2000. Dialyzed fetal bovine serum (Thermo Scientific- Hyclone dialyzed fetal bovine serum), fetal bovine serum (ThermoScientific-HyClone Fetal Bovine Serum), culture flasks and plates (Corning), 4-chambered glass microscope slides (Lab-TekII, 154526), Cryo-vials (Corning).

3.1.2- Cancer cell lines: Breast- 4t1 (ATCC CRL-2539), BT474 (ATCC HTB-20), SKBR3 (ATCC HTB-30), MCF7 (Nephew Laboratory), MCF7F (Nephew Laboratory), HCC1187 (Nephew Laboratory), HCC1937 (Nephew Laboratory), BT549 (ATCC). NSCLC- H460 (Moran Laboratory). Liver- HuH7 (Japanese Collection of Research Bioresources, JCRB-0403). Lymphoma- CEM (Moran Laboratory).

3.1.3- siRNA: siRNA constructs were purchased from the following venders as pre-designed double-stranded oligomers and resuspended in sterile water at a concentration of 20 µg/µl (20 pmol): si-Beclin1 (Qiagen), si-mTOR (Qiagen), si-p70 (Qiagen), si-LASS6 (Qiagen). A set of 4 pre-designed sequences that were functionally validated by the manufacturer, referred to as a FlexiTube GeneSolution, was used for each protein to be knocked down. The siRNA construct details are listed in Table 1, as detailed by the manufacturers website (www.qiagen.com).

Table 1: siRNA constructs. A Qiagen FlexiTube GeneSolution, containing 4 pre-designed and functionally validated siRNA sequences, was used for siRNA knockdown experiments. The specific sequence details for each are listed for each targeted protein as defined by the manufacturer.

	Gene ID	Qiagen- FlexiTube GeneSolution catalog #	FlexiTube siRNA ID
si-Beclin1	BECN1	GS8678	Hs_BECN1_3 (SI00055587)
			Hs_BECN1_4 (SI00055594)
			Hs_BECN1_1 (SI00055573)
			Hs_BECN1_2 (SI00055580)
si-mTOR	MTOR	GS2475	Hs_FRAP1_5 (SI00300244)
			Hs_FRAP1_6 (SI02662009)
			Hs_FRAP1_4 (SI00070462)
			Hs_FRAP1_7 (SI03023587)
si-p70α subunit	RPS6KB1	GS6198	Hs_RPS6KB1_5 (SI00301721)
			Hs_RPS6KB1_2 (SI00048594)
			Hs_RPS6KB1_4 (SI00048608)
			Hs_RPS6KB1_3 (SI00048601)
si-LASS6	CERS6	GS253782	Hs_LASS6_5 (SI02758245)
			Hs_LASS6_2 (SI00468335)
			Hs_LASS6_3 (SI00468342)
			Hs_LASS6_4 (SI00468349)

3.1.4- DNA constructs: Vector control plasmids- pEGFP-C3 parent vector (Clontech), pcDNA3.1 parent vector (Invitrogen), pBABE-puro Retroviral vector (Cell Biolabs). Cloned plasmid constructs: pEGFP-LC3 (Spiegel Laboratory), dncaspase-9 (Vector Biolabs), Bcl-XL (Vector Biolabs), pcDNA3 c-FLIP-s (Wafik Eldeiry Laboratory), camTOR (Addgene), cap70 (Addgene), caAkt (Addgene), dnAkt (Addgene), dncaspase-9 (Addgene), dnSrc (Addgene), dnMEK1 (Addgene), and I2PP2A (Addgene).

3.1.5- DNA propogation in bacteria: DNA propogation cell strains DH5α and One Shot TOP10 (Invitrogen), Miller Luria Bertani Broth and Miller Luria Bertani broth with Agar (Difco), SOC media (Invitrogen), ampicillin and kanamycin (Sigma-Aldrich), DNA plasmid purification kit (Qiagen), 1 Kb Plus DNA standard molecular weight marker (Invitrogen), 6X Sample Loading Dye (Promega), ethidium bromide (Sigma), agarose (Fisher Scientific), agarose gel running apparatus (Hoefer, submarine agarose gel unit).

3.1.6- Chemotherapeutic drugs: Pemetrexed/ Altima® was purchased from LC laboratories. Sorafenib/ Nexavar® was purchased from Sellechem (Bay-43-9006).

3.1.7- Sodium dodecyl sulfate- polyacrylamide gel electrophoresis (SDS-PAGE): The following items were purchased from Biorad: Running apparatus and Transfer apparatus (Mini PROTEAN Tetracell 1703810) and all necessary components, protein molecular weight marker (Dual Color Precision Plus Protein Standards– 161-0374), 40% Acrylamide/Bis-acrylamide (29:1) (16100146), Tween 20 (170-6531). Fisher Scientific: 0.22µM nitrocellulose membrane (EP2HY00010), Immunogilin FL PVDF membrane (IPFL00010), 2-mercaptoethanol (03446I), 20% sodium docecyl sulfate (BP1311), TEMED (BP150). LICOR: Blocking Solution (927-40000).

3.1.8- Western blotting/ Immunohistochemistry

The primary antibodies used in these studies were purchased from the following venders. Cell Signaling: mTOR (cs2972), p-mTOR S2448 (cs2971), p70 alpha regulatory subunit (cs2041), p-PDGFRβ Y1009 (cs3124), FGFRI (cs3472), ATG5 (cs2630), Mcl-1 (cs4572), Bcl-XL (cs2762), Src (cs2109), p-Src Y416 (cs2101), cleaved caspase-3 (cs9664). Santa Cruz Biotechnologies: GAPDH (sc-32233), p-p70 S421/T424 (sc-7984R), LASS6 (sc-100554), Beclin1 (sc-11427), ERK (sc-135900), p-ERK T202/Y204 (sc-7383), Akt 1/2/3 (sc-8312R), p-Akt S473 (sc-7985R), PDGFRβ (sc-339). R&D Systems: p-p70 T389 (AF8963). Novus Biologicals: LC3I/II (NB100-2331) and Ki67 (NB500-170).

Secondary antibodies were purchased conjugated to fluorophores for detection by fluorescence scanning, these include: goat α-mouse IgG- Alexa Fluor 680 (Invitrogen), goat α-rabbit IgG-IRDye800 (Rockland).

3.1.9- Fluorescence-based techniques: LysoTracker® Red DND-99 (Invitrogen- 7528), Annexin V-PI (Abcam- ab14085), Tunnel Apoptosis Detection Kit (Upstate- 17-141), H&E kit (Ricca Chemical Company- 3530-32)

3.1.10- *In vivo* studies: All animal protocols were conducted under approval of the VCU IACUC. Athymic nude female mice were obtained through the Virginia Commonwealth University's Division of Animal Resources. Tumors harvested at the end point were frozen in Optimal Cutting Temperature Compound (Tissue-Tek 4583). Tissue sectioning was performed using the Leica Cryostat. Antibodies and fluorescent dye stains used in these studies are listed in previous materials sections. Pemetrexed was reconstituted in sterile PBS (Invitrogen) and sorafenib was reconstituted in Cremophore EL (Sigma)

3.1.11- General Supplies: Twenty µM filter units (Nalgene), syrine and vacuum filters (Millipore), hemacytometer (Hausser Scientific, 0.1 mM deep)

Chemicals: Fisher- Dimethyl sulfoxide (BP231), Tris Base (BP152), potassium chloride (BP366), sodium chloride (S5271), Triton X-100 (BP151), 5N sodium hydroxide solutioin (S5256), hydrogen chloride (AKH212), chloroform (BP1145), sodium dodecyl sulfate (BP160), N-propanol (A451), methanol (A411), N-butanol (BP505). Sigma Aldrich- ammonium persulfate

(248614), acetone (179973). American Bioanalytical- glycine (AB00730). Pharmco-AAPER- 200 proof ethanol (111HPLC20S). JT Baker Chemical Company- glycerol (3-2136)

Reagents: Myriocin (Fisher), 3-methyladenine (Sigma), 0.4% Trypan Blue Dye Solution (MP Biomedicals), Protease Inhibitor Cocktail (Roche Applied Science), Amphotericin B (Quality Biologicals Inc.), bovine serum albumin (Fisher BP1600).

3.1.12- Instrumentation: LICOR Odyssey V3.0 Infrared Imager**,** Perkin Elmer Victor3 1420 Multilabel Reader**,** Zeiss Axiovent fluorescent microscope**,** Accuscope light microscope, Becton Dickinson FACScan flow cytometer, Lipid quantification: two tandem triple quadrupole/linear ion trap mass spectrometers (Applied Biosystems 4000 Q TRAP and an Applied Biosystems 3200 Q TRAP), Leica Cryostat tissue sectioner, and a Denver Instrument UB10 UltraBasic pH meter

3.2- Methodology

3.2.1- Cell Culture: All breast carcinoma cell lines and H460 NCSLC cells were cultured at 37 ^{o}C (5% (v/v CO_2) *in vitro* using RPMI supplemented with dialyzed 5% (v/v) fetal bovine serum (FBS), 10% (v/v) non-essential amino acids, and 1% penicillin/ streptomycin. HuH7 hepatoma cells were cultured at 37 ^{o}C (5% (v/v CO_2) *in vitro* using DMEM supplemented with dialyzed 5% (v/v) FBS, 10% (v/v) non-essential amino acids, and 1% penicillin/ streptomycin. Cells growing in non-dialyzed fetal bovine serum containing thymidine were gradually weaned into dialyzed serum lacking thymidine over 2 weeks, and used for experimental analyses. Once thawed, cells were used for 3 weeks before discarding.

3.2.2- DNA propogation in bacteria: Plasmids (0.2 µg) were transformed into DH5α or TOP10 cells using the manufacturer's protocol. Cells were plated on LB-Agar plates containing the appropriate selection reagent (Ampicillin at 100 µg/mL or Kanamycin at 30 µg/mL) and colonies were grown overnight at 37ºC. Individual colonies were inoculated into LB cultures containing the appropriate selection reagent overnight at 37ºC. The following day, cells were isolated by centrifugation and plasmid DNA was isolated from each using a plasmid DNA purification kit as suggested by the manufacturer. Plasmid DNA was de-salted/ further purified by adding 3 times the volume of 100% ethanol and 0.1 times the volume of 3M sodium acetate pH 5.2. DNA was isolated by centrifugation and washed with 70% cold ethanol. DNA pellets were allowed to dry at room temperature, and then resuspended in approximately 100 µL sterile TE Buffer supplied by the manufacturer. DNA concentrations were determined by UV spectrometry at 260 nm and 280 nm wavelengths. The 260 nm (A260) value was used in the following equation specific for double-stranded DNA (unknown µg/mL = 50µg/mL / 1.0 A260) to provide a concentration in the unit of ng/µL. DNA stocks were diluted to 1µg/µL for use in DNA transfection experiments. The 260/280 ratio was between 1.8 - 2.0 for all DNA preparations demonstrating acceptable DNA: protein ratios in terms of DNA purity.

3.2.3- Agarose gel electrophoresis: DNA preparations were evaluated by agarose gel electrophoresis to examine the quality of purified DNA. 0.8% agarose gels were prepared containing 0.015% ethidium bromide. 1 µg of each DNA sample was diluted in 6X DNA sample buffer and sterile, deionized water. Samples, alongside a DNA standard molecular weight marker, were run at 100 volts for 1 hr then visualized on a ChemiDoc Molecular imager using the ethidium bromide filter setting. Images were examined for levels of supercoiled DNA versus nicked DNA as judged by the DNA standard molecular weight marker and determined to be of reasonable quality for transfection experiments.

3.2.4- DNA transfection/ protein overexpression: Cells were plated at 2 X 10^5 in 60 mm dishes or 2 x 10^4 cells per well of a 12-well plate or microscopy slide and cultured for 24 hr prior to transfection. Cells were transfected with 1µg/mL DNA, pertaining to the volume of media used for the respective dish/ well, using Lipofectamine 2000 following the manufacturer's suggested protocol. For preparation of cell lysates, cells were incubated for 48 hr after transfection; then treated with vehicle, individual drugs, or pemetrexed/sorafenib prior to harvesting whole cell lysate. For all other assays, cells were incubated for 36 hr prior to treatment with drugs.

3.2.5- siRNA transfection/ protein knockdown: Cells were plated and cultured similarly to that for plasmid transfections. For transfection, 60 pmol of the annealed double-stranded siRNA, targeting our gene of interest or the negative control (a "scrambled" sequence with no significant homology to any known gene sequences from mouse, rat or human cell lines) was transfected into each 60 mm dish using Lipofectamine 2000 as per the manufacturer's suggested protocol. siRNA (scrambled or experimental) was diluted in Opti-MEM at 100 pmol/ 50 µl reaction volume. Three µl Lipofectamine 2000 was diluted in Opti-MEM at 1 µl/ 50 µl reaction. Prior to introduction of siRNA, the diluted lipofectamine 2000 was allowed to equilibrate then gently mixed with the diluted siRNA and incubated at room temperature for 20 min to allow lipid-siRNA complex formation. The solution was then added dropwise to the corresponding dish and tilted gently to mix. For preparation of cell lysates, cells were incubated for 48 hr after transfection; then treated with vehicle, individual drugs, or pemetrexed/sorafenib prior to harvesting whole cell lysate. For all other assays, cells were incubated for 36 hr prior to treatment with drugs.

3.2.6- Validation of dialyzed fetal bovine serum: Dialyzed serum was purchased from Thermo Scientific (Hyclone dialyzed fetal bovine serum, lot# ARG26916) and compared against the previous lot from Gemini Bioproducts (lot# A655110). A comparison was made using CEM lymphoma cells grown in suspension with 5% dialyzed FBS from either the new lot or the previous lot. Cells were plated in 10 cm dishes at 10^5 cells/ mL and the number of cells/ mL was determined every 2 days for 6 days by counting the number of cells per dish using a Beckman Coulter cell counter. Cells were collected from each condition by centrifugation at 1000 rotation per minute (rpm.), and then resuspended in 1 ml Diluent II Solution. Each cell sample was counted to obtain the number of cells/ mL and plotted in Sigma Plot 11.2 to obtain growth curves for the old lot versus the new lot of dialyzed serum to verify no significant growth changes between the lots of serum.

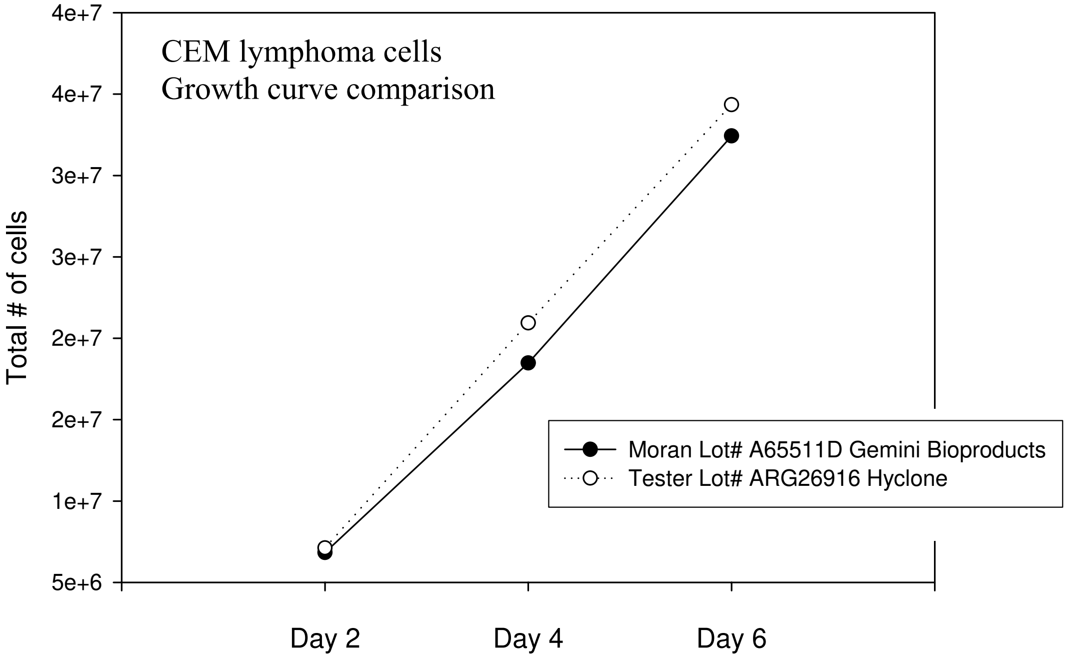

Figure 3-1: Validation of dialyzed fetal bovine serum in CEM lymphoma cells. CEM cells were plated at 10^6 cells per dish in triplicate and grown for 6 days. Every 2 days the cell concentration was determined for each dialyzed FBS lot using a Coulter counter machine. We purchased a Thermo Scientific Hyclone dialyzed FBS lot, which we tested against the previous lot used for these experiments. No significant changes in growth rates were noted between the two lots.

3.2.7- SDS-PAGE: Cells were plated at 5 x 10^5 cells / cm^2 and treated with drugs at the indicated concentrations and after the indicated time of treatment, lysed in 2X protein sample buffer for whole cell lysates, then boiled for 10 min. The boiled samples were loaded (10-100 µg/lane, based on the gel size), alongside a protein standard molecular weight marker, onto 8-14% SDS-PAGE gels and electrophoresis was run for 1 hr at 150 volts. Samples were electrophoretically transferred onto 0.22 µm nitrocellulose or PVDF membrane for 2 hr at 250 volts. Membranes were blocked with LICOR Odyssey Blocking Buffer for 1 hr at room temperature or 4° C overnight.

SDS-PAGE Buffer Recipes:

5X Running Buffer	10X Transfer Buffer	2x Protein Loading Buffer
30 g Tris Base	30.3 g Tris Base	1M Tris-HCl pH 6.8
144 g Glycine	144 g Glycine	20 mL glycerol
50 mL 20% SDS	50 mL 20% SDS	20 mL 20% SDS
deionized water to 2L	deionized water to 1L	2 mL BME
Filter sterilize. Store @ 4ºC.	0.05 g bromophenol blue	deionized water to 10 mL

SDS-PAGE gel components:

	5% Stacking gel	10% Resolving gel
40% Acrylamide:Bis-acrylamide (29:1)	12.5 mL	1.25 mL
1.5M Tris-HCl pH 8.8	12.5 mL	0
0.5M Tris-HCl pH 6.8	0	2.5 mL
10% APS	500 μL	100 μL
TEMED	20 μL	10 μL
Deionized water	up to 50 mL	up to 10 mL

Resolving gel percentages were adjusted by proportionately manipulating the volumes of acrylamide and deionized water.

3.2.8- Western Blotting/ Immunohistochemistry: Membranes containing blocked protein samples were incubated in primary antibody (0.5 – 1 μg/mL) overnight at 4ºC, washed, and then incubated in the corresponding secondary antibody (0.15 – 0.3 μg/mL) for 2 hr prior to analysis. All secondary antibodies used in these studies were conjugated to fluorophores (Alexa Fluor 680 or IRDye 800) for examination using the LICOR Odyssey Infrared Imager. For presentation, immunoblots were digitally assessed using the provided Odyssey Imager software (the data sets presented are the –Fold increase +/- SEM (n = 3) in expression of the indicated protein compared to GAPDH loading control; for phospho-proteins the –Fold increase +/- SEM (at least n = 3) is normalized to the total protein level of the indicated kinase or substrate). Errors are not numerically shown due to space restrictions in the figure panels; any indicated significant differences between the expression / phosphorylation levels of proteins are indicated by an asterisk or other annotation and have a $p < 0.05$. Images have their color removed and were transferred to Powerpoint for formatting.

3.2.9- Normalization of protein levels by densitometry: All western blotting samples shown in the results chapters were harvested in 2X sample loading buffer containing bromophenol blue. Sample volumes were adjusted according to the number of cells present prior to lysis. The corresponding sample volumes were subject to SDS-PAGE and examined using the LICOR Odyssey Infrared Imager. Each blot was evaluated for glyceraldehydes-3-phosphate dehydrogenase (GAPDH) expression and the band intensity for each sample was determined using the LICOR Odyssey V3.0 software. The sample band intensity for each protein of interest was also determined on the instrument, then expression values were calculated based on normalization to the determined GAPDH band densities. The expression values given for each western blot are all based on values normalized to that of each sample's GAPDH expression value.

3.2.10- Cell Death Analysis: For short term cell death assays and immunoblotting studies, cells were plated at a density of 3×10^3 per cm^2 ($\sim 2 \times 10^5$ cells per well of a 12 well plate) and 24h after plating treated with various drugs, as indicated. *In vitro* pemetrexed and sorafenib treatments were from 1mM and 10 mM stock solutions, respectively, and the maximal concentration of vehicle (DMSO) in media was 0.02% (v/v). Cells were treated with vehicle or pemetrexed / sorafenib for times indicated within the figure legends. For cell viability assays, cells were isolated at the indicated times, and either subjected to a trypan blue exclusion assay by counting 10 μL of each sample on a hemacytometer using the light microscope or fixed to slides and stained using a commercially available Diff Quick Geimsa assay kit. Alternatively, the

Annexin V/ propidium iodide assay was utilized to determine cell viability as per the manufacturer's instructions using a Becton Dickinson FACScan flow cytometer. Samples were evaluated in triplicate and plotted as the average means of cell death for each sample condition using Sigma Plot 11.2 software. Images were transferred to Powerpoint for formatting.

3.2.11- Quantification of GFP-LC3 incorporation into early autophagic vesicles: Cells were transfected with a plasmid to express an LC3-GFP fusion protein, as well as plasmids and/or siRNA constructs as indicated, then cultured for 36 hrs. Cell cultures were then treated with drugs for the indicated times. Using the FITC filter setting on the Zeiss Axiovert 200 fluorescent microscope at 40X magnification, GFP-LC3+ vesicle formation was determined by counting the number of GFP-LC3+ vesicles present in an individual cell for a minimum of 60 unique cells per sample condition amongst a minimum of 10 fields of view within each sample. These values were plotted in SigmaPlot 11.2, and then transferred to Powerpoint for figure formatting.

3.2.12- LysoTracker Red staining for visualization of acidification of late endosomes: Cells were plated in the wells of 4 chambered microscopy slides at 2 x 10^4 cells per well, then cultured for 24 hr. Cells were either exposed to drugs or transfected with DNA and/or siRNA at 1 µg or 20 pmol per well, respectively, using 1µl of Lipofectamine 2000 per reaction. Cells were cultured in antibiotic-free media for 36 hr prior to treatment with vehicle or drugs for the indicated times. LysoTracker Red dye was diluted in fresh, pre-warmed 37ºC medium at a final concentration of 15 nM. Culture media was aspirated from each sample, and the diluted LysoTracker Red stain was added to each cell sample and allowed to incubate at 37ºC for 30 min. Post-staining, the dye-containing media was aspirated, cell samples were gently washed 2 times with PBS, then finally resuspended in 250µl cold PBS per well. Cell samples were analyzed using the rhodamine filter setting on a Zeiss Axiovert 200 fluorescent microscope at 40X magnification using an exposure time of 3.355 seconds (brightness). Twenty representative images were taken of each sample and samples were performed in triplicate. A representative image for each condition and time point was selected for figure illustration generated using Powerpoint.

3.2.13- Analysis of PP2A activity: Cells were plated at 2 x 10^5 cells in 60 mM dishes in triplicate and cultured for 24 hr. Cells were then either treated with vehicle or drugs for 12 hrs or transfected with control siRNA or siRNA against LASS6 for 36 hr, and then treated with vehicle or drugs. After 12 hr drug treatments, cells were washed twice with cold low phosphate lysis buffer to remove residual phosphatases present in the culture media, and then harvested in 500 µl of fresh low phosphate lysis buffer. Samples were prepared according to the PP2A Phosphatase Activity Assay Kit protocol using filter-sterilized buffers prepared as described in the protocol. Three separate protein amounts (60 µg, 120µg, 180 µg) for each condition were immunoprecipitated with a monoclonal antibody against PP2A coupled to sepharose beads provided in the kit. After immunoprecipitation, PP2A Antibody-couple sepharose beads were washed and bound protein cleaved using the manufacturer provided reagent at equal volumes for each sample. The initial protein loading amounts varied slightly between each sample, however densitometry values obtained for the loading control were used to normalize quantified values. Samples were then transferred to a 96-well plate for the remainder of the protocol. After incubation with the detection substrate, samples were evaluated using a Malachite Green protocol for determination of Absorbance at 595nm λ using a Victor 3 platereader. Triplicate values obtained for each sample type, and 3 variable protein loading amounts, were averaged and plotted in SigmaPlot 11.2 as fold-change in PP2A Activity relative to that of the si-control transfected vehicle-treated condition. The SigmaPlot generated graph was then transferred to Powerpoint for figure formatting.

3.2.14- Quantification of ceramide and dihydroceramide levels: Cells were plated at 2 x 10^5 cells in 60 mm dishes in duplicate every day for 3 days for a total of 6 repeats per condition and cultured for 24 hr prior to transfection. Cells were transfected with siRNA against LASS6 (Qiagen) using Lipofectamine 2000 as described above, cultured for 36 hr, then treated with vehicle or drug combination for 24 hr. Cells were then harvested in 220 µl of cold PBS and 20 µl taken for lysis and protein determination using the Bradford Assay (BioRad). Protein levels were normalized based on total protein levels for each sample. Lysates were run on a denaturing SDS-PAGE gel to confirm normalized protein levels by evaluating the GAPDH densitometry values obtained using the LICOR Odyssey V3.0 software. The remaining 200 µL cell samples were transferred to glass screw cap tubes containing 500 µl methanol and 250 µL chloroform and stored at -80ºC until all sample replicates were obtained. A solution containing the internal standards was added to each cell sample. Cell samples were sonicated and then incubated in a 48ºC water bath with a shaker overnight (approximately 16 hr) to ensure complete digestion of cellular components. The following day, samples were cooled to 37ºC in a water bath and 75 µL of 1 M potassium hydroxide (in methanol) was added to each sample for further sonification. The samples were allowed to shake in a 37ºC water bath for an additional 2 hr after potassium hydroxide addition. Twelve µL of glacial acetic acid was added to each sample and samples were sonificated again. Lipids were harvested by centrifugation at 4000 rpm for 10 min. The supernatant was transferred to a clean glass screw cap tube using a Pasteur pipette and the supernatant was evaporated to dryness using a speed vacuum. Once completely dry, the lipids were reconstituted in 300 µL reconstitution solvent [60:40 (60:40 methanol: deionized water): methanol]. Reconstituted samples were sonificated, then centrifuged at 14000 rpm for 5 min. 200 µL of each sample was transferred to injection vials for sample analysis by mass spectrometry. The peaks obtained in each sample were identified based on comparison to the internal standard peaks. Data for each sample replicate (n = 6) was quantified using the instruments software program and plotted ($p < 0.05$, ± SEM) for each sample condition using Sigma Plot 11.2. Data figures were transferred to Powerpoint for formatting.

3.2.15- *In vivo* studies: To generate an orthotopic model of breast cancer, 10^5 cells were injected into the 3rd mammary fat pad of athymic nude female mice. Tumors were allowed to grow to approximately 50-100 mm^3. Mice were batched according to tumor sizes. Animals were treated every day for 5 days with vehicle, pemetrexed (50 mg/kg), sorafenib (25 mg/kg), or a combination of the drugs. The mice were rested for 2 days before a second round of 5 day treatment. During the experiment, mouse tumors were measured every 3 days. Mice reaching tumor volumes of 1700 mm^3 during the experiment were humanely sacrificed. Comparison of the effects of each treatment group was performed using ANOVA and the Student's t test. Differences with a *p*-value of <0.05 were considered statistically significant. Experiments were shown as a mean of multiple individual end points (± SEM). Representative tumors from each group (n= 3-6 mice) were excised and frozen in optimal cutting temperature compound for immunohistochemial analysis. From these mice, normal tissues (brain, kidney, lung, heart, spleen, liver) were also taken for analysis of toxicity in normal tissue cells by immunohistochemical analysis. Cryostat sectioned tissue (10 µm sections) were fixed to slides using cold acetone, rinsed with PBS, and proteins blocked on the fixed slides (10% rat sera, 1% bovine serum albumin, 0.1% Triton X, 0.01% Tween 20). Tissue sections were incubated in primary antibody overnight at 4ºC, washed, and then incubated in secondary antibody for 2 hr at room temperature. For experiments requiring a one-step dye staining procedure, tissue sections were fixed to the slides and incubated in the corresponding dye stain for 2 hr, then analyzed by fluorescence microscopy using the Axiovert Zeiss Fluorescent microscope. Representative images for each treatment group were selected.

Chapter 4: Sorafenib enhances Pemetrexed cytotoxicity through an autophagy-dependent mechanism in cancer cells

4.1 Pemetrexed treatment causes a dose-dependent activation of autophagy and cell death in multiple cancer cell types

NSCLC cells were grown in media containing thymidine-less serum to mimic the growth conditions within a patient. Increasing concentrations of clinically relevant doses of pemetrexed were given to H460 cells for various time points and autophagy was evaluated using a GFP-tagged form of LC3 to determine the number of autophagic vesicle formed per cell *in vitro*. Incorporation of GFP-LC3 into the autophagosome can be visualized by fluorescence microscopy and the average number of GFP-LC3+ vesicles per cell determined. Western blot analysis of cell lysates was performed after treatment of cells with vehicle or pemetrexed for 12 hr.

In drug-treated samples, western blot analysis indicated that the levels of LC3II (lipidated-LC3) were significantly higher than that of the vehicle-treated controls, indicating an enhancement of autophagic vesicle formation (Figure 4-1A). In agreement with this data, the number of GFP-LC3+ vesicles per cell increased in a pemetrexed dose-dependent manner at 6 and 12 hr time points in H460 cells (Figure 4-1B). These results demonstrated that pemetrexed was able to induce autophagy in H460 NSCLC cells. To determine whether induction of autophagy was a protective or cytotoxic response in these cells, cell viability was evaluated using a trypan blue exclusion assay after 12 hr treatment with increasing concentrations of pemetrexed. H460 cell viability decreased in a pemetrexed concentration-dependent manner (Figure 4-1C). Pre-treatment of cells with 3-MA, a Vsp34 PI3K class III inhibitor known to inhibit induction of autophagy, prior to exposure with a range of pemetrexed concentrations, resulted in an increase in cell viability as compared to cells treated only with pemetrexed at comparable dosages (Figure 4-1C). Cell viability was also determined by Annexin V-PI staining for H460 cells transfected with control siRNA or siRNA specifically targeting the Beclin1 gene. Results from these studies indicated that pemetrexed treatment elicited a dose-dependent decrease in cell viability at 24 hr, which was significantly diminished upon knockdown of Beclin1 (Figure 4-1D).

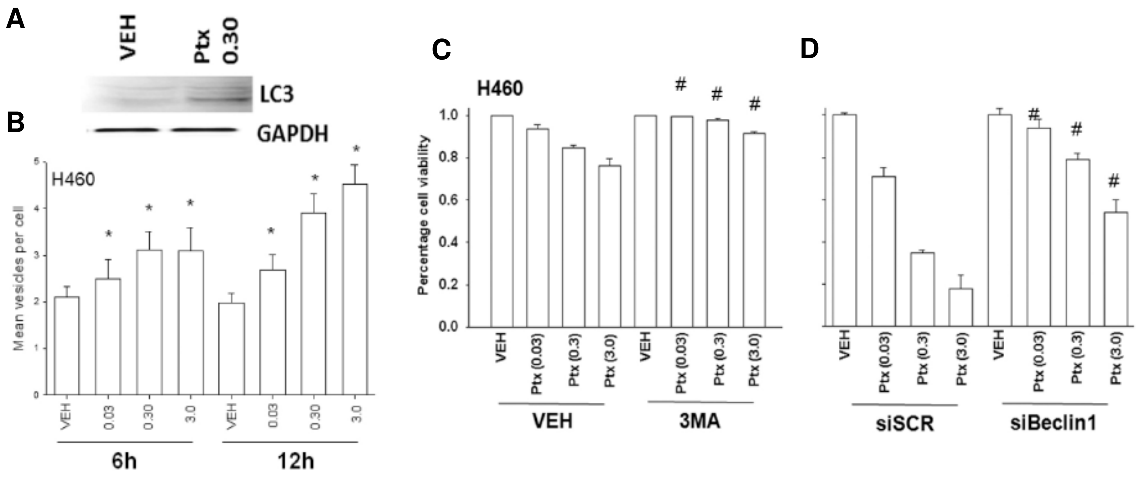

Figure 4-1: Pemetrexed induces autophagy and cell death in H460 NSCLC cells that are suppressed by treatment with 3-MA or knockdown of Beclin1. Cells were cultured in dialyzed media not containing exogenous thymidine, then treated vehicle (PBS) or pemetrexed for the indicated times. (A) 6 hr and (B) 12 hr treatment of H460 cells with pemetrexed causes an increase in LC3II protein levels as judged by western blot analysis. H460 cells were transfected with a plasmid to express control GFP or GFP-LC3, then treated with vehicle or increasing concentrations of pemetrexed for the indicated times. The number of GFP-LC3+ vesicles per cell at 6 and 12 hr time points was analyzed using fluorescence microscopy (*$p<0.05$ greater than vehicle control). (C) 3-MA (5mM, 30 min prior to drug treatment) protects H460 cells from the cytotoxic effects of pemetrexed at 24hr drug treatment. Cell viability was determined by Annexin V-PI staining. (# $p<0.05$ greater than corresponding value in vehicle treated cells) (D) Knockdown of Beclin1 protects H460 cells from the cytotoxic effects of pemetrexed at 24 hr drug treatment. Cell viability was determined by Annexin V-PI staining (# $p<0.05$ greater than corresponding value in vehicle treated cells).

Studies were performed to determine whether pemetrexed treatment causes a similar dose response relationship in other tumor cell types. In spontaneous mouse mammary (4T1), human mammary (BT474), and human hepatic (HuH7) carcinoma cell lines pemetrexed treatment was shown to induce a dose-dependent increase in autophagic vesicle formation as judged by the number of GFP-LC3+ vesicles per cell (Figure 4-2A-C).

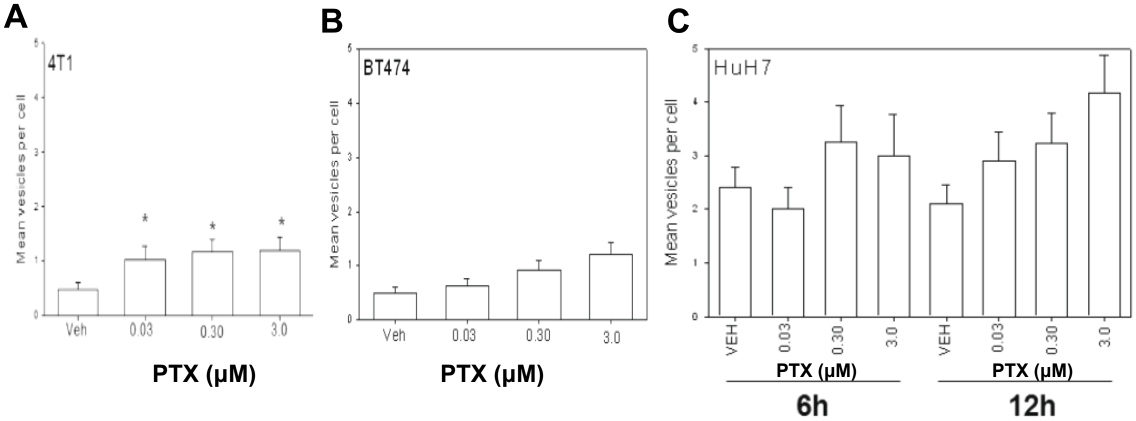

Figure 4-2: Treatment with pemetrexed causes an increase in autophagic vesicle formation in mammary and hepatic carcinoma cells. Cells were plated in dialyzed media, transfected with GFP-LC3 expressing plasmid, then cultured for 36 hr prior to drug treatment. Cells were treated with vehicle (PBS) or varying concentrations of pemetrexed for 12 hr, then analyzed for GFP-LC3+ vesicle formation by fluorescence microscopy. Samples were performed in triplicate and 40 random cells selected from each sample for determining the average number of autophagic vesicles per cell. (A) Pemetrexed causes a dose-dependent increase in autophagic vesicle formation at 12 hr in 4T1 murine breast carcinoma cells (*$p<0.05$ greater than vehicle control) and (B) BT474 mammalian breast carcinoma cells. (C) Pemetrexed causes an increase in autophagic vesicle formation at 6 hr and a dose-dependent response at 12 hr drug treatment in HuH7 hepatic carcinoma cells.

Knockdown of Beclin1 or pre-treatment with 3-MA in these cell lines resulted in a significant reduction in the cytotoxic effects of the pemetrexed, even in cells treated with the highest dose of pemetrexed used in these studies. (Figure 4-3). These findings were comparable to that of H460 NSCLC cells, suggesting that these tumor types also rely on an autophagy-dependent mechanism for pemetrexed-induced cell death. Data for other tumor cell types (glioblastoma, pancreatic and bladder carcinomas) treated with similar concentrations of pemetrexed also demonstrated a dose-dependent reduction in cell viability (data not shown).

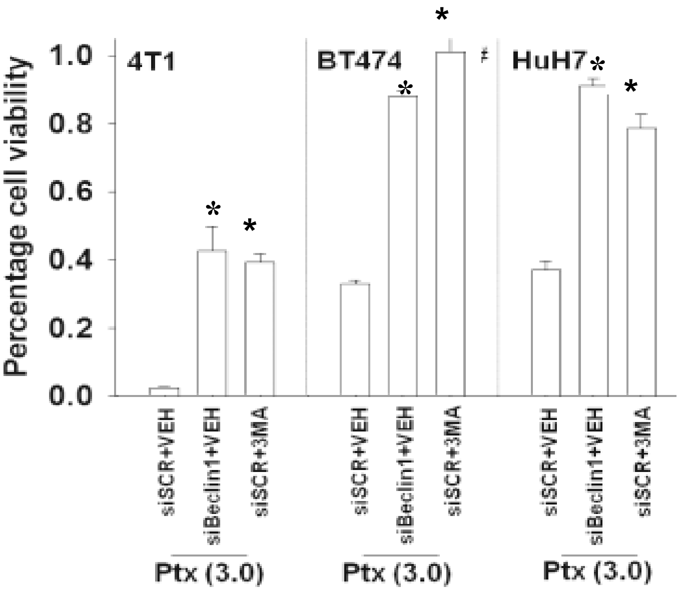

Figure 4-3: Pemetrexed lethality is autophagy-dependent in multiple tumor types. Cells were plated in media containing dialyzed serum and transfected with control siRNA or siRNA targeting Beclin1, then cultured for 36 hr prior to drug treatment. Cell samples were treated with PTX (3μM) for 24 hr then evaluated for cell viability by Annexin V-PI staining. Treatment with pemetrexed resulted in a decrease in cell viability; which is prevented (* $p < 0.05$) by knockdown of Beclin1 or treatment with 3-MA in 4T1, BT474, and HUH7 cells.

4.2 Sorafenib interacts with pemetrexed to enhance pemetrexed toxicity and induce autophagy in multiple tumor types

Sorafenib, a multi-kinase inhibitor of class III RTKs (PDGFRβ, VEGFRs, cKit, FLT3), has been shown to promote both cytoprotective and cytotoxic forms of autophagy in several tumor cell types (295-297). In H460 NSCLC cells, varying concentrations of pemetrexed and sorafenib interacted in a greater than additive fashion to enhance cell death (Figure 4-4). This response was noted using concentrations of pemetrexed and sorafenib below each drugs clinically relevant dose.

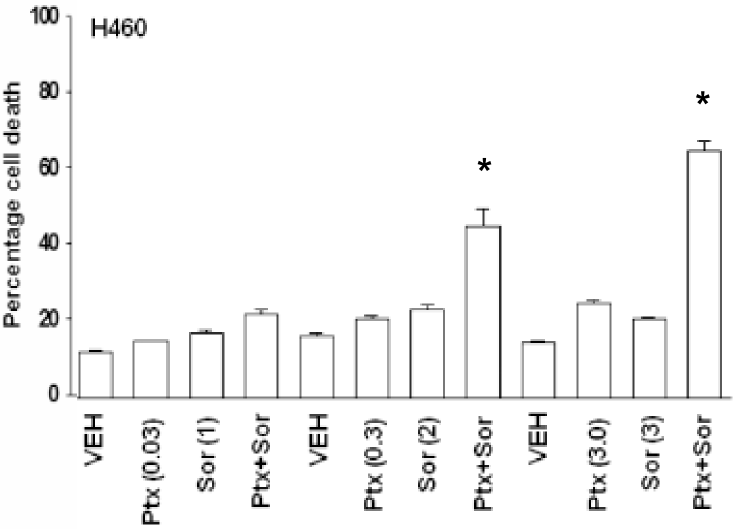

Figure 4-4: Co-treatment with pemetrexed and sorafenib enhanced toxicity in H460 NSCLC cells. Cells were cultured in media containing thymidine-less serum and treated with vehicles (PBS and DMSO), individual drugs, or a combination of pemetrexed and sorafenib for 24 hr. Samples were performed in triplicate and cell death evaluated using a trypan blue exclusion assay. A greater than additive enhancement in cell death was demonstrated for values having a *p<0.05 greater than vehicle control.

To determine the effectiveness of pemetrexed/sorafenib toxicity in multiple cancer cell types, breast and hepatic carcinoma cell lines were subject to the same treatment conditions used above. Cell death was evaluated in these cell types using a trypan blue exclusion assay for samples treated with vehicle, individual drugs, or a combination of the two at the lowest effective concentrations of each used to generate the previous data figure. A greater than additive enhancement of cell death was noted in 4T1, H460, BT474, and HuH7 cells when exposed to combination therapy in comparison to vehicle or individual drug controls (Figure 4-5A-D). Knockdown of Beclin1 was shown to suppress the cytotoxic interaction of pemetrexed/sorafenib in these cells (Figure 4-5A-D).

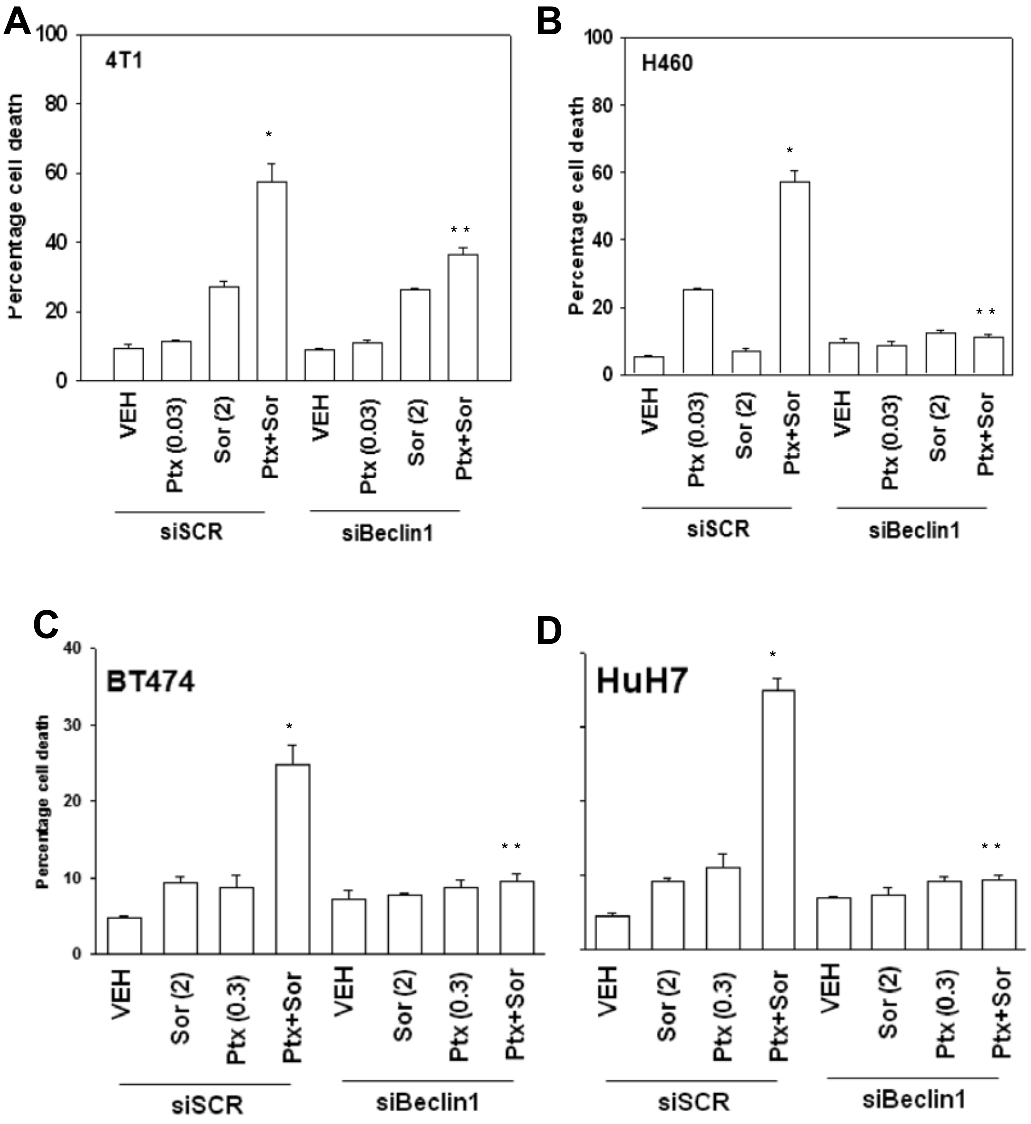

Figure 4.5- Pemetrexed interacts with sorafenib to enhance cell death that is suppressed by knockdown of Beclin1 in multiple tumor types. Cells were cultured in media containing thymidine-less serum, transfected with control siRNA or siRNA targeting Beclin1, then cultured for an additional 36 hr. Cells were then treated with vehicles (PBS and DMSO), individual drugs, or a combination of pemetrexed (μM) and sorafenib (μM) for 24 hr. Co-treatment of cells with pemetrexed and sorafenib for 24 hr causes a greater than additive increase in cell death for all tumor cell types* ($p<0.05$ greater than vehicle control), as compared to vehicle or individual drug controls; however knockdown of Beclin1 suppresses this effect** ($p<0.05$ less than corresponding value in siSCR cells) in (A) 4t1, (B) H460, and (C) BT474, and (D) HUH7 cells.

Autophagy was measured in breast and hepatic carcinoma cell lines co-treated with pemetrexed and sorafenib using the GFP-LC3+ vesicle formation assay, as described previously. Results indicated that HuH7, BT474, and 4T1 cells demonstrated a significant increase in autophagic vesicle formation for the drug combination treatment, compared to vehicle or individual drug-treatment controls (Figure 4-6A-C). Down-regulation of Beclin1 in these cells was shown to block this effect for each cell type (Figure 4-6A-C). These results suggest that pemetrexed and sorafenib cytotoxicity relies upon an autophagic dependent mechanism.

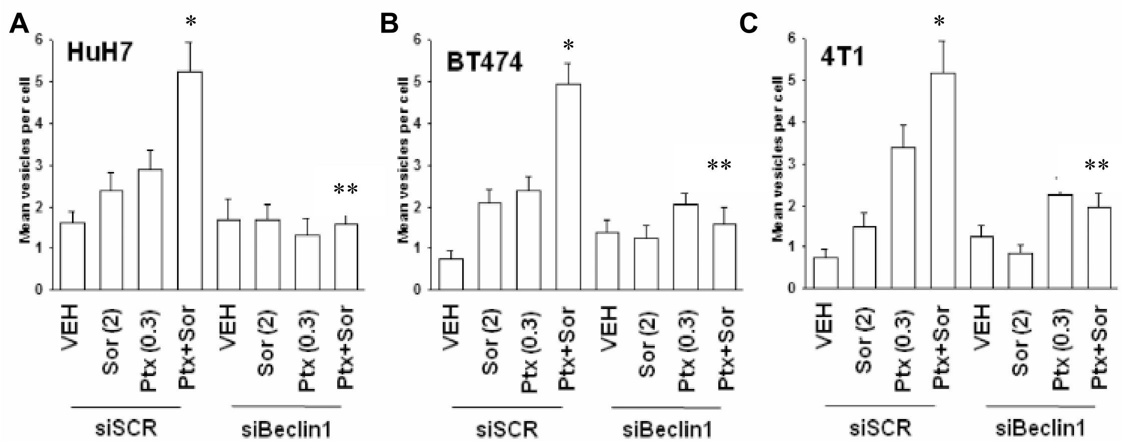

Figure 4-6: Pemetrexed interacts with sorafenib to enhance autophagy that is suppressed by knockdown of Beclin1 in multiple tumor types. Cells were cultured in media containing thymidine-less serum, transfected with a plasmid expressing GFP-LC3 and control siRNA or siRNA targeting Beclin1, then cultured for 36 hr prior to drug addition. Cells were treated with vehicles (PBS and DMSO), individual drugs (µM), or a combination of the drugs for 12 hr prior to analysis of GFP-LC3+ vesicle formation by fluorescence microscopy. Samples were performed in triplicate and 40 random cells selected for evaluation of each sample. Combination treatment caused a significant increase in the number of GFP-LC3+ vesicles per cell* ($p<0.05$ greater than vehicle), when compared to vehicle and single drug treatment controls. This effect is blocked by knockdown of Beclin1** in these cells ($p<0.05$ less than corresponding value in siSCR-transfected cells.

4.3 Pemetrexed/ sorafenib combination therapy is an effective therapeutic for triple negative breast cancer

Development of estrogen independence as a result of exposure to estrogen receptor inhibitors in ER+ breast cancers is one of the most prevalent types of acquired drug resistance in cancer therapy. For this reason, development of novel chemotherapeutic strategies for treatment of estrogen-independent breast cancer is important and necessary. As a result, studies were performed to assess the effectiveness of pemetrexed/sorafenib combination therapy in the treatment of Her2+ and triple-negative breast cancer cells, wherein the cell no longer responds to estrogen. Cell death was evaluated following drug combination treatment of BT549 (triple negative), SKBR3 (Her2+), HCC1187 (triple negative), and HCC1937 (triple negative) cells. Results indicated that individually, sorafenib and pemetrexed were able to induce a dose-dependent increase in cell death in all cell lines tested. In addition, the drug combination was able to induce a greater than additive enhancement of cell killing (Figure 4-7A-D).

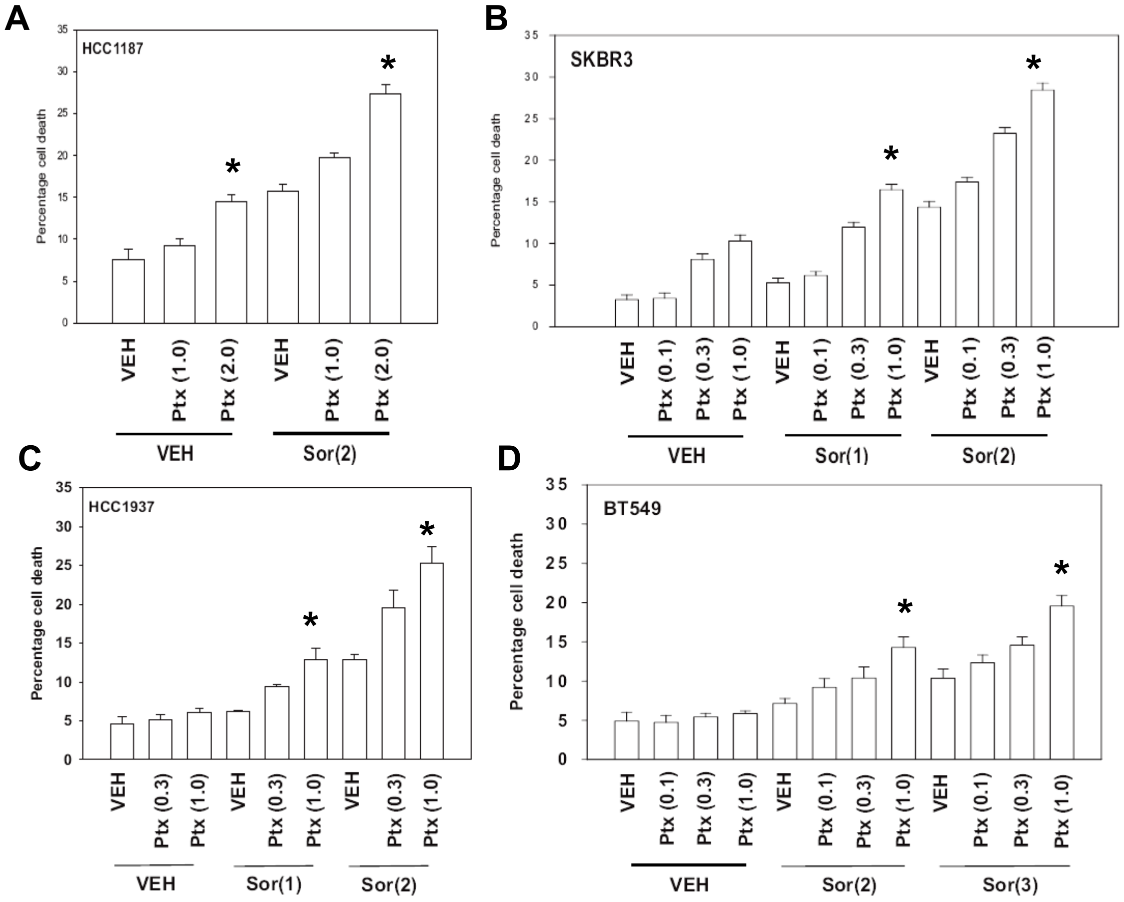

Figure 4-7: Pemetrexed and sorafenib interact in a dose-dependent manner to cause cell death in Her2+ and triple negative breast cancer cells. Cells were plated in media containing dialyzed serum for 24 hr prior to drug treatment. Co-treatment with pemetrexed (µM) and sorafenib (µM) for 24 hr resulted in a significant increase in cell death* ($p<0.05$ greater than vehicle) as compared to vehicle or individual drug-treatments in (A) HCC1187, (B) SKBR3, (C) HCC1937, and (D) BT549 cells, as judged by trypan blue exclusion.

Faslodex (Fulvestrant) has proven beneficial for the treatment of ER+ metastatic breast cancer cells in post-menopausal patients previously treated with, but now resistant to tamoxifen. This effect is likely due to the distinct mode of action by which fulvestrant inhibits estrogen signaling (298-299). Fulvestrant is typically issued as a second-line therapy to breast cancer patients having developed a resistance to a first-line chemotherapeutic regimen, while there are many patients that will also develop a resistance to fulvestrant (299-300). MCF7 is a well-characterized ER+ mammary ductal epithelial cell line isolated from a pleural effusion of a post-menopausal woman (301). Nephew and colleagues developed a fulvestrant-resistant MCF7 model (MCF7F) through stringent selection of cells able to bypass estrogen-dependence after exposure to fulvestrant at high dosage for an extended period of time (302). Studies were performed to examine whether the pemetrexed/sorafenib combination would be equally as toxic for fulvestrant-resistant and non-resistant breast cancer cells. Both parental MCF7 and fulvestrant-resistant MCF7 (MCF7F) cells demonstrated a dose-dependent increase in cell death for individual drug treatments. When analyzing drug combination lethality, both cell lines responded in at least an additive fashion, compared to that of the individual drugs; however MCF7F cells were more sensitive to the drug combination treatment (Figure 4-8).

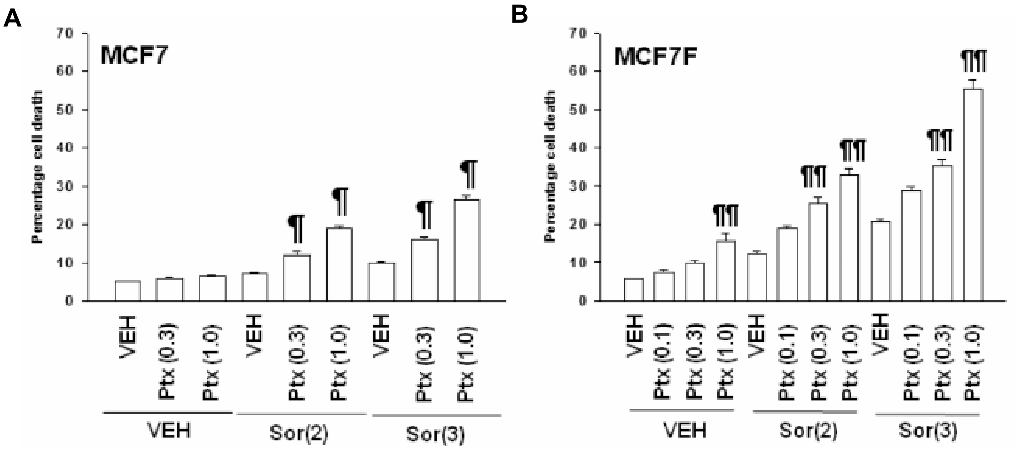

Figure 4-8: Co-treatment with pemetrexed and sorafenib cause a dose-dependent increase in cell death in parental and Fulvestrant-resistant MCF7 cells. Cells were plated in media containing thymidine-less serum for 24 hr prior to drug treatment. Cells were treated with vehicles (PBS and DMSO), individual drugs (µM), or drug combinations of increasing dosages for 24 hr. Cell death was analyzed by trypan blue exclusion. Treatment with pemetrexed and sorafenib resulted in as dose-dependent enhancement in cellular toxicity for single drug treatment conditions, as well as illustrated a greater than additive enhancement of cell killing in (A) parental, estrogen-dependent MCF7¶ ($p<0.05$ greater than vehicle control) and (B) Fulvestrant-resistant MCF7-F¶¶ ($p<0.05$ greater than vehicle control) cells.

4.4 MCF7F cells express higher levels of autophagy-related proteins and are more sensitive to pemetrexed/ sorafenib treatment than their estrogen-dependent counterparts

Data in this dissertation has indicated that the autophagic cellular machinery is important for sorafenib/pemetrexed induced toxicity in multiple tumor cell types. The expression levels of the proteins involved in autophagy were assessed to further validate these findings. Western blot analysis of several of the key proteins involved in the regulation of autophagy was determined for parental and fulvestrant-resistant MCF7 cells after treatment with vehicle, individual drugs, or the pemetrexed/ sorafenib combination (Figure 4-9). In both MCF7 and MCF7F cells, treatment with pemetrexed/ sorafenib caused an increase in the levels of LC3II (the lipidated form of LC3 necessary for autophagosomal membrane formation) and decreased levels of p62 (a marker for autolysosome activity when reduced). Clinical studies evaluating patient tumor samples have implicated the loss of Beclin1 in the process of tumor formation of breast and lung carcinoma (303-304). These studies suggested that autophagy exists as a protective mechanism in these cells. Interestingly, MCF7 cells are documented as a haplotype for expression of the Beclin1 gene (307-308). MCF7F cells express significantly higher basal levels of Beclin1 and the ATG5-12 complex than the parental strain. However, Beclin1 and ATG5-12 levels increased significantly for parental MCF7 cells when co-treated with pemetrexed and sorafenib, while there was no significant change in levels of these proteins for combination drug-treated MCF7F cells. The protein expression of anti-apoptotic Mcl-1 was reduced for both cell strains when treated with sorafenib and further reduced with combination treatment in MCF7F cells. The expression of Bcl-XL was reduced for MCF7F cells when treated with individual drugs or the combination (Figure 4-9).

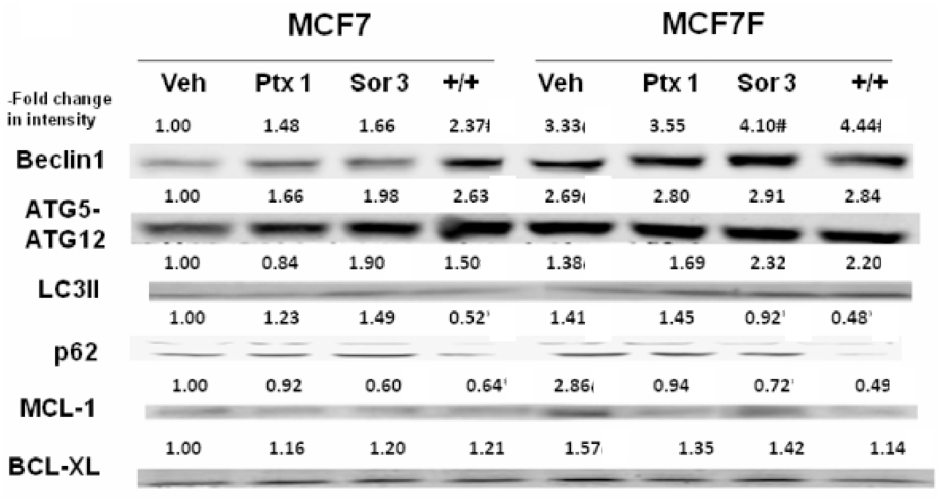
MCF7
MCF7F
Veh
Ptx 1
Sor 3
+/+
Veh
Ptx 1
Sor 3
+/+
-Fold change in intensity
1.00 1.48 1.66 2.37 3.33 3.55 4.10# 4.44
Beclin1
1.00 1.66 1.98 2.63 2.69 2.80 2.91 2.84
ATG5-ATG12
1.00 0.84 1.90 1.50 1.38 1.69 2.32 2.20
LC3II
1.00 1.23 1.49 0.52 1.41 1.45 0.92 0.48
p62
1.00 0.92 0.60 0.64 2.86 0.94 0.72 0.49
MCL-1
1.00 1.16 1.20 1.21 1.57 1.35 1.42 1.14
BCL-XL

Figure 4-9: Fulvestrant-resistant MCF7F cells express higher basal levels of autophagy related proteins than do their estrogen-dependent counterparts. Cells were plated in media containing thymidine-less serum for 24 hr prior to drug treatment. Cells were treated with vehicle, individual drugs, or a combination of pemetrexed and sorafenib for 24 hr. The levels of autophagy-related proteins were evaluated for each condition by western blot analysis. The expression values provided for each condition were calculated based on their respective GAPDH densitometry values. MCF7F expressed higher basal levels of Beclin1, ATG5-12, LC3II, p62, Mcl-1, and Bcl-XL. Pemetrexed/ sorafenib combination treatment caused a significant increase in the levels of Beclin1, ATG5, and LC3II (lapidated-LC3I) in both parental and fulvestrant-resistant MCF7 cells. P62 levels were significantly reduced in combination treated cell samples, as compared to vehicle or individual drug samples.

Pemetrexed and sorafenib co-therapy leads to an induction of autophagy, as well as an enhancement in cell death for multiple tumor types. Judging by alterations in the expression levels of autophagy-related proteins in cells treated with both drugs compared to controls, one would expect the mechanism of cell death to be one that could involve the intrinsic portion of the apoptotic pathway which utilizes the mitochondria. To examine this, the amount of cell death in cells over-expressing a dominant-negative form of caspase-9 (dncaspase-9) was evaluated. Over-expression of a non-functional form of caspase-9 caused a minor decrease in pemetrexed/ sorafenib lethality in MCF7, while causing a moderate decrease in combination-treated MCF7F cells. These results suggest that the intrinsic apoptotic pathway may have a role in drug combination lethality (Figure 4-10A-B). Overexpression of the anti-apoptotic Bcl-XL led to reduction in cell death in both cell lines. Overexpression of c-FLIP-s (an inhibitory protein of caspase-8 within the extrinsic pathway) caused no significant change in drug combination induced cytotoxicity in MCF7 or MCF7F cells (Figure 4-10A-B).

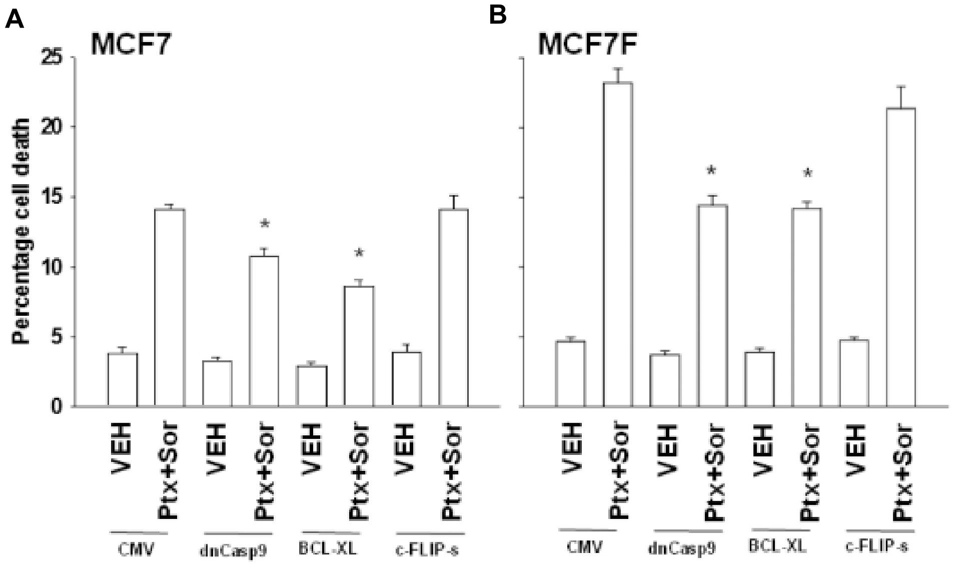

Figure 4-10: Toxicity resultant of combination treatment with pemetrexed and sorafenib follows an intrinsic, rather than extrinsic, death signaling mechanism. Cells were plated in media containing dialyzed serum and cultured for 24. Cell samples were infected with a vector control plasmid or a plasmid expressing the gene of interest for 36 hrs prior to drug treatment. Overexpression of a dominant negative form of caspase 9 or Bcl-XL decreases drug combination lethality in (A) MCF7 and (B) MCF7F cells, however overexpression of c-FLIPs has no effect on combination drug induced death* ($p<0.05$ less than CMV vector control-transfected cells).

Phosphorylation levels of the major signal transduction pathway proteins within these cells were examined, in an attempt to further define the mechanisms by which pemetrexed/sorafenib treatment propagates a cytotoxic cell death signal. MCF7F cells contain higher basal levels of PDGFRβ and FGFR, known sorafenib targets, than the parental strain (Figure 4-11A). Based on this observation, analysis of the phosphorylation levels of signaling proteins involved in propagation of these growth factor-induced responses were assessed. Combination therapy more significantly enhanced downregulation of phospho-mTOR S2448 in MCF7 and MCF7F cells, than did either of the individual drugs alone (Figure 4-11A). Phospho-Erk1/2 levels were significantly enhanced in drug combination samples for parental MCF7 cells. MCF7F cells demonstrated an increase in ERK1/2 phosphorylation, while the effect was not as dramatic as that for parental MCF7 cells. Thus, even in the presence of sorafenib, Erk1/2 was activated in this system. Treatment with pemetrexed or sorafenib as single agents modestly inhibited the levels of phospho-p70 T421/S424 and phopho-p70 T389 in parental MCF7 and estrogen-independent MCF7F cells (Figure 4-11A). MCF7F cells were found to express higher basal levels of phospho-ERK1/2, p70, and mTOR than the parental MCF7 strain (Figure 4-11B).

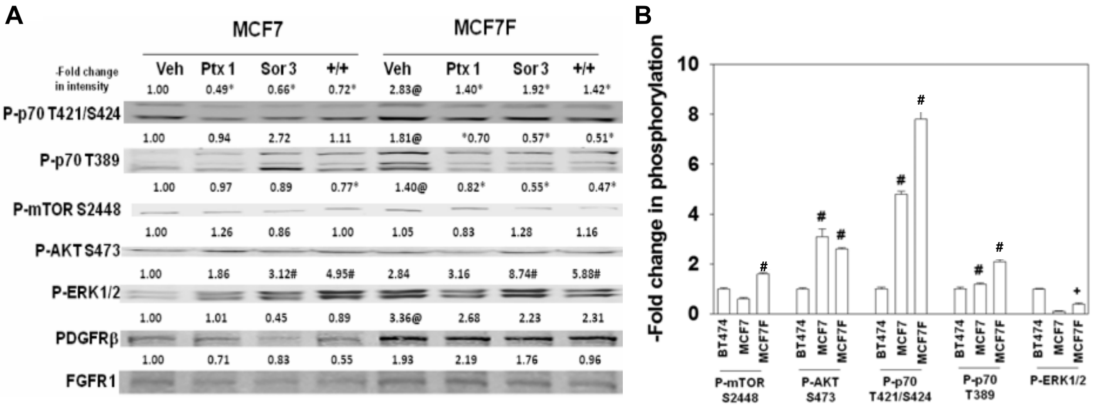

Figure 4-11: Pemetrexed/ sorafenib co-treatment alters signaling through mTOR and MAPK pathways. Cells were plated in media containing thymidine-less serum for 24 hr prior to treatment. Cells were treated with vehicles (PBS and DMSO), individual drugs, or a combination of pemetrexed and sorafenib for 24 hr. Lysates were harvested and denaturing gels run to determine phospho-protein levels. (A) Combination treatment with pemetrexed and sorafenib downregulates mTOR* and p70* activation ($p<0.05$), while strongly activating the Erk1/2$^\#$ signaling pathway ($p<0.05$). Basal levels$^@$ of p-p70 S6 kinase T389 and T421/S424, p-mTOR S2448, and total PDGFRß were higher in Fulvestrant-resistant MCF7 cells, as compared to their estrogen-dependent counterparts ($p<0.05$). (B) Quantification of protein levels were plotted illustrating the basal levels of the indicated phospho-proteins for BT474, MCF7, and MCF7F cells. MCF7F cells have higher basal activity for ERK1/2, p70, and mTOR.

The importance of the signaling proteins implicated in the western blot findings was determined. Initially, the levels of PDGFRβ were manipulated in MCF7 and MCF7F cells. Knockdown of PDGFRβ could potentially mimic the effects of sorafenib treatment if the drug was preferential for this receptor using this particular dose range. Western blot analysis confirmed the reduction in PDGFRβ levels by siRNA in both cell lines (Figure 4-12A). Results indicated that knockdown of PDGFRβ led to an enhanced cell death, in a pemetrexed mediated dose-dependent manner in MCF7 and MCF7F cells, this effect was more pronounced in MCF7F (Figure 4-12B).

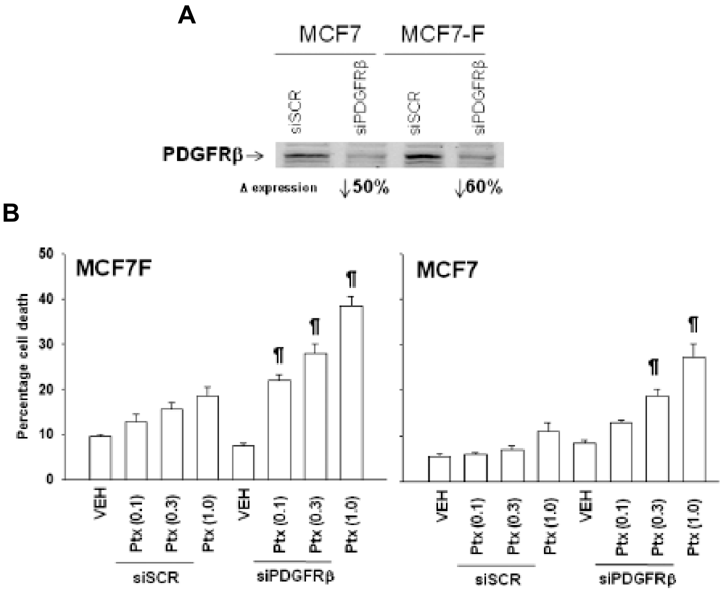

Figure 4-12: MCF7F cells are more sensitive to pemetrexed treatment than the estrogen-dependent parental strain and pemetrexed-induced toxicity can be enhanced by knockdown of PDGFRβ. Cells were plated in media containing dialyzed serum and cultured for 24 hr prior to transfection with control siRNA or a siRNA targeting PDGFRβ. 36 hr post transfection, cells were treated with pemetrexed at the indicated dosages. 24 hr after treatment cells either (A) harvested for lysate to demonstrate knockdown of PDGFRβ or subject to a (B) trypan blue exclusion assay to determine cell death percentages. Both parental and Fulvestrant-resistant MCF7 cells became more sensitive to pemetrexed treatment upon knockdown of PDGFRβ¶ ($p<0.05$).

The importance of mTOR and p70 S6K in the interactions of pemetrexed and sorafenib was determined, by transiently knocking down expression of these proteins. Western blot analysis of mTOR and p70 verified a reduction in the levels of these proteins by siRNA methods (Figure 4-13A). Simultaneous knockdown of p70 and mTOR was shown to enhance drug combination lethality in both cell lines; however the effect of knocking down both of these proteins simultaneously must be considered when evaluating these findings. Comparatively speaking, MCF7F cells appeared to be more sensitive to combination treatment following knockdown for mTOR and p70 (Figure 4-13B-C). Knockdown of mTOR and p70 may have sensitized MCF7F to pemetrexed-only treatment; while taking into consideration the consequent effects of knockdown of these proteins in cells (Figure 4-13C). Downregulation of either protein alone did not appear to promote combination drug toxicity (data not shown).

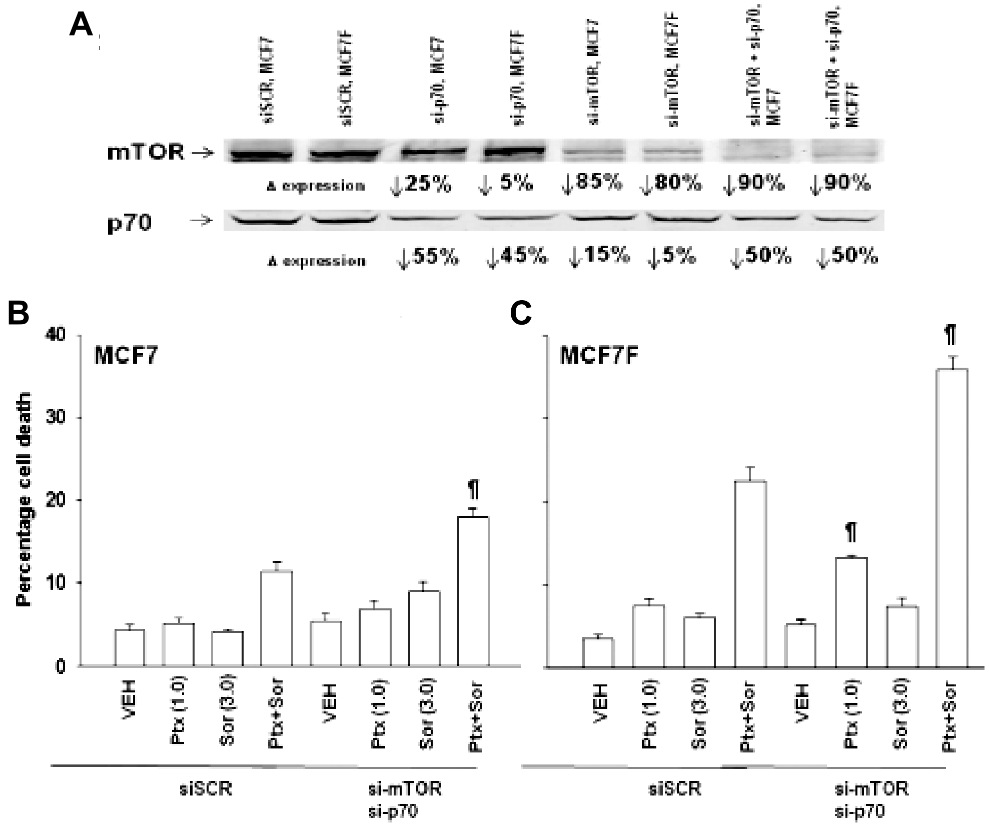

Figure 4-13: mTOR and p70 S6 kinase pathways play an important role in pemetrexed/ sorafenib lethality. Cells were plated in media containing thymidine-less serum 24 hr prior to transfection with control siRNA or siRNA targeting mTOR and p70, simultaneously. Transfected cells were cultured for 36 hr prior to treatment with vehicle, individual drugs, or a combination of pemetrexed and sorafenib for 24 hr. (A) The levels of mTOR and p70 were determined by western blot analysis to verify knockdown of the genes. (B) Knockdown of mTOR and p70 sensitize MCF7¶ and MCF7F¶ cells to combination treatment, as judged by trypan blue exclusion ($p<0.05$ greater than vehicle).

Using a separate approach, constitutively active forms of mTOR and p70 were overexpressed in MCF7 and MCF7F cells and these cells were then subjected to the same analysis. Results from these studies demonstrated that overexpression of constitutively active forms of either protein led to reductions in pemetrexed toxicity in parental MCF7 cells, while combination treatment further enhanced a reduction in cell death in these cells (Figure 4-14A-B). These results may be suggestive of lower levels of TS expression in the parental cell line because sensitivity of MCF7F cells to pemetrexed as a single agent was enhanced. Similar to the siRNA knockdown data for these proteins, when constitutively active forms of both mTOR and p70 were co-expressed, there was a more pronounced effect than either individually. Overexpression of constitutively active forms of mTOR and p70 caused a more pronounced reduction in cell death for MCF7F cells than MCF7 (Figure 4-14B).

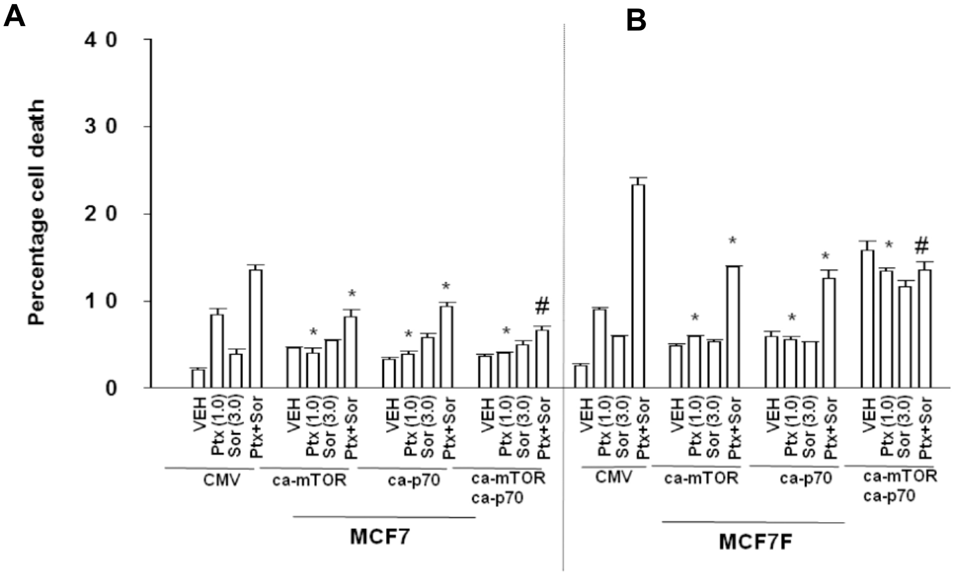

Figure 4-14: Constitutive activation of mTOR and p70 S6 kinase pathways desensitizes MCF7 cells to pemetrexed/ sorafenib cotherapy. Cells were plated in media containing thymidine-less serum and cultured for 24 hr prior to transfection. Cells were transfected with vector control plasmid or plasmids to express constitutively active forms of mTOR (ca-mTOR), p70 (ca-p70), or both. Cells were treated with vehicle, individual drugs, or a combination of pemetrexed and sorafenib for 24 hr prior to determination of cell death using a trypan blue exclusion assay. Overexpression of constitutively active mTOR or constitutively active p70 caused a reduction* in toxicity for combination drug treatments ($p<0.05$ less than corresponding value in CMV vector-transfected cells) in (A) MCF7 and (B) MCF7F cells, as compared to vector control cells. Overexpression of constitutively active mTOR and constitutively active p70 in combination further reduced$^\#$ cell death in both cell lines below that of individual manipulations ($p<0.05$).

4.5 Pemetrexed and sorafenib interact to promote cell death in vivo

The ultimate goal of this study is to have pemetrexed/sorafenib co-therapy translated into the clinical setting. In order to examine the effectiveness of this drug combination in an *in vivo* tumor environment, these drugs were tested in an orthotopic BT474 mammary carcinoma mouse model. Pemetrexed/sorafenib co-treatment significantly reduced tumor growth in mice, when compared to vehicle and individual drug treatment (Figure 4-15A). Immunohistochemistry was performed on tissue slices from mice under different treatment conditions to evaluate the levels of cell proliferation and apoptosis. Tumor growth data correlated with immunohistochemistry data (Figure 4-15B). A decrease in Ki-67 staining (for proliferation), demonstrated a reduction in proliferation for combination drug-treated cells. In addition, apoptosis was enhanced for pemetrexed/ sorafenib-treated tumors, which correlated with tumor growth data.

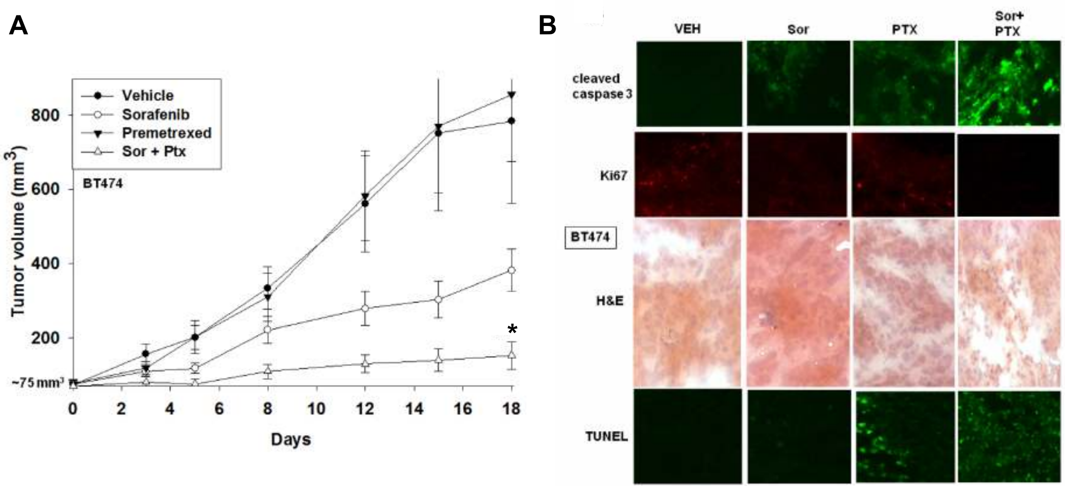

Figure 4-15: Pemetrexed and sorafenib interact to reduce tumor growth in a breast cancer-induced mouse model. Cells were injected into the 4th mammary fat pad of athymic nude mice and allowed to form tumors (~75mm^3), then batched according to tumor size. Animals were treated with vehicles (PBS or chromophore), individual drugs, or a combination of pemetrexed (50 mg/kg) and sorafenib (25 mg/kg) once a day for 2 rounds of 5-day treatment, separated by 2 days. Tumor sizes were recorded every 3 days during the course of the experiment. Mean tumor volumes were plotted per group. (A) Combination treatment with pemetrexed/ sorafenib resulted in a significant growth reduction for BT474 cells, as compared to vehicle and individual drug treatments* ($p<0.05$). (B) Tumor tissue slices were harvested 14 days after the last drug treatment and immunohistochemistry preformed to evaluate the levels of apoptosis and cell proliferation, as well as cell morphology in comparison to healthy tissue controls. All *in vivo* studies were conducted by Dr. Hossein Hamed.

Chapter 5: Results- Sorafenib and pemetrexed toxicity in cancer cells is mediated via Src-Erk signaling

The studies in this chapter sought to understand in greater detail how the anti-folate pemetrexed and the multi-kinase inhibitor sorafenib interact to kill mammary carcinoma cells. A previous study combining pemetrexed and sorafenib in prostate cancer cells demonstrated a pronounced activation of Erk1/2 in response to combination treatment (295). This chapter addresses the involvement of MEK1/2-Erk1/2, Src, the tumor suppressor PP2A, the inhibitor 2 of protein phosphatase 2A (I2PP2A/ SET), and the *de novo* ceramide synthetic machinery in drug combination-induced cell killing.

5.1 Pemetrexed induces a cytotoxic form of autophagy in Her2+ and triple negative breast cancer cells

In Her2+ BT474 cells, pemetrexed/ sorafenib combination drug therapy was shown to cause a significant Beclin 1-dependent increase in early autophagic vesicle formation, as judged by GFP-LC3+ autophagic punctae formation (Figures 5-1A and 5-1B). Treatment of BT474 and MCF7F cells with pemetrexed and sorafenib resulted in a pronounced increase in cell death, while this effect was significantly attenuated by knockdown of Beclin1 (Figure 5-1C).

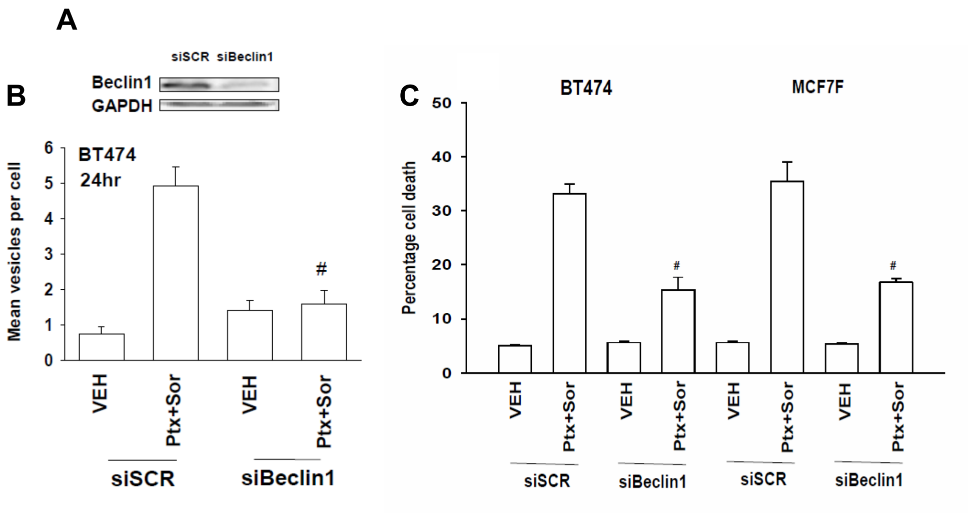

Figure 5-1: Pemetrexed-induced autophagy and tumor cell killing is suppressed by knockdown of Beclin1. Cells were plated in media containing dialyzed serum and cultured for 24 hr prior to transfection GFP-LC3 and control siRNA or siRNA targeting Beclin1, as well as the GFP-LC3 expression plasmid. Cells were treated with vehicle or pemetrexed/ sorafenib combination prior to analysis of autophagasome formation. (A) Western blot analysis for verification of Beclin1 knockdown. (B) Autophagosomal lysosome formation was quantified by determination of GFP-LC3+ vesicles per cell after 24 hr exposure to vehicle or combination drug treatment. Pemetrexed/ sorafenib treatment caused a significant increase in autophagic vesicle formation in BT474 cells, which was attenuated upon knockdown of Beclin1$^{\#}$ ($p<0.05$ less than corresponding value in siSCR cells). (C) Pemetrexed/ sorafenib cotreatment for 24 hr caused an increase in cell death for BT474 and MCF7F cells, which was reduced upon knockdown of Beclin1$^{\#}$ ($p<0.05$ less than corresponding value in siSCR cells).

These breast cancer cell models were further examined for progression of early autophagic vesicles to late stage endosomes when treated with the drug combination using Lysotracker Red staining, which is sensitive for late stage endosome acidification. The presence and intensity of red staining is indicative of the levels of proteosomal degradation occurring in these vesicles (305). Treatment of BT474 and MCF7F cells demonstrated a time-dependent increase in late stage endosomal acidification (Figure 5-2A). The most prominent increase in endosomal activity was seen at 24 hr. Knockdown of Beclin1 suppressed this effect in both BT474 and MCF7F cells (Figure 5-2B-C).

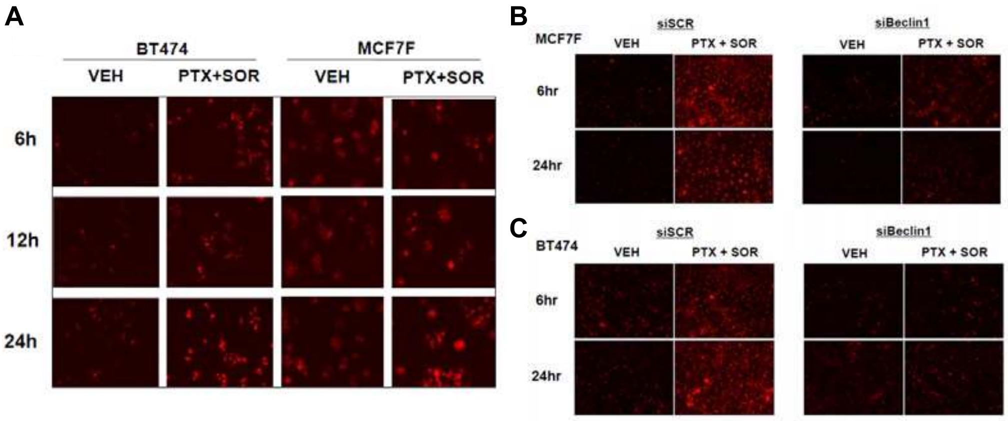

Figure 5-2: Pemetrexed interacts with sorafenib in a time-dependent fashion to increase autophagy which is suppressed by knockdown of Beclin1. Cells were plated in media containing dialyzed serum and cultured for 24 hr prior to drug treatment for variable times or transfection with control siRNA or siRNA targeting Beclin1. For non-transfected cell samples, cells were treated with vehicle or a combination of pemetrexed and sorafenib various time points than evaluated for (A) lysosomal protein degradation at various time points. For transfected samples, 36 hr post-transfection with si-Beclin1, cells were treated with vehicle or a combination of pemetrexed and sorafenib for 6 or 24 hr time points, then evaluated for lysosomal protein degradation in (B) MCF7F and (C) BT474 cells. Both cell lines demonstrated an increase in acidic lysosome formation upon treatment with pemetrexed and sorafenib at various time points, compared to vehicle-treated cells; while knockdown of Beclin1 reduced this effect.

5.2 Pemetrexed/ sorafenib toxicity is dependent upon the generation of ROS

In many cases, chemotherapeutic drug toxicity is preceded by the generation of ROS, which may promote oxidative stress in cells. Increased levels of ROS can result in oxidation of lipids, proteins, and DNA, ultimately leading to cell death (306). Due to their highly reactive nature, ROS disrupt the integrity of the lysosomes causing lysosomal membrane permeabilization and the release of molecules that trigger autophagy and caspase-induced cell death. To further validate the importance of late stage endosome formation for pemetrexed/ sorafenib-induced cellular toxicity in the cell models used in this study, we pre-treated cells with ammonium chloride (NH_4Cl), an agent known to inhibit endosomal acidification by neutralization of this compartment; thus preventing LC3 degradation in autophagolysosomes (307-308). Results indicated a significant reduction in drug combination-induced cell toxicity in BT474 and MCF7F cells pre-treated with NH_4Cl (Figure 5-3A-B). This data further confirms the importance of lysosomal function for promoting pemetrexed/ sorafenib toxicity in breast cancer cells.

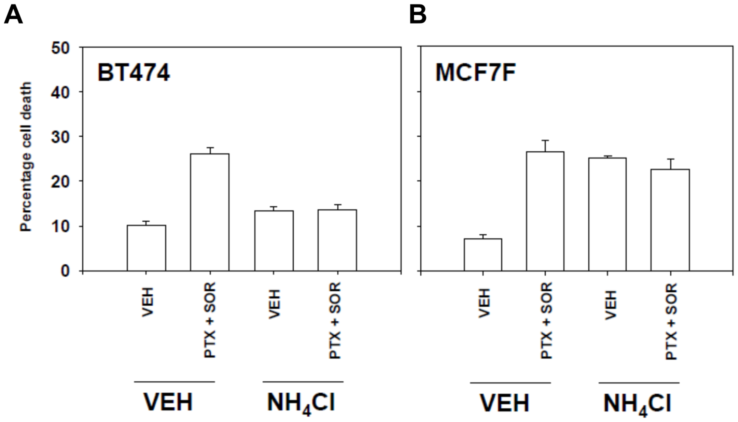

Figure 5-3: Inhibition of autophagy at the mitochondrial level abolishes drug combination-induced cell death. Cells were plated in dialyzed serum-containing media and cultured for 24 hr prior to vehicle or pemetrexed/ sorafenib treatment +/- NH_4Cl. Cells were evaluated for viability using a trypan blue exclusion assay. Treatment with NH_4Cl resulted in an abolishment of pemetrexed/ sorafenib induced drug lethality, as compared to vehicle treated cells for both BT474 and MCF7F cells.

5.3 Pemetrexed/ Sorafenib cytotoxicity is regulated by Src

PDGFRβ, a known sorafenib target, was identified in preliminary experiments to be a possible factor in the pemetrexed/ sorafenib co-therapy response. PDGFRβ was shown to be expressed at higher levels in fulvestrant-resistant MCF7 cells, compared to parent MCF7 cells (illustrated in the Chapter 4). MCF7F tumor cells are more aggressive in terms of tumorigenicity, while they demonstrate a greater sensitivity to drug combination treatment than the estrogen-dependent parental strain. To further define the mechanisms contributing to apoptosis following drug-induced reductions in PDGFRβ, we examined one of its prominent downstream effector kinases, c-Src. Earlier studies in our laboratory reported that sorafenib treatment can lead to inhibition of

PDGFRβ and activation of Src through a CD95-dependent mechanism (256-257,286). Upregulation of Src has been strongly correlated with invasion and cell motility, which are characteristic of tumor cell progression (309). Src becomes activated by PDGFRβ at the plasma membrane, an event which is mediated through its interactions with phosphorylated Tyr579 and Tyr581 residues of PDGFRβ (310). Src can transmit its signal to a number of downstream targets including MEK/Erk and Akt. In the first chapter of results, Erk1/2 was shown to be activated in response to pemetrexed/ sorafenib treatment in parental and estrogen-independent breast cancer cells. The MEK/Erk and Akt pathways communicate with one another on multiple levels to regulate Src signaling. For this reason, the mechanisms by which Src mediates its biological effects are not always clear.

We examined a possible role for Src in the Erk1/2-mediated response of tumor cells to pemetrexed/ sorafenib co-therapy. Knockdown of PDGFRβ in BT474 cells was accompanied by an approximate 2-fold increase in phospho-Src Y416 levels (Figure 5-4A, left). Overexpression of a dominant negative form of Src (dnSrc) was verified by western blot (Figure 5-4A, right). Overexpression of dnSrc suppressed drug-induced autophagic vesicle formation in BT474 cells (Figure 5-4B). MCF7F cells demonstrated a reduced percentage of drug combination-induced cell death when overexpressing dnSrc, as compared to vector-transfected cells (Figure 5-4C).

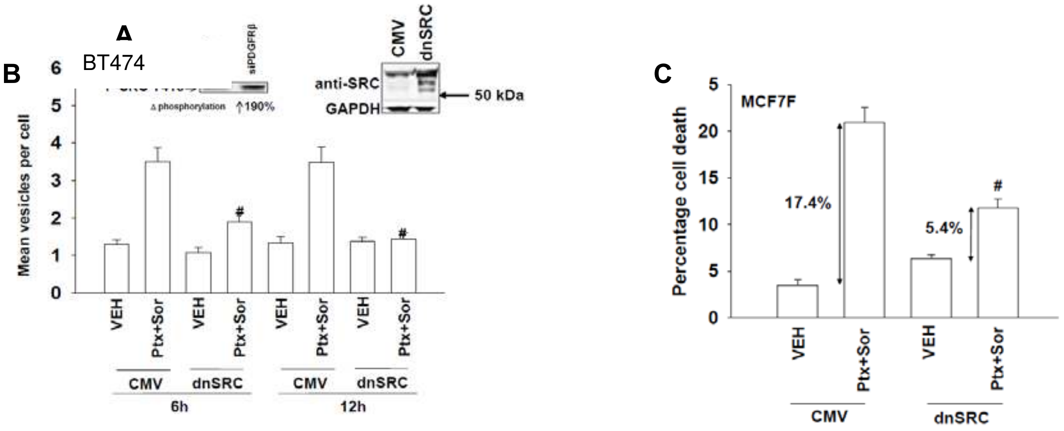

Figure 5-4: Src is an important player in the mechanistic means by which pemetrexed and sorafenib enhance cell death. Cells were plated in dialyzed serum- containing media then cultured for 24 hr prior to transfection with vector control plasmid or a dnSRC-expressing construct. 36hr post-transfection, cells were treated with vehicle or a combination of pemetrexed and sorafenib for the indicated times, then evaluated for GFP-LC3 vesicle formation or cell lethality. (A) Western blot analysis of p-Src Tyr416 (left) in BT474 cells when PDGFRβ is downregulated by treatment with sorafenib, as well as western blot analysis to verify overexpression of dominant-negative Src. (B) Overexpression of dominant-negative Src attenuates drug combination-induced autophagic vesicle formation in BT474 cells$^{\#}$ ($p<0.05$ less than corresponding value in CMV vector control-transfected cells) and (C) reduces cell toxicity in MCF7F cells, as compared to the vector control-transfected cotreatment samples$^{\#}$ ($p<0.05$ less than corresponding value in CMV vector control-transfected cells).

5.4 Pemetrexed/ sorafenib toxicity is mediated by the MEK/Erk pathway

A pronounced increase in phospho-Src Y416 levels upon co-treatment of breast cancer cells with pemetrexed and sorafenib led us to the question of which downstream effector pathways are being activated by Src during this response. Src is known to regulate several pathways in the cell including the Erk1/2 pathway, found in the previous chapter of results to be activated by the pemetrexed/sorafenib drug combination. Overexpression of dnSrc was shown to suppress drug-induced activation of (phospho)-Erk1/2 in parental MCF7 cells (Figure 5-5A), whilst overexpression of a dominant negative form of MEK1 (dnMEK1) was shown to inhibit Erk1/2 phosphorylation in these cells (Figure 5-5B). dnMEK1 overexpression led to a significant reduction in pemetrexed/ sorafenib-enhanced cell lethality in BT474, MCF7, and MCF7F cells (Figure 5-5C).

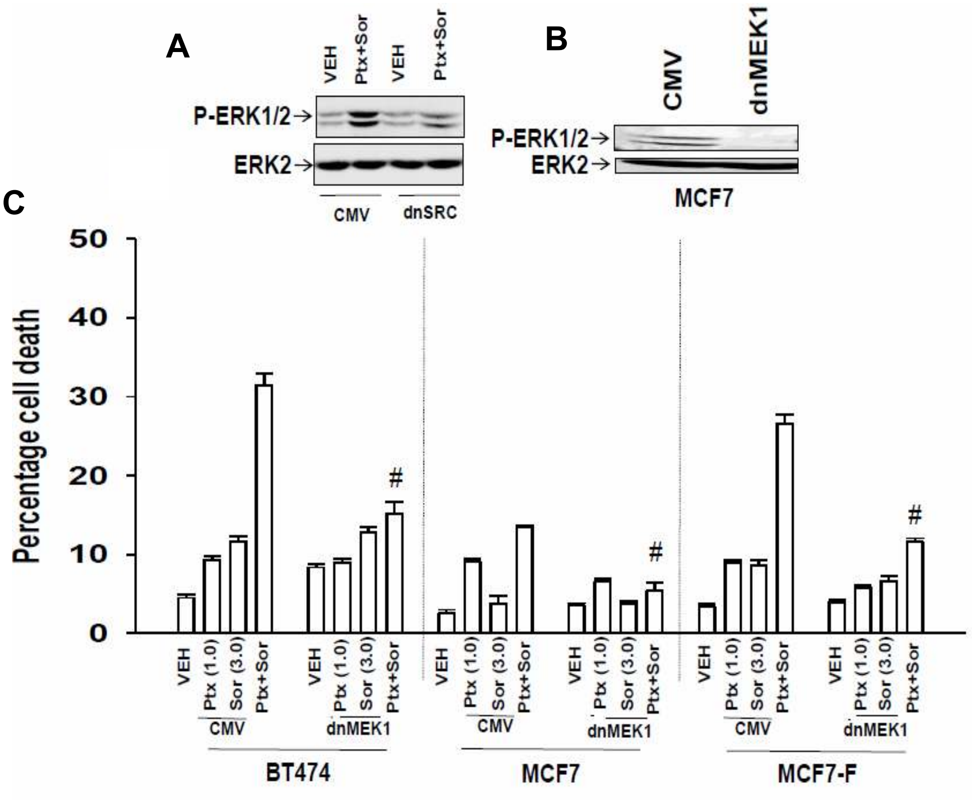

Figure 5-5: Src regulates an Erk1/2-mediated response to pemetrexed/ sorafenib in mammary carcinoma cell lines. Cells were plated in media containing dialyzed serum and cultured for 24 hr prior to transfection with control plasmid or a plasmid to express a dominant-negative form of MEK1. Per western blot analysis: (A) Upon overexpression of dnSrc, activation of ERK1/2 is reduced for pemetrexed/ sorafenib co-treatment samples, as compared to vector control transfected in MCF7 cells. (B) dnMEK1 overexpression in these cells results in a suppression of ERK1/2 activation. (C) Overexpression of dnMEK1, when compared to vector control transfected cells, causes a significant reduction in drug combination-induced cell lethality# ($p<0.05$) in BT474, MCF7, and MCF7F cells, when compared to their respective vector controls.

The amount of autophagic vesicle formation was examined in MCF7F cells overexpressing dnMEK1, to determine whether activation of Erk1/2 by MEK1 is also necessary for drug-induced activation of autophagy. Overexpression of dnMEK1 elevated the basal levels of early autophagic vesicle formation. However, overexpression of dnMEK1 was shown to suppress the pemetrexed/ sorafenib-induced enhancement in LC3+ vesicle formation; more so at the 12 hr time point than the 24 hr time point, possibly due to upregulation of TS in a compensatory effort to reestablish normal DNA synthesis levels (Figure 5-6). A similar effect was noted for BT474 and MCF7F cells overexpressing dnMEK1 when examining late-stage endosomal activity using Lysotracker Red staining. The increase in endosomal acidification caused by pemetrexed/ sorafenib cotreatment was reduced in cells overexpressing dnMEK1 (Figure 5-7).

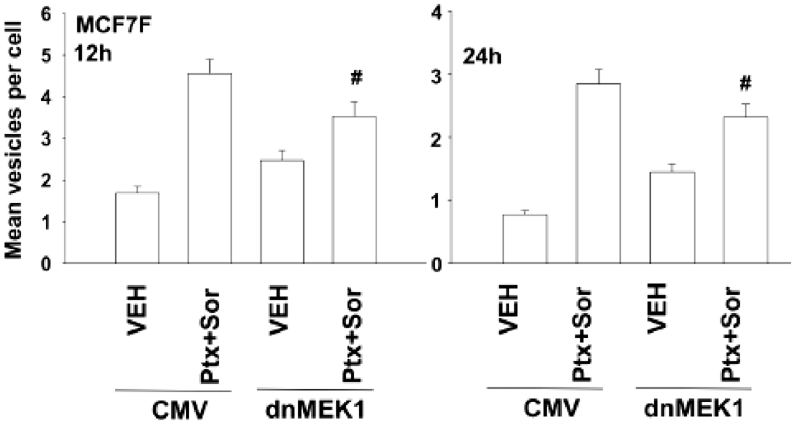

Figure 5-6: Overexpression of a non-functional form of MEK1 attenuates activation of autophagy in pemetrexed/ sorafenib-treated cells. Cells were plated in media containing dialyzed serum and cultured for 24 hr prior to transfection with vector control plasmid or a plasmid to overexpress a dominant-negative form of MEK1. (A) Overexpression of dnMEK1 reduces the levels of autophagosome formation resultant of combination treatment with pemetrexed and sorafenib in MCF7F cells, as compared to vector control transfected cells[#] ($p<0.05$ less than CMV control cell sample values). (B) Overexpression of dnMEK1 reduces the toxic side effects of pemetrexed/ sorafenib co-treatment, as compared to vector control transfected cells for MCF7F and BT474 cell strains[#] ($p<0.05$ less than empty vector (CMV) value).

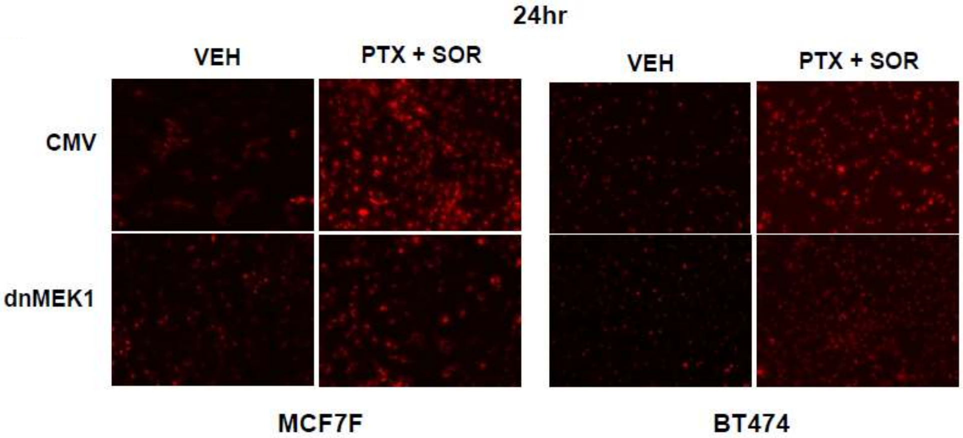

Figure 5-7: Overexpression of dnMEK1 suppresses drug combination-induced acidic lysosome formation. Cells were plated in media containing dialyzed serum and cultured for 24 hr prior to transfection with vector control plasmid or a plasmid to overexpress a dominant-negative form of MEK1. Overexpression of dnMEK1 reduces the levels of acidic lysosome formation in MCF7F (left) and BT474 (right) cells, as compared to vector-transfected and vehicle-treated controls.

Collectively, the data presented here demonstrates that down-regulation of PDGFRβ promotes the activation of Src Tyr416 and subsequent phosphorylation of Erk1/2 by MEK1, through a mechanism unidentified as of yet. Each of these signaling components is important for induction of autophagy-dependent cellular toxicity in the breast cancer cell models used in this study. MEK/Erk signaling is generally associated with pro-survival events, however, some studies have shown that Erk1/2 activation can coincide with cell death, as it does in this particular combination therapy response. There are several levels of enzymatic control exerted over the Erk1/2 pathway including other kinases, as well as protein phosphotases, namely PP2A. For this reason, we assessed whether PP2A plays a role in Src-Erk1/2-mediated drug combination lethality in the breast cancer cell models used in this study.

5.5 Protein phosphatase PP2A is involved in the cytotoxic response of parental and Fulvestrant-resistant MCF7 cells to pemetrexed/ sorafenib treatment

Protein phosphatases serve as important regulators of intracellular signaling cascades. Protein phosphatase 1 (PP1) and protein phosphatase 2A (PP2A) account for approximately 90% of serine/threonine phosphatase activity in most mammalian cells and have been shown to regulate nearly all cellular events (311). PP2A is promiscuous for a wide variety of protein substrates owing to a dynamic relationship within its tri-subunit holoenzyme complex, which delegates specific binding to regulatory molecules and proteins (312). These interactions mediate function through sub-cellular localization to specific compartments within the cell for specific targeting to downstream effector proteins. PP2A is known to have numerous downstream targets which enable its involvement in almost all cellular events, both pro-survival or pro-apoptotic. Attenuation of PP2A activity has been linked to increased tumorigenicity in cancer cells, suggestive of the theory that PP2A functions as a tumor suppressor (311-312). PP2A is regulated by endogenous inhibitory proteins, inhibitor 1 of PP2A (I1PP2A) and inhibitor 2 of PP2A (I2PP2A/SET) (313). These inhibitors act noncompetitively to regulate PP2A depending on its sub-cellular localization. I2PP2A expression has been linked to tumorigenicity in NSCLC, leukemia, prostate cancer, and breast cancer cells (313-315). For this reason, it is important to take into consideration the changes in I2PP2A levels when evaluating PP2A activity and the levels of Erk1/2 phosphorylation regulated by PP2A.

Based on previous data in this study suggesting that fulvestrant-resistant MCF7F cells express higher basal levels of Erk1/2 activity and previous reports that describe MCF7F cells as being more aggressive than parental MCF7 cells, we next we determined the possibility that phosphatases have a role in the mechanism by which these drug acheive their toxic effect. We began by evaluating PP2A activity, while this phosphatase is reported to play a role in many chemotherapeutic drug interactions. Our data showed that PP2A mediates pemetrexed/ sorafenib- induced Erk1/2 activation and tumor cell toxicity. The manipulation of I2PP2A expression as a means of down-regulating PP2A activity was performed in the following experiments. MCF7F cells express higher SET/ I2PP2A levels than MCF7 cells, whilst I2PP2A expression was shown to increase for both cell lines when treated with pemetrexed and sorafenib (Figure 5-8A). Basal levels of PP2A activity are higher in parental MCF7 cells than fulvestrant-resistant MCF7F cells. Treatment of MCF7F cells with pemetrexed and sorafenib resulted in an approximate 2-fold enhancement in PP2A activity, which was negated by overexpression of I2PP2A (Figure 5-8B). As previously noted, MCF7F cells have higher basal expression of Erk1/2 activity (Figure 5-8C). Overexpression of I2PP2A in MCF7F cells resulted in an increase in basal Erk1/2 activity, whilst treatment with pemetrexed and sorafenib did not result in any further change in phospho-Erk1/2 expression (Figure 5-8D). Thus, drug-induced activation of Erk1/2 is likely required for drug-induced killing. Cell killing is not simply induced by a cell exhibiting elevated Erk1/2 activity. Collectively these findings argue that PP2A activity status can be manipulated by overexpression of I2PP2A and that its activity regulates Erk1/2 signaling in pemetrexed/ sorafenib-treated breast cancer cells.

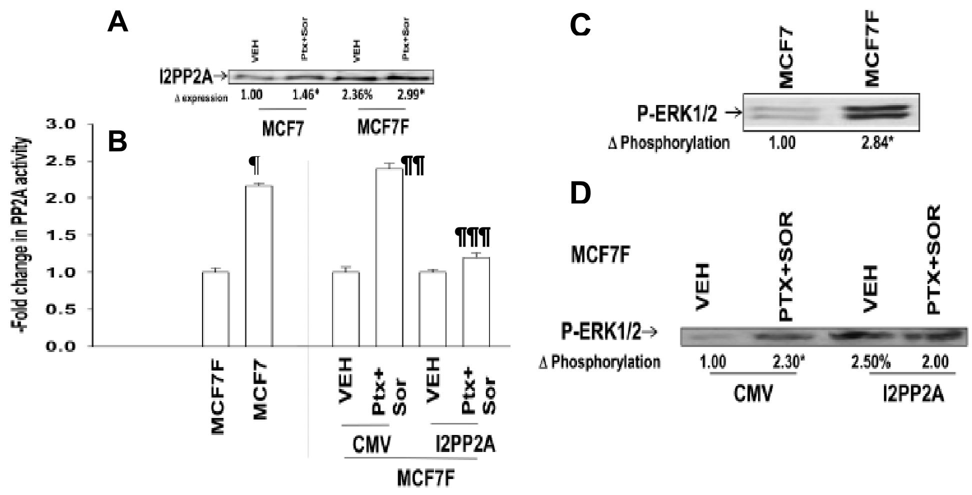

Figure 5-8: PP2A is activated in response to pemetrexed/ sorafenib cotreatment in MCF7F cells. Cells were plated in media containing dialyzed serum and cultured for 24 hr prior to transfection. 36 hr after transfection, cells were treated with vehicle or the drug combination. Parent and fulvestrant-resistance MCF7 cells were treated with vehicle or pemetrexed (1µM) + sorafenib (3µM) for 24 hr, lysates harvested, then expression levels were evaluated using immunoblotting techniques or PP2A activity quantified. All protein levels were normalized to GAPDH, then quantified to represent –Fold change in protein levels. (A) The levels of I2PP2A increased upon treatment with Ptx and Sor, as compared to basal levels in vehicle-treated cells* ($p<0.05$) MCF7F cells express higher basal levels of I2PP2A than the parental strain$^{\%}$ ($p<0.05$) (B) Basal PP2A activity was evaluated in MCF7 and MCF7F cells and quantified to represent –Fold change in activity. PP2A activity was approximately 2-fold greater in MCF7F cells¶ ($p<0.05$). Treatment of MCF7F cells with Ptx and Sor caused a 2-fold enhancement in PP2A activity, as compared to vehicle treated cells¶¶ ($p<0.05$). Overexpression of I2PP2A suppressed the enhancement of PP2A activity caused by drug combination treatment¶¶¶ ($p<0.05$). (C) MCF7F cells express much higher basal levels of P-ERK1/2, than do MCF7. (D) In MFC7F cells, treatment with Ptx and Sor enhances the levels of P-ERK1/2* ($p<0.05$). Overexpression of I2PP2A in these cells results in higher basal levels of p-ERK1/2$^{\%}$ ($p<0.05$) however it prevents the increase in P-ERK1/2 caused by drug combination treatment.

The impact of I2PP2A expression on drug-induced autophagy and cell killing was investigated. Overexpression of I2PP2A was shown to reduce drug combination-induced enhancement of autophagic vesicle formation, as well as drug combination toxicity in MCF7F cells (Figure 5-9A-B). Thus, overexpression of I2PP2A, causing a decrease in PP2A activity, is able to protect breast cancer cells from pemetrexed/ sorafenib-induced cell lethality indicative of the theory that PP2A may be involved in drug combination-enhanced cellular toxicity.

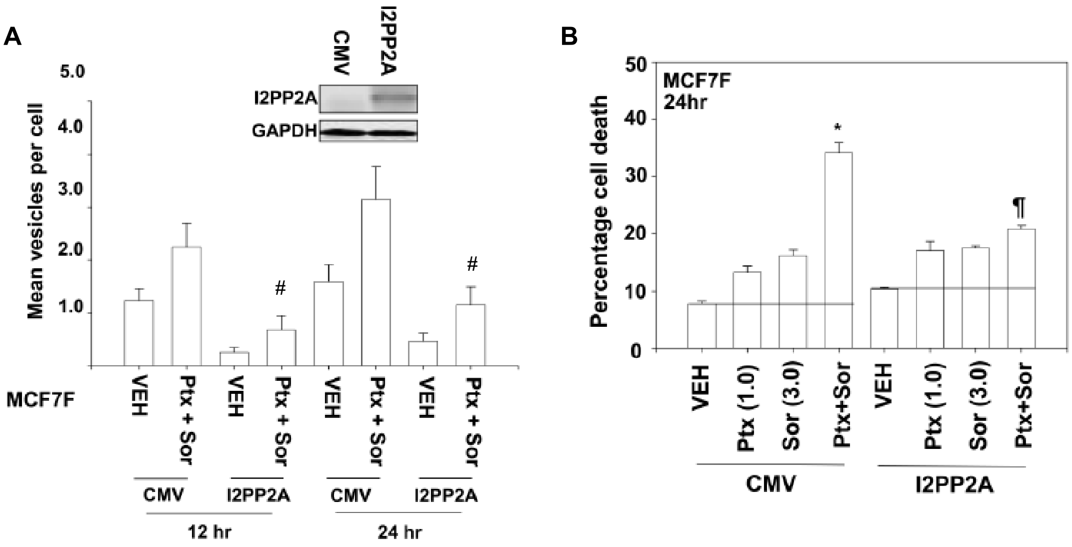

Figure 5-9: Overexpression of I2PP2A suppresses drug-induced autophagy and toxicity in MCF7F cells. Cells were plated in media containing dialyzed serum and cultured for 24 hr prior to transfection with a vector control plasmid or plasmid to overexpress I2PP2A. 36 hr after transfection, cells were treated with vehicle or pemetrexed (1µM) and sorafenib (3µM) for the indicated times. (A) Western blot analysis verifying overexpression of I2PP2A in MCF7F cells (upper). Overexpression of I2PP2A suppresses drug combination-induced autophagic vesicle formation at 12 and 24 hr time points$^{\#}$ ($p<0.05$ less than corresponding value in CMV vector control-transfected cells). (B) Pemetrexed/ sorafenib treatment causes an enhancement in cell death* ($p<0.05$) which is abolished upon overexpression of I2PP2A¶ ($p<0.05$ less than corresponding value in CMV vector control-transfected cells).

Collectively, these findings strongly suggest that PP2A activity is a factor in pemetrexed/ sorafenib-induced cytotoxicity in mammary carcinoma cells, based on overexpression of I2PP2A. One avenue of investigation for enhancement of PP2A activity resulting from combination drug therapy involves the generation of bio-active lipids, such as ceramides. In recent years, I2PP2A was found to interact with ceramides, preventing its inhibitory association with PP2A. The PP2A heterotrimer itself also has been shown to interact with ceramide, with ceramide promoting

PP2A activation. These phenomena were found to occur in multiple tumor types, arguing for a tumor suppressive role for PP2A (208). Because PP2A activity was shown to promote drug combination sensitivity in the tumor models used in this study, we theorized that ceramide levels may also be elevated in these cells as a result of drug-induced cellular stress.

5.6 Drug combination interactions in breast cancer cells are ceramide-dependent

To determine if PP2A activation was ceramide-dependent, we first examined whether loss of ceramide synthase 6 (LASS6), the enzyme responsible for *de novo* ceramide synthesis of 16 carbon (C16) lipids, could alter drug combination-enhanced PP2A activation. Knockdown of LASS6 in MCF7F and BT474 cells blocked the enhancement of PP2A activity caused by pemetrexed/ sorafenib treatment (Figure 5-10).

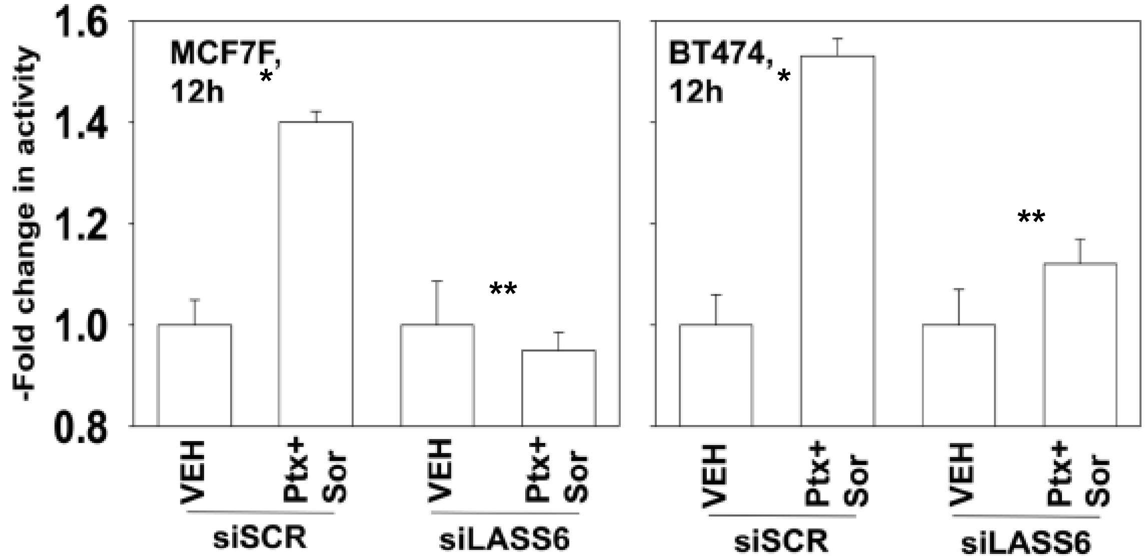

Figure 5-10: Knockdown of LASS6 abolishes drug combination-induced activation of PP2A in breast cancer cells. Cells were plated in triplicate with media containing dialyzed serum and cultured for 24 hr prior to transfection with control siRNA or siRNA specifically targeting LASS6. 36 hr after transfection, cells were treated with vehicle or pemetrexed (1μM) and sorafenib (3μM) for 12 hr. Lysates were collected and PP2A activity was evaluated. Activity values were quantified by cell number for each sample, which agreed with GAPDH normalization values, then represented as –Fold change in activity. Treatment of MCF7F and BT474 cells caused a significant increase in PP2A activity at 12 hr[*] ($p<0.05$). Knockdown of LASS6 significantly reduced drug combination-induced enhancement of PP2A activity in these cells[**] ($p<0.05$).

Studies were performed to determine if pemetrexed/ sorafenib treatment caused an increase in ceramide and dihydroceramide levels in breast cancer cells. In BT474 cells, co-treatment with these drugs increased the levels of C16:0, C22:0, C24:1, and C24:0 dihydroceramides (Figure 5-11). The increase in dihydroceramide levels was reduced for C16:0 upon knockdown of LASS6. However, the increases in C22:0, C24:1, and C24:0 levels that occur as a result of drug combination treatment, were not altered by reducing the expression of LASS6 (Figure 5-11). The levels of C16:0, C22:0, C24:1, and C24:0 ceramides were not significantly altered by treatment with pemetrexed/ sorafenib or by knockdown of LASS6 in the cells used in this study (Figure 5-11).

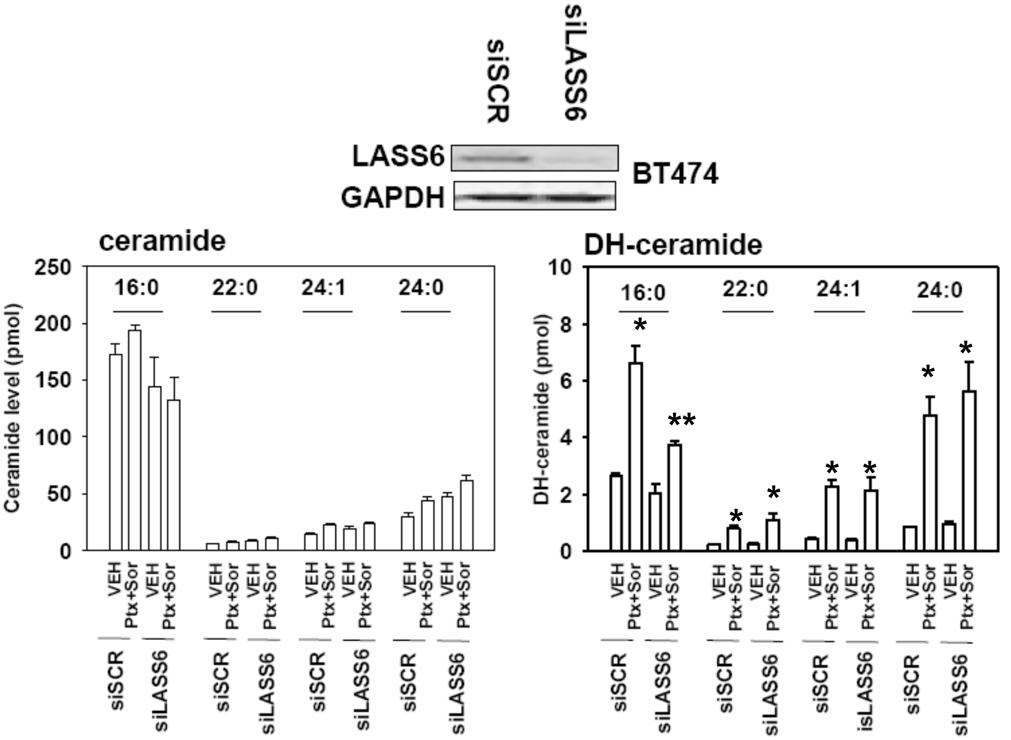

Figure 5-11: The *de novo* ceramide synthesis pathway plays a role in the toxic interaction of pemetrexed and sorafenib in BT474 cells. Cells were plated in triplicate with media containing dialyzed serum and cultured for 24 hr prior to transfection with control siRNA or siRNA specifically targeting LASS-6. 36 hr after transfection, cells were treated with vehicle or pemetrexed (1μM) and sorafenib (3μM) for 24 hr. Lysates were harvested and samples evaluated for ceramide levels using an HPLC-MS-MS analysis method. Values were normalized by cell number, which was verified by immunoblotting for GAPDH levels, then levels were quantified according to known standard concentration levels. Western blot analysis verifying the knockdown of LASS6 in BT474 cells (upper panel). Analysis of vector control versus si-LASS6 samples, when treated with vehicle or drug combination, yielded no significant variations is ceramide levels (bottom, left panel). Evaluation of the levels of dihydro-ceramides were all elevated as a result of pemetrexed/ sorafenib treatment* ($p<0.05$), however in the case of 16:0 dihydroceramide, knockdown of si-LASS6 suppressed combination drug-induced di-hydro-ceramide generation (bottom, right panel)** ($p<0.05$). Raw data for ceramide and dihydroceramide levels were obtained by Jeremy Allegood of the Lipidomics/ Metabolomics Facility at VCU.

The data presented here suggests that PP2A activity is enhanced in breast cancer cells treated with pemetrexed/ sorafenib and that it may be in part responsible for drug-induced autophagy and cell death. These findings also suggest that PP2A activity is dependent upon ceramide production and that C16:0 dihydroceramides levels are regulated by LASS6, which was found to likely play a role in the cytotoxic interaction of these drugs. Together, these findings suggest that there may be a link between PP2A activity and the generation of dihydroceramides, which are both conducive for a toxic form of autophagy caused by co-treatment of breast cancer cells with pemetrexed and sorafenib.

Chapter 6: Discussion

Pemetrexed, a second generation anti-folate drug approved for the treatment of malignant pleural mesothelioma and advanced or metastatic NSCLC, was reported to induce autophagy in tumor cells by causing an increase in intracellular ZMP^+ levels that lead to stimulation of AMPK. AMPK activation leads to inhibition of mTOR and promotion of early autophagic vesicle formation (243-244,249). No specific role for autophagy, whether pro-survival or pro-death was identified for pemetrexed-treated tumor cells in these studies. Studies in this thesis aimed to first address the role of autophagy in response to pemetrexed exposure in multiple cancer cell types. Data indicated that in H460 NSCLC cells, pemetrexed treatment caused an increase in autophagic vesicle formation and that drug-induced enhancement of autophagy correlates with a dose-dependent decrease in cell viability. Knockdown of Beclin1 or pre-treatment of the cells with 3-MA to inhibit formation of the autophagosome attenuates these effects. These results were also noted in 4T1 and BT474 mammary carcinoma cells, as well as HuH7 human hepatoma cells. Together, these data illustrate that pemetrexed lethality is dependent on a cytotoxic form of autophagy in multiple tumor types.

These findings may in part be explained by pemetrexed induced inhibition of a secondary target AICART, the second folate-dependent enzyme in the *de novo* purine biosynthetic pathway which catalyzes the conversion of ZMP^+ (AICAR) into formyl-AICAR. Inhibition of AICART results in intracellular accumulation of ZMP^+, a substrate for this reaction known to cause ER stress resulting in activation of the AMPK pathway for the purpose of restoring cellular homeostasis. Activation of AMPK leads to the inhibition of mTOR. mTOR is universally accepted to be the gatekeeper for autophagic cellular responses through its interactions with Akt and AMPK pathway members. Inhibition of mTOR enables the association of ATG proteins, which is necessary for formation of the autophagosome. Autophagy can be utilized as a mechanism by which the cell recycles its components to restore homeostasis in the cell or in some cases, as a means to cell death. In these studies, treatment of tumor cells with pemetrexed resulted in the latter, thus providing an explanation as to the mode of drug lethality (Figure 6-1).

Based on work in our laboratory and others, we hypothesized that sorafenib, a relatively promiscuous RTK inhibitor known to also induce a cytotoxic form of autophagy, may interact with pemetrexed in a manner which enhances pemetrexed cytotoxicity in these tumor cells (284-287). Our lab reported in earlier studies that combining sorafenib with vorinostat further induced vorinostat cytotoxicity in gastrointestinal cancer cells that was dependent on ceramide generation resultant of CD95 and PERK activation (181,202,315-317,316-318). In H460 NSCLC cells, co-treatment with pemetrexed and sorafenib at concentrations well below the maximal achievable dose for each caused a dose-dependent enhancement of autophagy which corresponded with a dose-dependent increase in cell death. Combination drug treatment elucidated similar effects in breast and hepatic carcinoma cell models. We also tested the effectiveness of pemetrexed/ sorafenib co-treatment in several breast cancer cell types of variable lineages, to determine if this combination therapy was effective in, both, Her2+ (SKBR3, BT474) and estrogen-independent triple negative (BT549, HCC1187, HCC1937) breast tumor cells. All breast cancer cell lines demonstrated a dose-dependent increase in cell death when treated with pemetrexed and sorafenib at variable concentrations, BT549 cells required a higher dosage to achieve the same lethal effect. Taken together, these data support the notion that pemetrexed/ sorafenib co-therapy is effective in the treatment of both ER+ and triple negative mammary carcinoma cells.

Acquired drug resistance as a result of developing estrogen independence is a major obstacle in the treatment of breast cancer patients undergoing continued drug treatments. Faslodex (fulvestrant) has proven beneficial for the treatment of ER+ metastatic breast cancer in post-menopausal patients who had been previously been treated with tamoxifen then become resistant. This effect is likely due to the distinct mode of action by which fulvestrant inhibits estrogen signaling (298-299). Fulvestrant is typically issued as a second-line therapy, in breast cancer patients who have developed a resistance to a first-line chemotherapeutic regimen, whilst there are many patients that will also develop a resistance to fulvestrant (299-300). MCF7 is a well-characterized ER+ mammary ductal epithelial cell line isolated from a pleural effusion of a post-menopausal woman (301). Nephew and colleagues developed a fulvestrant-resistant MCF7 model (MCF7F) through stringent selection of cells able to bypass estrogen-dependence after exposure to 1 μM fulvestrant for 18 months (302). MCF7F cells are known to express higher levels of EGFR and breast cancer resistance protein (BCRP) than their parental counterparts. For this reason, we compared the drug combination sensitivities of parental MCF7 to fulvestrant-resistant MCF7F cells. We found that cell death was enhanced in both cell lines in a greater than additive fashion, when compared to individual drug treated cells, MCF7F cells were more sensitive to the drug combination.

In an attempt to elucidate the biochemical mechanisms by which these drugs interact, as well as to further characterize the mechanisms by which fulvestrant-resistant MCF7F cells are more responsive to pemetrexed/ sorafenib cotreatment, studies were undertaken to compare the expression patterns of autophagy-related proteins for estrogen-dependent and fulvestrant-resistant MCF7 cells. It is well accepted that many primary breast cancers including MCF7 cells, express a haplotype of Beclin1 that leads to an insufficiency of the protein causing these cells to be less effective at inducing autophagy than non-transformed mammary epithelial cells (303). Parental MCF7 cells were compared to fulvestrant-resistant MCF7F cells which are no longer responsive to estrogen. MCF7F cells expressed higher basal levels of autophagy-related proteins (Beclin1, ATG5-12, LC3II, p62) than parental MCF7 cells. Both, MCF7 and MCF7F cells, demonstrated an increase in the levels of Beclin1 when treated with individual drugs which was further enhanced by drug combination. The levels of ATG5-12 and LC3II were also enhanced in both cell lines when treated with individual drugs and the drug combination. In agreement with these findings, the levels of p62 were reduced in both cell lines when treated with the drug combination, demonstrating that autophagy was progressing to the late stage endosomal state where p62 becomes enzymatically cleaved for recycling of amino acids. Higher basal expression of autophagy related proteins suggests that a protective form of autophagy may be occurring as a result of biochemical changes made within the cell to establish estrogen independence. In comparison to parental MCF7 cells, MCF7F cells also expressed higher basal levels of protective Mcl-1 and Bcl-XL proteins, this may further explain how MCF7F cells engage in a protective form of autophagy basally. However, when treated with the drug combination, MCF7F cells demonstrated a significantly greater reduction in the levels of Mcl-1 and Bcl-XL, which may suggest an explanation as to how these cells are more sensitive to pemetrexed/ sorafenib co-therapy. In summation: the expression patterns of protective Bcl-2 family member proteins, as well as proteins involved autophagy, suggest that MCF7F cells demonstrate higher basal levels of autophagy, which may exist as a result of a protective effort to maintain a natural energy and nutrient state resultant of biochemical changes that have occurred as a result of establishing estrogen independence. The level of autophagy-dependent protein expression were enhanced in both cells lines when treated with the pemetrexed/ sorafenib combination, whilst the levels of protective Mcl-1 and Bcl-XL proteins were significantly reduced in MCF7F cells. These findings suggest that the enhanced induction of autophagy in MCF7F cells exists as a protective means of maintaining cellular homeostasis post-establishment of estrogen independence, and that drug combination induced changes in protective Bcl-2 family members and autophagy related proteins and may in part explain why these cells are more sensitive to the drugs than their estrogen dependent counterparts.

Autophagy and the intrinsic apoptosis pathway are inter-connected processes. These pathways have been reported to interact to alter cell viability during ER stress caused by ROS generation in the cell. There are multiple means by which intracellular generation of ROS and ER stress can promote cell death. One of the best characterized mechanisms of ROS-stimulated cell death involves protein kinase RNA-like endoplasmic reticulum kinase (PERK) (202). PERK phosphorylates eukaryotic initiation factor 2α (eI2Fα), which attenuates transcription leading to a reduction in translation of protective Bcl-2 family member proteins, namely Mcl-1, thereby enabling Beclin1 to carry out its role in initiation of autophagosomal membrane formation (202,318-320). Treatment with pemetrexed and sorafenib was shown to cause a reduction in Mcl-1 and Bcl-XL protein expression, as well as an increase in the levels of Beclin1 unsequestered by these protective BH3-domain containing proteins in parental and fulvestrant-resistant MCF7 cells. The roles of extrinsic apoptosis, intrinsic apoptosis, and autophagy were assessed in our combination treated cells. Overexpression of c-FLIP-s in MCF7 and MCF7F cells did not significantly alter drug combination induced toxicity, overexpression of a dominant-negative form of caspase-9 or protective Bcl-XL reduced pemetrexed/ sorafenib toxicity in these cells. These results suggested that pemetrexed/ sorafenib induced cell killing was not dependent upon the extrinsic apoptotic pathway, rather a mitochondria dependent mechanism.

To determine the mechanisms by which pemetrexed/ sorafenib treatment propagates a cytotoxic death signal in MCF7 and MCF7F cells, the activation status of several important protein kinases involved in cell survival and cell death by evaluating phosphorylation at their regulatory sites was examined. MCF7F cells express higher basal levels of protein expression of activated p70 S6K and mTOR than parental MCF7 cells, as well as demonstrating a more significant reduction in activation of these proteins when treated with pemetrexed and sorafenib. Knockdown of p70 S6K and mTOR in MCF7F cells exhibited a greater enhancement of cell death when treated with the pemetrexed/ sorafenib combination than did parental MCF7 cells. These results are in agreement with the initial observations suggesting MCF7F cells were more sensitive to drug combination treatment. Likewise, overexpression of constitutively active forms of p70 S6K or mTOR resulted in a decrease in drug combination induced cell death in MCF7 and MCF7F cells. This data indicated that higher basal expression of p70 S6K and mTOR, as well as higher basal expression of activated p70 S6K and mTOR, may offer a survival advantage in breast cancer cells having established estrogen independence. Akt activity is known to regulate both of these pathways, the levels of Akt phosphorylation were not significantly altered by pemetrexed/ sorafenib treatment in either cell line. This may be explained by an increase in Erk1/2 phosphorylation, as signaling through Erk1/2 has been linked to increased autophagy in several different cell types (326-327,321-322). Erk1/2 activation was enhanced in both parental and fulvestrant-resistant MCF7 cells treated with the drug combination, while it was found to be more significant in parental MCF7 cells. This data suggested a complex mechanism by which these drugs interact to induce a cytotoxic response in breast cancer cells.

A comparison of RTK expression levels for MCF7 and MCF7F cells demonstrated that MCF7F cells express higher basal expression of FGFR1 and PDGFRβ, both secondary targets of sorafenib. These results suggested that these membrane receptors may be important targets for sorafenib in breast cancer cells at the concentrations used in the studies presented here. The effects of PDGFRß knockdown in these cell lines were evaluated to determine the contribution of PDGFRβ in the toxic interactions of pemetrexed and sorafenib. Treatment of MCF7 and MCF7F cells with pemetrexed post-knockdown of PDGFRβ enhanced cell death percentages in each cell line, suggesting that PDGFRβ might important target for sorafenib in these breast cancer cells. MCF7F express higher basal levels of PDGFRβ, offering one possible rationale as to why these cells may be more sensitive than parental MCF7 cell to the pemetrexed/ sorafenib cotherapy.

To summarize: MCF7F cells are more sensitive to pemetrexed/ sorafenib combination treatment than parental MCF7 cells. Data presented here offers several plausible explanations as to how this might occur. First, MCF7F cells express higher basal levels of autophagy related proteins, likely as a protective effort in these cells. However, when expression of these proteins is further enhanced by treatment with pemetrexed and sorafenib; the balance shifts in favor of a cytotoxic form of autophagy that leads to cell death. MCF7F cells also express higher basal levels of protective Bcl-2 family member proteins, Mcl-1 and Bcl-XL, which correlates with the notion that higher basal levels of autophagy serve to protect these cells under normal conditions. Upon co-treatment with pemetrexed and sorafenib, MCF7F cells demonstrated a greater reduction in the levels of Mcl-1 and Bcl-XL, illustrating the possibility that these proteins may be key regulators of the shift from a cytoprotective to cytotoxic form of autophagy. In addition, enhanced basal PDGFRβ expression levels may offer an explanation as to how MCF7F cells are more sensitive to treatment with pemetrexed alone or pemetrexed/ sorafenib cotreatment, as PDGFRβ appears to be a key target of sorafenib in these cells.

In the second chapter of results, possible roles for Src, PP2A, I2PP2A, and *de novo* ceramide synthesis in the Erk1/2-dependent interaction of pemetrexed and sorafenib in mammary carcinoma cells were investigated. Again, we show that pemetrexed and sorafenib co-therapy stimulated autophagy and cell death in breast cancer cells (BT474 and MCF7F), which was suppressed by knockdown of Beclin1. Studies concerning the progression of early autophagic vesicles to the stage of the late endosome, where proteolytic degradation of autophagolysosome components takes place suggested that in both cell lines, treatment with pemetrexed and sorafenib enhanced late stage endosomal activity in a dose dependent manner. This effect was shown to be suppressed by knockdown of Beclin1, this potentially indicated that an induction of early autophagosome formation was necessary for this response. The requirement for acidic endosome acidification in this response was assessed by cell death analysis. Results indicated that inhibiting endosome acidification by treatment with NH_4Cl completely abolished drug combination-induced toxicity in BT474 and MCF7F cells.

According to an earlier study reported by our laboratory and others, sorafenib treatment can lead to inhibition of PDGFRβ and activation of Src, which in turn promotes activation of the CD95 death cell receptor and induction of the extrinsic apoptotic pathway (315-317). In BT474 cells knocked down for PDGFRβ, led to an almost two-fold increase in p-Src Y416. This led to the evaluation Src activation in the response of BT474 and MCF7F cells to pemetrexed/ sorafenib cotherapy. When examining the formation of early autophagic vesicles in BT474 cells overexpressing dnSrc, it was found that Src was required for the pemetrexed/ sorefenib interaction in these cells. Examination of Src Tyr416 phosphorylation in BT474 cells, when knocked down for PDGFRβ, indicated that Src activation is enhanced by a reduction in activation of PDGFRβ. This have may occured as a result of Src becoming available to interact with an alternative upstream activator, possibly another RTK on the plasma membrane (Figure 6-1). Overexpression of dnSrc in MCF7F cells was shown to suppress drug combination-induced cell killing, suggesting that in Her2-negative cells, Src activation was also important for the pemetrexed/ sorafenib interaction. Src interacts intra-cellularly with multiple RTKs,, Indeed, Src is well-documented to interact with EGFR/Her1 and Her2/neu receptors that are known to be overexpressed in 20-30% of breast cancer patients (323-324). Other Src activating RTKs include FGFR1 and Met, these receptors also happen to be known secondary targets of sorafenib. It is possible that inhibition of PDGFRβ releases Src from its interactions with this receptor, enabling Src interactions with other RTKs such as EGFR and Her2 through the aid of adaptor proteins. In the case of BT474, which expresses both receptors and to overexpress Her2, Src may interact with either receptor to become activated and signal to downstream effectors to promote activation of the MEK/Erk pathway and enhancement of lipid metabolism. In the case of MCF7F cells, which are Her2 negative, Src may still interact with EGFR to promote the same downstream signaling outcomes. This is just one explanation as to the activation of Src in breast cancer cells where PDGFRβ signaling is inhibited as a result of pemetrexed/ sorafenib co-treatment, more specifically sorafenib treatment. Src may also be activated by other RTKs as well as multiple cytoplasmic kinases upon treatment with pemetrexed and sorafenib.

An assessment of whether Src activation was required for MEK/Erk activation in the pemetrexed/ sorafenib response was performed. Overexpression of dnSrc attenuated the drug-induced levels of activated Erk in BT474 cells. To further validate these signaling phenomena dnMEK1 was overexpressed in BT474, MCF7, and MCF7F cells. Results indicated that the lethal effects of co-treatment with pemetrexed and sorafenib were significantly reduced by the effects of overexpressing a non-functional form of MEK. Overexpression of dnMEK1 in MCF7F cells was shown to reduce drug-combination induction of early autophagosome formation. Overexpression of dnMEK1 also dramatically reduced late stage endosomal activity in these cells. Together, these data suggest that Src may mediate activation of MEK/Erk which we found is strongly upregulated in breast cancer cells in response to pemetrexed/ sorafenib-treatment.

Protein phosphatases are important modulators of signal transduction pathways. PP1 and PP2A account for 90% of serine/ threonine phosphatase activity in mammalian cells. Their activation is regulated by multiple protein signals, including the Src signaling network. PP2A is know to be an important regulator of the Erk1/2 pathway and is thought to become less active as a tumor progresses to an advanced state. We analyzed the role of PP2A in the Erk1/2-dependent interaction between pemetrexed and sorafenib in breast cancer cells by overexpressing I2PP2A, an inhibitory protein for PP2A. Results indicated that MCF7F cells expressed higher basal levels of I2PP2A and phospho-Erk1/2 when compared to parental MCF7 cells, I2PP2A levels were enhanced in both cells lines when exposed to pemetrexed/ sorafenib co-therapy. Based upon evaluation of PP2A activity in these cells using a PP2A-specific activity assay kit, PP2A basal activity was determined to be greater in parental MCF7 cells when compared to MCF7F cells. This finding can at least in part be explained by the differences in I2PP2A expression levels in these cell lines. Treatment of MCF7F cells with the drug combination caused an increase in Erk1/2 activation and PP2A activity, which was suppressed by overexpression of I2PP2A. It is important to note that the basal expression of phospho-Erk1/2 in MCF7F cells was increased in response to overexpression of I2PP2A, while there was no further activation of Erk1/2 when the cells were treated with pemetrexed and sorafenib. Overexpression of I2PP2A in MCF7F cells also led to a significant reduction in pemetrexed/ sorafenib-stimulated early autophagic vesicle formation and cell lethality. PP2A activity was also shown to be altered during pemetrexed/ sorafenib-induced cell death for MCF7F cells.

Many studies have reported that PP2A activity can be regulated by bio-active lipids, more specifically ceramides (177,179,181-183,186,189,196,198,200,208-209,294,325-326) (Figure 6-1). It is also well documented that Src activation can mediate lipid metabolism in breast cancer cells (324). Having identified a clear role for PP2A activation in cellular response to pemetrexed/ sorafenib exposure, the importance of ceramide generation in regulating drug combination enhanced activation of PP2A was evaluated. The *de novo* ceramide synthesis pathway can be responsible for activation of PP2A and induction of autophagy, LASS6 generation of C16 dihydroceramides has also been identified in several studies as a key player in ceramide synthesis (202,327-328). Results of the examination of PP2A activity in MCF7F and BT474 cells indicated that pemetrexed/ sorafenib-stimulated PP2A activation was significantly reduced by knockdown of LASS6. Drug combination mediated enhanced PP2A activity appeared to be more strongly reduced by knockdown of LASS6 in BT474 cells than in MCF7 cells. The proportions of C:16, C22:0, C24:1, and C24:0 ceramides and dihydroceramides were evaluated for drug treated BT474 cells knocked down for LASS6 using an adapted version of an established HPLC Mass Spectroscopy method (329). Normal ceramide levels were not significantly altered by knockdown of LASS6 or drug treatment Pemetrexed/ sorafenib treatment was shown to induce an increase in all dihydroceramide levels examined. LASS6 knockdown led to a suppression of the drug induced enhancement of C16:0 dihydroceramide level, this was expected, since LASS6 is the *de novo* enzyme responsible for specifically generating this lipid. The observed increase in C22:0, C24:1, and C24:0 dihydroceramide levels caused by pemetrexed/ sorafenib treatment were not affected by inhibiting LASS6 expression. Knockdown of LASS6 also led to suppression of drug combination stimulated formation of early autophagic vesicles and cell killing in BT474 cells. Treatment of BT474 cells with myriocin, a small molecule inhibitor of serine palmitoyltransferase of the *de novo* synthesis pathway, effectively enhanced the suppression of drug-induced cell death. These findings suggest that *de novo* ceramide synthesis is involved in the toxic interaction of pemetrexed/ sorafenib in breast cancer cells and that C16:0 dihydroceramimdes are somehow important in this response. Other dihydrocermides may be critical for this response; however only C16:0 dihydroceramide generation by manipulating the expression of LASS6 was evaluated in this study. Other *de novo* ceramide synthetic enzymes may have an effect similar to that of LASS6, however these enzymes were not specifically examined. Together with previous data, it can be concluded that *de novo* ceramide synthesis is required for activation of PP2A and that this event is critical for induction of autophagy and cell death in breast cancer cells (Figure 6-1). Several chemotherapeutic agents have been identified which cause upregulation of *de novo* ceramide synthesis in co-ordination with cell death, for example: daunorubicin, cisplatin, etoposide, gemcitabine, camptothecin, and fludurabine (325-326). Dihydroceramides may not themselves induce apoptosis, although earlier studies have suggested that a dehydrogenase becomes activated to promote generation of ceramides which promote apoptosis in these tumor cells (326).

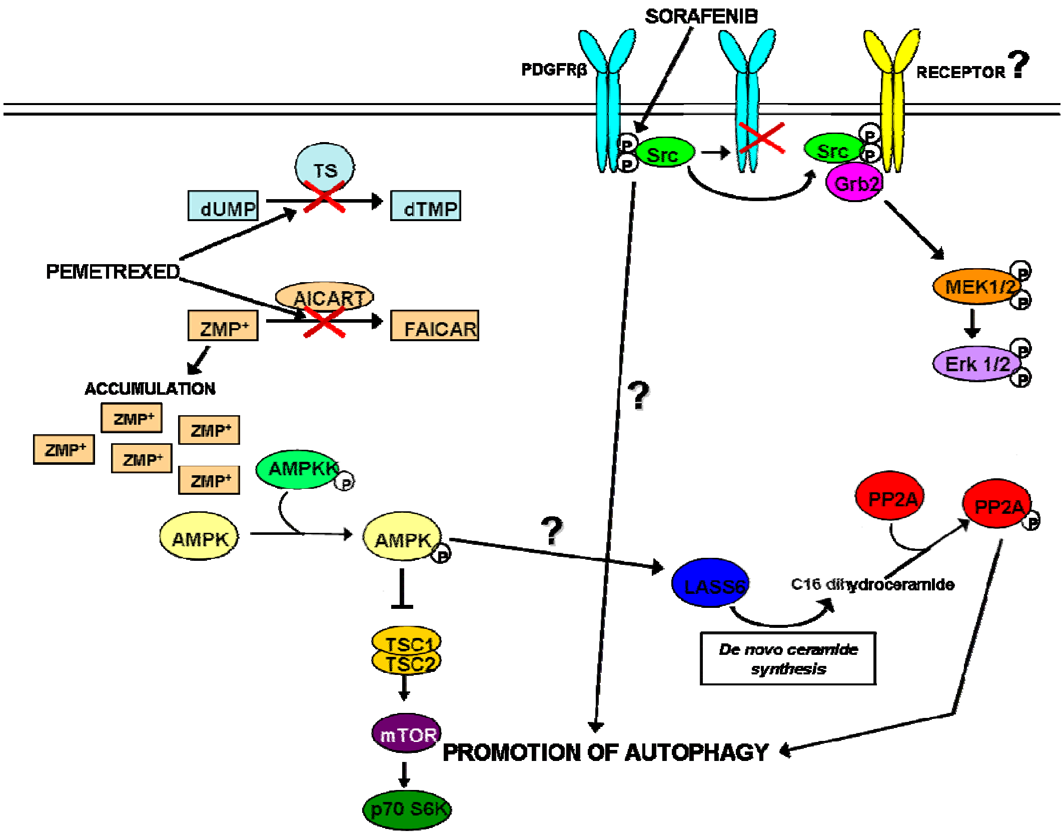
SORAFENIB
PDGFRβ
RECEPTOR ?
P
P
Src
Src
P
P
Grb2
TS
dUMP
dTMP
PEMETREXED
AICART
ZMP+
FAICAR
MEK1/2
P
P
Erk 1/2
P
P
ACCUMULATION
ZMP+
ZMP+
ZMP+
ZMP+
ZMP+
?
AMPKK
P
AMPK
AMPK
P
?
PP2A
PP2A
P
LASS6
C16 dihydroceramide
De novo ceramide synthesis
TSC1
TSC2
mTOR
PROMOTION OF AUTOPHAGY
p70 S6K

Figure 6-1: A working model of the mechanisms which promote cytotoxicity as a result of cotreatment of breast cancer cells with pemetrexed and sorafenib. Pemetrexed inhibition of its secondary target, AICART, leads to an increase in intracellular ZMP$^+$ levels to induce AMPK activation and subsequent inhibition of mTOR, thus promoting autophagy. AMPK activation is known to induce *de novo* ceramide synthesis, while the mechanism by which this occurs is not known. PP2A becomes activated as a result of the changes in dihydroceramide levels, which can be explained by several mechanisms. Exposure of breast cancer cells to sorafenib was demonstrated to interfere with PDGFRβ activity, a known target for the drug, resulting in disruption of the PDGFRβ-Src interaction; therefore enabling an interaction between Src and an alternate RTK. Src is hyperactivated by the alternate RTK and signaling is transduced through the MEK/ERK pathway. Sorafenib enhances pemetrexed-induced toxic autophagy through a mechanism which has yet to be determined. Together, pemetrexed and sorafenib, act in at least an additive fashion to promote cell lethality.

In addition to these *in vitro* findings, an *in vivo* orthotopic model of breast cancer was generated using BT474. Results in this model system indicated that combination therapy with pemetrexed and sorafenib was able to suppress BT474 tumor cell growth in a greater fashion than individual drugs alone. The *in vivo* data correlated with increased levels of apoptosis, as well as reduced proliferation in these tumors. In additional studies involving pemetrexed and sorafenib combination treatment, the same effect was seen using an *in vivo* orthotopic model of GBM6 human glioblastoma cells stably expressing the luciferase gene. GBM6-luciferase cells demonstrated a marked decrease in tumor cell growth, as well as an increase in overall survival for mice co-treated with the drugs when compared to individual drugs alone (31). Sections from normal tissue/ organs were analyzed from both breast carcinoma and glioblastoma models and no deleterious effects were noted. *In vivo* experiments supported the notion that combination treatment with pemetrexed and sorafenib was an effective combination therapy for the treatment of multiple cancer cell types.

Collectively, the studies detailed in this dissertation illustrate the effectiveness of pemetrexed/ sorafenib co-therapy for the treatment of multiple tumor types. Experimental results illustrated a clear role for a toxic form of autophagy in drug combination lethality. *In vivo*, the drugs interact to significantly reduce tumor growth for orthotopic mammary carcinoma and glioblastoma mice models. Development of estrogen independence as a result of acquired chemotherapeutic drug resistance appeared to play a role in the sensitivity of the breast cancer cell lines tested to pemetrexed/ sorafenib co-therapy. These findings suggested that this combination treatment regimen may be an effective means of treating triple negative breast cancer patients who have received earlier treatments with drugs for which they are no longer responsive.

Literature Cited

Literature Cited

1. American Cancer Society. "Cancer Facts & Figures 2012". Atlanta: American Cancer Society; 2012.

2. Lindsey CW. Allosteric Akt(PKB) inhibitors: Discovery and SAR of isoenzyme selective inihibitors. Med Chem Letters 2005; 15: 761-764.

3. Wada T, Penninger JM. Mitogen-activated protein kinases in apoptosis regulation. Oncogene 2004; 23(16): 2838-2849.

4. Wang X, Tournior C. Regulation of cellular functions by ERK5 signaling pathway. Cell Signaling 2006; 18(6): 753-760.

5. Heasley LE, Han SY. JNK regulation of oncogenesis. Molecules and Cells 2006; 21(2): 167-173.

6. Mittelstadt PR, Salvador JM, Fornace AJ Jr, Ashwell JD. Activating p38 MAPK: New tricks for an old kinase. Cell Cycle 2005; 4(9): 1189-1192.

7. Chuderland D, Seger R. Protein-protein interactions in the regulation of the extracellular signal-regulated kinase. Molecular Biotechnology 2005; 29(1): 57-74.

8. Barros JC, Marshall CJ. Activation of either ERK1/2 or ERK5 MAP kinase pathways can lead to disruption of the action cytoskeleton. Journal of Cell Science 2005; 118: 1663-1671.

9. Nishimoto S, Nishida E. MAPK Signaling: ERK5 versus ERK1/2. Embo Reports 2006; 7(8): 792-786.

10. Ranganathan A, Pearson GW, Chrestensen CA, Sturgill TW, Cobb MH. The MAP kinase binds to and phosphorylates p90 RSK. Arch Biochem Biophys 2006; 449(1-2): 8-16.

11. Wagner EF, Nebreda AR. Signal integration by JNK and p38 MAPK pathways in cancer development. Nature Reviews in Cancer 2009; 9(8): 537-549.

12. McCubrey JA, Stealman LS, Chappel WH, Abrams SL, Wong EW, Chang F, Lehmann B, Terrian DM, Millella M,m Tafuri A, Stivala F, Libra M, *et al*. Raf/ MEK/ ERK pathway in cell growth, malignant transformation, and drug resistance. Biochim Biophys Acta 2007; 1773(8): 1263-1284.

13. Kim EK, Chol EJ. Pathalogical roles of MAPK signaling pathways in human disease. Biochim Biophys Acta 2010; 1802(4): 396-405.

14. Kato T, Tapping RI, Huang S, Watson MH, Ulevitch RJ, Lee JD. Bmk1/ERK5 is required for cell proliferation induced by epidermal growth factor. Nature 1998; 395(6703): 713-716.

15. Raman M, Chen W, Cobb MH. Differential regulation and properties of MAPKs. Oncogene 2007; 26: 3100-3112.

16. Yang T, Lu Z, Meng L, Wel S, Hong K, Zhu W, Huang C. The novel agent ophiobolin O induces apoptosis and cell cycle arrest of MCF7 cells through activation of MAPK signaling pathways. Bioorg Med Chem Lett 2011; 22(1): 579-585.

17. Rubinfeld H, Seger R. The ERK cascade: a prototype of MAPK signaling. Mol Biotechnol 2005; 31(2): 151-174.

18. Kohno M, Tanimura S, Ozaki K. Targeting the extracellular signal-related kinase pathway in cancer therapy. Biol Pharm Bull 2011; 34(12): 1781-1784.

19. Kolch W. Meaningful relationships: the regulation of the Ras/Raf/MEK/Erk pathway by protein interactions. Biochemistry Journal 2000; 351(Pt 2): 289-305.

20. Maurer G, Tarkowski B, Baccariui M. Raf kinases in cancer: roles and therapeutic opportunities. Oncogene 2011; 30: 3477-3488.

21. Davies H, *et al*. Mutations of the BRAF gene in human cancer. Nature 2002; 417: 949-954.

22. Trakul N, Rosner MR. Modulation of the MAP kinase signaling cascade by Raf kinase inhibitory protein. Cell Research 2005; 15(1): 19-23.

23. Yan M, Templeton DJ. Identification of 2 serine residues of MEK1 that are differentially phosphorylated during activation by Raf and MEK kinase. Journal of Cell Biology 1994; 269(29): 19067-19073.

24. Ramos JW. The regulation of extracellular signal-related kinase (ERK) in mammalian cells. The International Journal of Biochemistry and Cell Biology 2008; 40(12): 2707-2719.

25. Ahn NG, Seger R, Bratlien RL, Diltz CD, Tonks NK, Krebs EG. Multiple components of an epidermal growth factor-stimulated protein kinase cascade. In vitro activation of a

myelin basic protein/ microtubule-associated protein 2 kinase. Journal of Biological Chemistry 1991; 266(7): 4220-4227.

26. Warn-Cramer BJ, Cottrell GT, Burt JM, Lan AF. Regulation of connexin 43 gap junctional extracellular communication by MAP-activated protein kinase. Journal of Biological Chemistry 1998; 273(15): 9188-9196.

27. Fukuda Y, Gotoh Y, Nishida E. Interactions of MAP kinase with MAP kinase kinase: its possible role in the control of nucleocytoplasmic transport of MAP kinase. EMBO Journal 1997; 16: 1901-1908.

28. Kohno M, Pouyssegui J. Targeting the ERK signaling pathway in cancer therapy. Annalysis of Medicine 2006; 38: 200-211.

29. Yoon S, Seegar R. The extracellular signal-related kinase: multiple substrates regulate diverse cellular functions. Growth factors 2006; 24:21-44.

30. Favoni PE, Pattarozzi A, Lo Casto M, Barbieri F, Gatti M, Paleari L, Bajetto A, Porcile C, Mutti L, Corte G, Florio T. Gefitinib targets EGFR dimerization and ERK1/2 phosphorylation to inhibit pleural mesothelioma cell proliferation. Curr Cancer Drug Targets 2010; 10(2): 176-191.

31. Bareford MD, Park MA, Yacoub A, Hamed H, Tang Y, Cruickshanks N, Eulitt P, Hubbard N, Tye G, Burow ME, Fisher PB, Moran RG, Nephew KP, Grant S, Dent P. Sorafenib enhances pemetrexed cytotoxicity through an autophagy-dependent mechanism in cancer cells. Cancer Research 2011; 71(14): 4955-4967.

32. Li P, Wood K, Mamon H, Haser W, Roberts R. Raf-1: A kinase currently without a cause but not lacking in effects. Cell 1991; 64: 479-482.

33. Ries S, Biederer C, Woods D, Shifman O, Shira Saua S, Sasazuki T, *et al*. Opposing effects of Ras on p53: transcriptional activation of mdm2 and iduction of p19ARF. Cell 2000; 103: 321-330.

34. Han JA, Kim JI, Ongusana PP, Hwang DH, Ballou LR, Mahale A, *et al*. p53-mediated induction of Cox-2 counteracts p53- or genotoxic stress-induced apoptosis. EMBO Journal 2002; 21: 5635-5644.

35. Fan S, Meng Q, Laterra JJ, Rosen EM. Ras effector pathways modulate scatter factor-stimulated NF-(kappa) B signaling and protection against DNA damage. Oncogene 2007; 26: 4774-4796.

36. Golding SE, Rosenberg E, Niell S, Dent P, Povirk LF, Valerie K. Extracellular signal-related kinase positively regulates ataxia telangiectasia mutated, homologous

recombination repair, and the DNA damage response. Cancer Research 2007; 67: 1046-1053.

37. Kasid U, Suy S, Dent P, Ray S, Whiteside TL, Sturgill TW. Activation of Raf by ionizing radiation. Nature 1996; 382: 813-816.

38. Dai Y, Chen S, Pei XY, Almenara JA, Kramer LB, Venditti CA, *et al*. Interruption of the Ras/MEK/ERK signaling cascade enhances Chk1 inhibitor-induced DNA damage in vitro and in vivo in human multiple myeloma cells. Blood 2008; 112: 2439-2449.

39. Zheng B, Jeong JH, Asara JM, Yuan YY, Granter SR, Chin L, *et al*. Oncogenic B-RAF negatively regulates the tumor suppressor LKB1 to promote melanoma cell proliferation. Molecular Cell 2009; 33: 237-247.

40. Alexia C, Lasfer M, Groyer A. Role of constitutively-activated and insulin-like growth factor-stimulated ERK1/2 signaling in human hepatoma cell proliferation and apoptosis: evidence for heterogenicity of tumor cell lines. Annals of the New York Academy of Science 2004; 1030: 219-229.

41. Wang X, Martindale JL, Holbrook NJ. Requirement for ERK activation in cisplatin-induced apoptosis. Journal of Biological Chemistry 2000; 275: 39435-39443.

42. Zheng A, Kallio A, Harkonen P. Tamoxifen-induced rapid death of MCF-7 breast cancer cells is mediated via extracellularly signal-regulated kinase signaling and can be abrogated by estrogen. Endocrinology 2007; 148(6): 2764-2775.

43. Drew BA, Burow ME, Beckam BS. MEK5/ERK5 pathway: The first fifteen years. Biochim Biophys Acta 2012; 1825(1): 37-48.

44. Wagner EF, Nebreda AR. Signal integration by JNK and p38 MAPK pathways in cancer development. Nature Reviews Cancer 2009; 9: 537-549.

45. Nebrada AR, Porras A. p38 MAP kinases: Beyond the stress response. Trends in Biochem Sci 2000; 25: 257-260.

46. Kyria Kis JM, Auruch J. Mammalian mitogen-activated protein kinase signal transduction pathways activated by stress and inflammation. Physiol Rev 2001; 81: 807-819.

47. Yan F, Wang XM, Liu ZC, Pan C, Yuan SB, Ma QM. JNK1, JNK2, and JNK3 are involved in p-glycoprotein-mediated multidrug resistance of of hepatocellular carcinoma cells. Pancreat Dis Int 2010; 9(3): 287-295.

48. Cuadrado A, Nebreda AR. Mechanisms and functions of p38 MAPK signaling. Biochemistry Journal 2010; 429: 403-417.

49. Lee JC, Laydon JT, McDonnell PC, Gallagher TF, Kumar S, Green D, McNulty D, Blumenthal MJ, Heys JR, Landvatter SW. A protein kinase involved in the regulation of inflammatory cytokine biosynthesis. Nature 1994; 372: 739-746.

50. Jiang Y, Chen C, Li Z, Guo W, Genger JA, Lin S, Han J. Characterization of the structure and function of a new mitogen-activated protein kinase (p38β). Journal of Biological Chemistry 1996; 271: 17920-17926.

51. Lechner C, Zahalkg MA, Grot JF, Moller NP, Ullrich A. ERK-6, a mitogen-activated protein kinase involved in C2C12 myoblast differentiation. PNAS 1996; 93: 4355-4359.

52. Jiang Y, Gram H, Zhao M, New L, Gu J, Feng L, Di Padova F, Ulevitch RJ, Han J. Characterization of structure and function of the fourth member of p38 group mitogen-activated protein kinases, p38δ. Journal of Biological Chemistry 1997; 272(48): 30122-30128.

53. Kocieniewski P, Faeder JR, Lipniacki T. The interplay of double phosphorylation and scaffolding in MAPK pathways. Journal of Theoretical Biology 2012; 295c: 116-124.

54. Ahn YH, Kurie JM. MKK4/SEK1 is negatively regulated through a feedback loop involving the E3 ubiquitin ligase itch. Journal of Biological Chemistry 2009; 284: 29399-29404.

55. Ono K, Han J. The p38 signal transduction pathway: activation and function. Cell Signal 2000; 12: 1-13.

56. Cuenda A, Rousseau S. p38 MAP kinase pathway regulation, functionm and role in human diseases. Biochim Biophys Acta 2007; 1771: 1358-1375.

57. Whitmarsh AJ, Davis RJ. Role of mitogen-activated protein kinase kinase 4 in cancer. Oncogene 2007; 26: 3172-3184.

58. Weston CR, Davis RJ. The JNK signal transduction pathway. Curr Opin Cell Biol 2007; 19(2): 142-149.

59. Ventura JJ, Hubner A, Zhang C, Flavell RA, Shokat KM, Davis RJ. Chemical genetic analysis of the time course of signal transduction by JNK. Molecular Cell 2006; 21(5): 701-710.

60. Den Y, Ren X, Yang L, Lin Y, Wu X. JNK-dependent pathway is required for TNFα-induced apoptosis. Cell 2003; 115: 61-70.

61. Das M, Jiang F, Suiss HK, Zhang C, Shokat KM, Flavell RM, Davis RJ. Suppression of p53-dependent senescence by JNK signal transduction pathway. PNAS 2007; 104(40): 15759-15764.

62. Karin M, Gallagher E. From JNK to pay dirt: jun kinases, their biochemistry, physiology, and clinical importance. IUBMB Life 2005; 57(4-5): 283-295.

63. Zhang H, Bajraszewski N, Wu E, Wang H, Moseman AP, Dabora SL, Griffin JD, Kwiatkowski DJ. PDGFRs are critical for PI3K/Akt activation and negatively regulated by mTOR. J Clin Investigation 2007; 117(3): 730-738.

64. Adams JR, Schachter NF, Liu JC, Zacksenhaus E, Egan SE. Elevated PI3K signaling drives multiple breast cancer subtypes. Oncotarget 2011; 2(6): 435-447.

65. Murphy E. Estrogen signaling and cardiovascular diseases. Circulation Research 2011; 109(6): 687-696.,

66. Vivanco I, Rohle Dm Versele M, Iwanami A, Kuga D, Oldrini B, Tanaka K, Dang J, Kubek S, Palaskas N, Hsueh T, Evans Mm, Mulholland Dm Wolle D, Rajasekaran S, Rajasekaran A, Liau LM, Cloughesy TF, Dikio I, Brennan C, Wu H, Mischel PS, Perera T. Mellinghoff IK. The phosphatase and tension homolog regulates epidermal growth factor receptor (EGFR) inhibitor response by targeting EGFR for degradation. PNAS 2010; 107(14): 6459-6464.

67. Yeramian A, Sorolla A, Velasco A, Santacana M, Dorcet X, Valls J, Abal L, Morena S, Eqido R, Casanova JM, Puig S, Vilella R, Llombart-Cussac A, Matias-Guiu X, Marti IM. Inhibition of activated receptor tyrosine kinases by Sunitinib induces growth arrest and sensitizes meleanoma cells to Bortezomib by blocking Akt pathway. Intl J Cancer 2011; 130(4): 967-978.

68. Manning BD, Cantley LC. Akt/PKB signaling: Navigating downstream. Cell 2007; 127(9): 1261-1274.

69. Andjelkovic DR, Alessi R, Meier R, Fernandez A, Lamb NJC, Frech M, Cohen P, Incocq JM, Hemmings BA. Role of translocation in the activation and function of protein kinase B. Journal of Biological Chemistry 1997; 272: 31515-31524.

70. LoPicollo J, Blumenthal GM, Bernstein WB, Dennius PA. Targeting the PI3K/Akt/mTOR pathway: Effective combinations and clinical considerations. Drug Resistance Updates 2008; 11(1-2): 32-50.

71. Ogita S, LoRusso P. Targeting phosphoinositol 3 kinase (PI3K)-Akt beyond rapalogs. Target Oncol 2011; 6: 103-117.

72. Leevers SJ, Vanhaesebroeck B, Waterfield MD. Signaling through phosphoinositide 3-kinases: the lipids take centre stage. Curr Opin Cell Biol 1999; 346: 9-29.

73. Song G, Ouyang G, Bao S. The activation of Akt/PKB signaling pathway and cell survival. J Cell Mol Medicine 2005; 9(1): 59-71.

74. Hers I, Vincent EE, Tavare JM. Akt signaling in health and disease. Cellular Signaling 2011; 23(10): 1515-1527.

75. Pearce LR, Komander D, Alessi DR. The nuts and bolts of AGC protein kinases. Nature Reviews in Molecular Cell Biology 2010; 11: 9-22.

76. Belandran A, Cassamayor A, Deak M, Paterson A, Gaffney P, Currie R, Dawnes CP, Alessie DR. PDK1 acquires PDK2 activity in the presence of a synthetic peptide derived from the carboxyl terminus of PRK2. Current Biology 1999; 9: 393-404.

77. Delcommenne M, Tan C, Gray V, Rue L, Woodgett J, Dedhar S. Phosphoinositide-3-OH kinase-dependent regulation of glycogen synthase kinase 3 and protein kinase B/AKT by the integrin-linked kinase. PNAS 1998; 95(19): 11211-11216.

78. Hill M, Feng J, Hemmings B. Identification of a plasma membrane raft-associated PKB Ser473 kinase activity that is distinct from ILK and PDK1. Current Biology 2002; 12(14): 1251-1255.

79. Santos SC, Lacronique V, Bauhaert I, Monni R, Bernard O, Gisselbrecht S, Gouilleux F. Constitutively active STAT5 variants induce growth and survival in hematopoietic cells through a PI3K/AKT dependent pathway. Oncogene 2001; 20(17): 2080-2090.

80. Toker A, Newton AC. Akt/ protein kinase B is regulated by autophosphorylation at the hypothetical PDK-2 site. Journal of Biological Chemistry 2000; 275: 8271-8274.

81. Brognard J, Sierecki E, Gao T, Newton AC. PHLPP and a second isoforms, PHLPP2, differentially attenuate the amplitude of AKT signaling by regulating distinct AKT isoforms. Molecular Cell 2007; 25: 917-931.

82. Hernandez-Aya LF, Gonzalez-Angulo AM. Targeting the phosphoinositol 3-kinase signaling pathway in breast cancer. Oncologist 2011; 16(4): 404-414.

83. Ravichandran LV, Chen H, Li Y, Quon MJ. Phosphorylation of PTP1B at Ser(50) by Akt impairs its ability to dephosphorylates the insulin receptor. Molecular Endocrinology 2001; 15(10): 1768-1780.

84. Cross DA, Alessi DR, Cohen P, Andjelkovich M, Hemmings BA. Inhibitor of glycogen synthase kinase-3 by insulin mediated by protein kinase B. Nature 1995; 378(6559): 785-789.

85. Everaert BR, Van Craenenbroeck EM, Hoymans VY, Haine SE, Van Nassauw L, Conraads VM, Timmermans JP, Vrints CJ. Current perspective of pathophysiological and

interventional effects of endothelial progenitor cell biology: focus on PI3K/AKT/eNOS pathway. International Journal of Cardiology 2010; 144(3): 350-366.

86. Jiang BH, Zheng JZ, Aoki M, Vogt PK. Phosphotidylinositol 3-kinase signaling mediates angiogenesis and expression of vascular endothelial growth factor in endothelial cells. PNAS 2000; 97(4): 1749-1753.

87. Ozes ON, Mayo LD, Gustin JA, Pfeffer SR, Pfeffer LM, Donner DB. NF-kappa B activation by tumor necrosis factor requires the Akt serine-threonine kinase. Nature 1999; 401: 82-85.

88. Liang J, Zubovitz J, Petrocelli T, Kotchetkov R, Connor MK, Han K, Lee JH, Ciarallo S, Catzavelos C, Beniston R, Franssen E, Slingerland JM. PKB/Akt phosphorylates p27, impairs nuclear import factor of p27 and opposes p27-mediated G_1 arrest. Nature Medicine 2002; 8: 1152-1160.

89. Diehl JA, Cheng M, Roussel MF, Sherr CJ. Glycogen synthase kinase-3 beta regulates cyclin D1 proteolysis and subcellular localization. Genes Dev 1998; 12: 3499-3511.

90. Vander Haar E, Lee SI, Bandhakavi S, Griffin TJ, Kim DH. Insulin signaling to mTOR mediated by the Akt/PKB substrate PRAS40. Nature Cell Biology 2007; 9: 316-323.

91. Datta SR, Dudek H, Xu T, Masters S, Haian F, Gotoh Y, Greenberg ME. Akt phosphorylation of BAD couples survival signals to the cell intrinsic death machinery. Cell 1997; 91(2): 231-241.

92. Nicholson KM, Anderson NG. Protein kinase B/ Akt signaling pathway in human malignancy. Cell Signaling 2002; 14: 381-395.

93. Sarbassov DD, Guertin DA, Ali SM, Sabatini DM. Phosphorylation and regulation of Akt/PKB by the Rictor-mTOR complex. Science 2005; 307: 1098-1101.

94. Cautley LC. The phosphoinositide 3-kinase pathway. Science 2002; 296: 1655-1657.

95. Li Y, Inoki K, Guan KL. Biochemical and functional characterizations of small GTPase Rheb and TSC2 GAP activity. Molecular and Cellular Biology 2004; 24(18): 7965-7975.

96. Zick Y. Insulin resistance: a phosphorylation-based uncoupling of insulin signaling. Trends in Cell Biology 2001; 11: 4347-441.

97. Bhaskar PT, Hay N. The two TORCs and AKT. Dev Cell 2007; 12(4): 487-502.

98. Hennessey BT, Smith DL, Ram PT, Lu Y, Mills GB. Exploiting the PI3K/AKT pathway for cancer drug discovery. Nature Reviews in Drug Discovery 2005; 4(12): 988-1004.

99. Beckman KE. The PI3KCA gene is mutated with high frequency in human breast cancers. Cancer Biology and Therapy 2004; 3: 772-775.

100. Kang S, Bader AG, Vogt PK. Phosphotidylinceitol 3-kinase mutations indentified in human cancers are oncogenic. PNAS 2005; 102: 802-807.

101. Samuels Y, Wang Z, Bardelli A, Silliman N, Ptak J, Szabo S, Konishi H, Karakas B, Blair BG, Lin C, Peters BA, Velculescu VE, Park BH. High frequency of mutations of the PI3KCA gene in human cancers. Science 2004; 304: 554.

102. Campbell IG, Russell SE, Choong DY, Montgomery KG, Ciavarella ML, Hooi CS, Cristiano BE, Pearson RB, Phillips WA. Mutation in the PI3KCA gene in ovarian and breast cancer. Cancer Research 2004; 64: 7678-7681.

103. Woenckhaus J, Steger K, Werner E, Fenic I, Gamerdinger U, Battmann A, Dreyer T. Genomic gain of PI3KCA and increased expression of p110α are associated with progression and dysplasia into invasive squamous cell carcinoma. Journal of Pathology 2002; 198: 335-342.

104. Ma YY, Wei Sj, Lin YC, Lung JC, Chang TC, Wheng-Peng J, Liu JM, Yang DM, Yang WK, Shen CY. 2000. PI3KCA as an oncogene in cervical cancer. Oncogene. 19: 2739-2744.

105. Mizoguchi M, Nutt CL, Mohapetra G, Louis DN. Genetic alterations of phosphoinositide 3-kinase subunit genes in human glioblastomas. Brain Pathology 2004; 14: 372-377.

106. Broderick DK, Di C, Parrett TG, Samuels YR, Cummins JM, McLendon RE, Fults DW, Velculescu VE, Binger DD, Yan H. Mutations in PI3KCA in anaplastic oligodendrigliomas, highgrade astrocytomas, and medulloblastomas. Cancer Research 2004; 64: 5048-5050.

107. Atkins MB, Hidalgo M, Stadler WM, Logan TF, Dutcher JP, Hudes GR, Park Y, Liou SH, Marshall B, Boni JP, Dukart G, Sherman ML. Randomized phase II study of multiple dose levels of CCI-779, a novel mammalian target of rapamycin kinase inhibitor, in patients with advanced refractory renal cell carcinoma. Journal of Clinical Oncology 2004; 22: 909-918.

108. Galanis E, Buckner JC, Maurer MJ, Kreisberg JI, Ballman K, Boni J, Peralba JM, Jenkins RB, Dakhil SR, Morton RF, Jaeckle KA, Scheithauer BW, Dancer J, Hildalgo M, Walsh DJ, North Central Treatment Cancer Group. Phase II trial of temsirolimus (CCI-779) in recurrent glioblastoma multiforme: a Northern Central Cancer Treatment Group study. Journal of Clinical Oncology 2005; 23(23): 5294-5304.

109. Chan S, Johnston S, Scheulen ME, Mross K, Morant R, Lahr A, Feussner A, Berger M, Kirsch T. First report: a phase 2 study of the safety and activity of CCI-779 for patients

with locally advanced or metastatic breast cancer failing prior chemotherapy. Proc Am Soc Clin 2002; 21: 175.

110. Mills GB, Lu Y, Kohn EC. Linking molecular therapeutics to molecular diagnostics: inhibition of the FRAP/RAFT/TOR component of the PI3K pathway preferentially blocks PTEN mutant cells in vitro and in vivo. PNAS 2001; 98: 1031-1033.

111. DeGraffenried LA, Chandrasekar B, Friedrichs WE, Donzis E, Silva J, Hidalgo M, Freeman JW, Weiss GR. Reduced PTEN expression in breast cancer cells confers susceptibility to inhibitors of the PI3 kinase/ Akt pathway. Annalytical Oncology 2004; 15: 1510-1516.

112. Kau TR, Schroeder F, Ramaswamy S, Wojciechowski CL, Zhao JJ, Roberts TM, Clardy J, Sellers WR, Silver PA. A chemical genetic screen indentifies inhibitors of regulated nuclear export of a Forkhead transcription factor in PTEN-deficient tumor cells. Cancer Cell 2003; 4: 463-476.

113. Defeo-Jones D, Barnett SF, Fu S, Hancock PJ, Haskell KM, Leander KR, McAvoy E, Robinson RG, Duggan ME, Lindsley CW, Zhao Z, Huber HE, Jones RE. Tumor cell sensitization to apoptotic stimuli by selective inhibition of specific Akt/PKB family members. Molecular Cancer Therapy 2005; 4: 271-279.

114. Lindsley CW, Zhao Z, Leister WH, Robinson RG, Barnett SF, Defeo-Jones D, Jones RE, Hartman GD, Huff JR, Huber HE, Duggan ME. Akt/PKB inhibitors: Discovery and SAR of isoenzyme selective inhibitors. Bioorg Med Chem Lett 2005; 15: 761-764.

115. Towler MC, Hardie DG. AMP-activated protein kinase in metabolic control and insulin signaling. Circulation Research 2007; 100(3): 328-341.

116. Steinberg GR, Kemp BE. AMPK in health and disease. Physiological Reviews 2009; 89(3): 1025-1078.

117. Mithcellhill KI, Mitchell BJ, House CM, Stapleton D, Dyck J, Gamble J, Ullrich C, Witters LA, Kemp BE. Posttranslational modifications of the 5’-AMP-activated protein kinase beta1 subunit. Journal of Biological Chemistry 1997; 272: 24475-24479.

118. Hong SP, Leiper FC, Woods A, Carling D, Carlson M. Activation of yeast Snf1 and mammanlian AMP-activated protein kinase by upstream kinases. PNAS 2003; 100: 8839-8843.

119. Hawley SA, Gradalla AE, Olson GS, Hardie DG. The antidiabetic drug metaformin activates the AMP-activated protein kinase cascade via an adenine nucleotide-independent mechanism. Diabetes 2002; 51: 2420-2425.

120. Momcilovic M, Hong SP, Carlson M. Mammalian Tak1 activates Snf1 protein kinase in yeast and phosphorylates AMP-activated protein kinase in vitro. Journal of Biological Chemistry 2006; 281: 25336-25343.

121. Markman B, Dienstmann R, Tabernero J. Targeting the PI3K/Akt/mTOR pathway- Beyond Rapalogs. Oncotarget 2010; 1(7): 530-543.

122. Abdel-Halim MN, Porter JW. A new mechanism of regulation of rat liver acetyl-Co A carboxylases activity. Journal of Biological Chemistry 1980; 225: 441-444.

123. Lizeano JM, Goransson O, Toth R, Deak M, Morrice NA, Basleau J, Hawles SA, Udd L, Mikela TP, Hardie DG, Alessi DR. LKB1 is a master kinase that activates PI3 kinase of the AMPK superfamily including MAPK/PAR-1. The Embo Journal 2004; 23(4): 833-843.

124. Baas AF, Boudeau GP, Sapkota L, Smit R, Medema NA, Morrile DR, Clevers A. Clevers HC. Activation of tumor suppressor kinase LKB1 by the STE20-like pseudokinase STRAD. The Embo Journal 2003; 22: 3062-3072.

125. Carlson CA, Kim KH. Regulation of hepatic acetyl coenzyme A carboxylases by phosphorylation and dephosphorylation. Journal of Biological Chemistry 1973; 248: 378-380.

126. Beg ZH, Allmann DW, Gibson DM. Modulation of 3-hydroxy-3-methylglutaryl coenzyme A reductase activity with protein fractions of rat liver cytosol. Biochem Biophys Res Commun 1973; 54: 1362-1369.

127. Carling D, Clarke PR, Zammit DA, Hardie DG. Purification and characterization of the AMP-activated protein kinase. Copurification of acetyl CoA carboxylases kinase and 3-hydroxy-3-methylglutaryl CoA reductase kinase activities. European Journal of Biochemistry 1989; 186: 129-136.

128. Wang Z, Wilson WA, Fujino MA, Roach PJ. Antagonistic controls of autophagy and glycogen accumulation by Snf1p, the yeast homolog of AMP-activated protein kinase, the cyclin-dependent kinase Pho85p. Molecular Cell Biology 2001; 21: 5742-5752.

129. Bergeron R, Russell RR 3rd, Young LH, Ren JM, Marcucci M, Lee A, Shulman GI. Effect of AMP activation on muscle glucose metabolism in conscious rats. J Physiol Endocrinol Metab 1999; 276: E938-E944.

130. Jorgensen SB, Viollet B, Andreelli F, Frosig C, Birk JB, Schjerling P, Valont S, Richter EA, Wojtaszewski JFP. Knockout of the alpha-2 but not alpha-1 5’-AMP-activated protein kinase isoform abolishes AICAR- but not contraction-induced glucose uptake in skeletal muscle. Journal of Biological Chemistry 2003; 279: 1070-1079.

131. Hardie DG. Sensing of energy and nutrients by AMP-activated protein kinase. The American Journal of Clinical Nutrition 2011; 93(4): 8915-8965.

132. Vakana E, Altman JK, Platanias LC. Targetting AMPK in the treatment of malignancies. Journal of Cell Biochemistry 2012; 113: 404-409.

133. Petranovic D, Tyo K, Vemuri GN, Nielsen J. Prospects of yeast systems biology for human health: integrating lipid, protein and energy metabolism. FEMS Yeast Research 2010; 10: 1046-1059.

134. Lee JW, Park S, Takahashi Y, Wang HG. The association of AMPK with ULK1 regulates autophagy. Plos One 2010; 5(11): e15394.

135. Wullschleger S, Loweith R, Hall MN. TOR signaling in growth and metabolism. Cell 2006; 124: 471-484.

136. Mihaylova MM, Shaw RJ. The AMPK signaling pathway coordinates cell growth, autophagy, and metabolism. Nature Cell Biology 2011; 13(9): 1016-1023.

137. Hadad S, Iwamoto T, Jordan L, Purdie C, Bray S, Baker L, Jellenea G, Deharo S, Hardie DG, Pusztai L, Moulder-Thompson S, Dewar JA, Thompson AM. Evidence for biological effects of metaformin in operable breast cancer: A preparative window of opportunity, randomized trial. Breast Cancer Res Treat 2011; 128: 783-794.

138. Liu B, Fan Z, Edgerton SM, Deng XS, Alimora IN, Lind SE, Thor AD. Metaformin induces unique biological and molecular responses in triple negative breast cancer cells. Cell Cycle 2009; 8(13): 2031-2040.

139. Zheng B, Jeong JH, Asara JM, Yuan YY, Granter SR, Chin L, Cantley LC. Oncogenic BRAF negatively regulates the tumor suppressor LKB1 to promote melanoma cell proliferation. Molecular Cell 2009; 33: 237-247.

140. Ji H, Ramsey MR, Hayes DN, Fan C, McNamara K, Kozlowski P, Torrice C, Wu MC, Shimamura T, Perera SA, Liang MC, Cai D, Naumov GN, Bao L, Contreras CM, Li D, Chen L, *et al*. LKB1 modulates lung cancer differentiation and metastasis. Nature 2007; 448: 807-810.

141. Chen MB, Shen WX, Yang Y, Wu XY, Gu JH, Lu PH. Activation of AMP-activated protein kinase is involved in vincistrine-induced cell apoptosis in B16 melanoma cells. Journal of Cell Physiology 2011; 226: 1915-1925.

142. Carretero J, Medina PP, Blanco R, Smit L, Tang M, Roncador G, Maestre L, Conde E, Lopez-Rios F, Clevers HC, Sanchez-Cespedes M. Dysfunctional AMPK activity signaling through mTOR and survival in response to energetic stress in LKB1-deficient lung cancer. Oncogene 2007; 26: 1616-1625.

143. Priebe A, Tan L, Wahl H, Kueck A, He G, Kwok R, Opipari A, Liu JR. Glucose deprivation activates AMPK and induces cell death through modulation of Akt in ovarian cancer cells. Gynecological Oncology 2007; 122(2): 389-395.

144. Peter ME, Krammer PH. The CD95 (APO-1/Fas) DISC and beyond. Cell Death and Differentiation 2003; 1: 26-35.

145. Aouad SM, Cohen LY, Sharif-Askari E, Haddad EK, Alam A, Sekaly RP. Caspase-3 is a component of Fas death-inducing signaling complex in lipid rafts and its activity is required for complete caspase-8 activation during Fas-mediated cell death. The Journal of Immunology 2004; 172: 2316-2323.

146. Hyer ML, Samuel T, Reed JC. The FLIP-side of Fas signaling. Clinical Cancer Research 2006; 12: 5929-5931.

147. Wolf BB, Shuler M, Echever F, Green DR. Caspase-3 is the primary activator of apoptotic DNA fragmentation via DNAse activation. Journal of Biological Chemistry 1999; 274(43): 30651-30656.

148. Grinberg M, Sarig R, Zaltsman Y, Frumkin D, Grammatikakis N, Reuvany E, Gross A. tBID homooligerimizes in the mitochondrial membrane to induce apoptosis. Journal of Biological Chemistry 2002; 277: 12237-12245.

149. Ishdorj G, Li L, Gibson SB. Regulation of autophagy in hematological malignancies: role of reactive oxygen species. Leuk Lymphoma 2012; 53: 26-53.

150. Lee J, Giordano S, Zhang J. Biochemistry Journal 2012; 441: 523-540.

151. Gutierrez MG, Masters S, Singh SB, Taylor GA, Colombo MI. Autophagy is a defense mechanism inhibiting BCG and mycobacterium tuberculosis survival in infected macrophages. Cell 2004; 119(6): 753-766.

152. Yorimitsu T, Klionsky DJ. Autophagy: molecular machinery for self-eating. Cell Death and Differentiation 2005; 12: 1542-1552.

153. Wirawan E, Lippens S, Berghe TV, Romagnoli A, Fimia GM, Piacentini M, Vandenabeele P. Beclin1- A role in membrane dynamics and beyond. Autophagy 2012; 8(1): 1-15.

154. Amaravadi RK, Lippincott-Schwartz J, Yin XM, Weiss WA, Takebe N, Timmer W, DiPaola RS, Lotze MT, White E. Principles and current strategies for targeting autophagy for cancer treatment. Clinical Cancer Research 2011; 17: 654-666.

155. Tang Y, Hamed H, Cruickshanks N, Fisher PB, Grant S, Dent P. Obatoclax and lapatinib interact to induce toxic autophagy through NOXA. Molecular Pharmacology 2012; 81(4): 527-540.

156. Lefranc F, Kiss R. Autophagy: The Trojan horse to combat glioblastomas. Neurosurgery Focus 2006; 20(4): E7.

157. Yorimitsu T, Nair U, Yang Z, Klionsky DJ. Endoplasmic reticulum stress triggers autophagy. Journal of Biological Chemistry 2006; 281: 30299-30304.

158. Ogata M, Hino S, Saito A, Morikawa K, Kondo S, Kanemoto S, Murakami T, Taniguchi M, Tanii I, Yoshinaga K, Shiosaka S, Hammarback JA, Urano F, Imaizumi K. Autophagy is activated for cell survival after endoplasmic reticulum stress. Molecular Cell Biology 2006; 26: 9220-9231.

159. Mizushima N, Levine B. Autophagy in mammalian development and differentiation. Nature Cell Biology 2010; 12: 823-830.

160. Yang Z, Klionsky DJ. Eaten alive: a history of macroautophagy. Nature Cell Biology 2010; 12: 814-822.

161. Yang Z, Klionsky DJ. Mammalian autophagy: core molecular machinery and signaling regulation. Curr Opin Cell Biol 2010; 22(2): 124-131.

162. Yang Z, Klionsky DJ. An overview of the molecular mechanism of autophagy. Current Opinion in Microbiology and Immunology 2009; 335: 1-32.

163. Scarlatti F, Maffei R, Bear I, Cigdogno P, Guidoni R. Role of noncanonical Beclin1-independent autophagy in cell death induced by resveratrol. Cell Death and Differentiation 2008; 15: 1318-1329.

164. Paglin S, Lee NY, Nakar C, Fitzgerald M, Plotkin J, Deuel B, Hackett N, McMahill M, Sphicas E, Lampen N, Yahalom J. Rapamycin-sensitive pathway regulates mitochondrial membrane potential, autophagy, and survival in irradiated MCF-7 cells. Cancer Research 2005; 65: 11061-11070.

165. Sini P, Vanus D, Chresta C, Gruichard S. Simultaneous inhibition of mTORC1 and mTORC2 by mTOR kinase inhibitor AZD-8055 induces autophagy and cell death in cancer cells. Autophagy 2010; 6: 553-554.

166. Wu YT, Tan HL, Shui G, Bauvy C, Huang Q, Wenk MR, Ong CN, Codogno P, Shen HM. Dual role of 3-methyl adenine in modulation of autophagy via different temporal patterns of inhibition on class I and II phosphoinositide 3-kinases. Plos One 2010; 285(14): 10850-10861.

167. Willis SN, Fletcher Jim, Kaufmann T, van Delft MG, Chen L, Czabotar PE, Ieriono H, Lei IF, Fairlie WD, Bouillet P, Strasser A, Kluck RM, Adams JM, Huang DCS. Apoptosis initiated when BH3 ligands engage multiple Bcl-2 homologs, not Bax or Bak. Science 2007; 315: 856-859.

168. Codogno Meijer AJ. Autophagy and signaling: their role in cell survival and cell death. Cell Death and Differentiation 2005; 12: 1509-1518.

169. Kung CP, Budina A, Balaburski G, Bergenstock MK, Murphy M. Autophagy in tumor suppression and cancer therapy. Crit Rev Eukaryot Gene Expr 2011; 21: 71-100.

170. Crechomska IA, Goemans GC, Skepper JN, Tolkovsky AM. Bcl-2 complexed with Beclin1 maintains full anti-apoptotic function. Oncogene 2009; 28: 2128-2141.

171. Du H, Wolf V, Schafer B, Moldovenu T, Chipuk JE, Kuwana T. BH3 domains other than Bim and Bid can directly activate Bax/Bak. Journal of Biological Chemistry 2001; 286(1): 491-501.

172. Esposito MD. The roles of BID. Apoptosis 2002; 7: 433-440.

173. Korsmeyer SJ, Wei MC, Saito M, Weiler S, Oh KJ, Schlesinger PH. Pro-apoptotic cascade activates BID, which oligerimizes Bak or Bax into pores that result in the release of cytochrome C. Cell Death and Differentiation 2000; 7: 1166-1178.

174. Notte A, Leclere L, Michiels C. Autophagy as a mediator of chemotherapy-induced cell death in cancer. Biochemical Pharmacology 2011; 82(5): 427-434.

175. Wolf BB, Schuler M, Echeverri F, Green DR. Caspase-3 is the primary activator of apoptotic DNA fragmentation via DNA fragmentation factor-45/ inhibitor of caspase-activated DNase inactivation. Journal of Biological Chemistry 1999; 274: 30651-30656.

176. Maceyka M, Milstein S, Spiegel S. Sphingosine-1-phosphate: the swiss army knife of sphingolipid signaling. Journal of Lipid Research 2009; 50: 5272-5276.

177. Hannun YA, Obeid LM. Principles of bioactive lipid signaling: lessons from sphingolipids. Nature Reviews in Molecular Cell Biology 2006; 9: 139-150.

178. Pitson SM. Regulation of sphingosine kinase and sphingolipids signaling. Trends in Biochemical Sciences 2011; 36(2): 97-107.

179. Mashima T, Seimiya H, Tsuruo T. De novo fatty acid synthesis and related pathways as molecular targets for cancer therapy. British Journal of Cancer 2009; 100: 1369-1372.

180. Andrieu-Abadie M, Levade T. Sphingomyelin hydrolysis during apoptosis. Biochim Biophys Acta 2002; 1585(2-3): 126-134.

181. Park MA, Mitchell C, Zhang G, Yacoub A, Allegood J, Haussinger D, Reinehr R, Larner A, Spiegel S, Fisher PB, Voelkel-Johnson C, Ogretmen B, Grant S, Dent P. 2010. Cancer Research. 70(15): 6313-6324.

182. Lepine S, Allegood JC, Park MA, Dent P, Milstein S, Spiegel S. Sphingosine-1-phosphate phosphohydrolase-1 regulates ER stress-induced autophagy. Cell Death and Differentiation 2011; 18(2): 350-361.

183. Suane M, Su ZZ, Dash R, Liu X, Norris JS, Sarkar D, Lee SG, Allegood JC, Dent P, Spiegel S, Fisher PB. Ceramide plays a prominent role in MDA-7/IL-24-induced cancer-specific apoptosis. Journal of Cell Physiology 2010; 222(3): 546-555.

184. Alexia C, Lasler M, Groyer A. Role of constitutively-activated and insulin-like growth factor-stimulated ERK1/2 signaling in human hepatoma cell proliferation and apoptosis: evidence for heterogeneity of tumor cell lines. Annals of the New York Academy of Sciences 2004; 1030: 219-229.

185. Siskind LG. Mitochondrial ceramide and the induction of apoptosis. Journal of Bioenergetics and Biomembranes 2005; 37(3): 143-153.

186. Jiang G, Rao X, Kim CY, Freiser H, Zhang Q, Jiang Z, Li G. Gamma-tocotrienol induces apoptosis and autophagy in prostate cancer cells by increasing intracellular dihydrosphingosine and dihydroceramide. International Journal of Cancer 2012; 130(3): 685-693.

187. Kitatani K, Idkowiak-Baldys J, Hannun YA. The sphingolipids salvage pathway in ceramide metabolism and signaling. Cellular Signaling 2008; 30(6): 1010-1018.

188. Gault CR, Obeid LM, Hannun YA. An overview of sphingolipids metabolism: from synthesis to breakdown. Adv Exp Med Biol 2010; 688: 1-23.

189. Menaldino DS, Bushnev A, Sun A, Liotta DS, Symolon H, Desai K, Dillehay DL, Peng Q, Wang E, Allegood J, Trotman-Pruett S, Sullards MC, Merrill AH Jr. Sphingoid bases and de novo ceramide synthesis: enzymes involved, pharmacology, and mechanisms of action. Pharmacological Research. 2003; 47(5): 373-381.

190. Aronova S, Wedaman K, Aronov PA, Fontes K, Ramos K, Hammock BD, Powers T. Regulation of ceramide biosynthesis by TOR complex 2. Metabolism 2008; 7(2): 148-158.

191. Yoon S, Lee MY, Park SW, Moon JS, Koh YK, Ahn YH, Park BW, Kim KS. Upregulation of acetyl-CoA carboxylases alpha and fatty acid synthase by human epidermal growth factor receptor 2 at the translational level in breast cancer cells. Journal of Biological Chemistry 2007; 282: 26122-26131.

192. Dickson RC. More chores for TOR: de novo ceramide synthesis. Cell Metabolism 2008; 7(2): 99-100.

193. Perry RJ, Ridgway ND. The role of de novo ceramide synthesis in the mechanism of action of the tricyclic xanthate D609. Journal of Lipid Research 2004; 45: 164-173.

194. Senkal CE, Ponnusamy S, Manevich Y, Meyers-Needham M, Saddoughi SA, Mukhopadyay A, Dent P, Bielawski J, Ogretmen B. Alteration of ceramide synthase 6/ C16-ceramide induces activating transcription factor 6-mediated endoplasmic reticulum (ER) stress and apoptosis via perturbation of cellular Ca^{2+} and ER/Golgi membrane network. Journal of Biological Chemistry 2011; 286(49): 42446-42458.

195. Bieberich E. Ceramide signaling in cancer and stem cells. Future Lipidol 2008; 3(3): 273-300.

196. Strub GM, Maceyka M, Hait NC, Milstein S, Spiegel S. Extracellular and intracellular actions of sphingosine-1-phosphate. Adv Exp Med Biol 2010; 688: 141-155.

197. Bourgin F, Reizman H, Capitani G, Grutter MG. Structure and function of sphingosine-1-phosphate lyase, a key enzyme of sphingolipids metabolism. Structure 2010; 18(8): 1054-1065.

198. Scallatti F, Sala G, Somenzi G, Signoielli P, Sacchi N, Gridoni R. Resveratrol induces growth inhibition and apoptosis in metastatic breast cancer cells via de novo ceramide signaling. The FASEB Journal 2003; 17: 2339-2341.

199. Malisan F, Testi R. Lipid signaling in CD95-mediated apoptosis. FEBS Letters 1999; 452(1-2): 100-103.

200. Reynolds CP, Maurer BJ, Kolesnick RN. Ceramide synthesis and metabolism as a target for cancer therapy. Cancer Letters 2004; 206: 169-180.

201. Park MA, Hamed HA, Mitchell C, Cruickshanks N, Dash R, Allegood J, Dmitriev IP, Tye G, Ogretmen B, Spiegel S, Yacoub A, Grant S, Cruiel DT, Fisher PB, Dent P. A serotype 5/3 adenovirus expressing MDA-7/IL-24 infects renal carcinoma cells and promotes toxicity of agents that increase ROS and ceramide levels. Molecular Pharmacology 2011; 79(3): 368-380.

202. Yacoub A, Hamed HA, Allegood J, Mitchell C, Spiegel S, Lesniak MS, Ogretment B, Dash R, Sarkar D, Broaddus WC, Grant S, Cruiel DT, Fisher PB, Dent P. PERK-dependent regulation of ceramide synthase 6 and thioredoxin play a key role in MDA-7/IL-24-indcued killing of primary glioblastoma multiforme cells. Cancer Research 2010; 70(3): 1120-1129.

203. White-Gilbertson S, Mullen T, Senkal C, Lu P, Ogretmen B, Obeid L, Voelkel-Johnson C. Ceramide synthase 6 modulates TRAIL sensitivity and nuclear translocation of active caspase-3 in colon cancer cells. Oncogene 2009; 28(8): 1132-1141.

204. Baran Y, Salas A, Senkal CE, Ganduz U, Bielawski J, Obeid LM, Ogretmen B. Alterations in ceramide/sphingosine-1-phosphate rheostat involved in the regulation of resistance to imatinib-induced apoptosis in K562 human chronic myeloid leukemia cells. Journal of Biologial Chemistry 2007; 282(15): 10922-10934.

205. Kraveka JM, Li L, Szulc ZM, Bielawski J, Ogretmen B, Hannun YA, Obeid LM, Bielawski A. Involvement of the dihydroceramide desaturase in cell cycle progression in human neuroblastoma cells. Journal of Biological Chemistry 2007; 282(23): 16718-16728.

206. Velda Chan SY, Helchie AL, Brown MG, Anderson R, Hoskin DW. Apoptosis induced by intracellular accumulation in MDA-MB-435 breast carcinoma cells is dependent of the generation of reactive oxygen species. Expiramental and Molecular Pathology 2007; 82(1): 1-11.

207. Valsecchi M, Aureli M, Mauri L, Illuzzi G, Chigorno V, Prinetti A, Sonnino S. Sphingolipidomics of A2780 human ovarian carcinoma cells treated with synthetic retinoids. Journal of Lipid Research 2010; 51(7): 1832-1840.

208. Mukhopadhyay A, Saddoughi SA, Song P, Sultan I, Ponnusamy S, Senkal CE, Snook CF, Arnold HK, Sears RC, Hannun YA, Ogretmen B. Direct interaction between the inhibitor 2 and ceramide via sphingolipid protein binding is involved in the regulation of protein phosphatase 2A activity and signaling. The FASEB Journal 2009; 23(3): 751-763.

209. Chalfant CE, Szulc Z, Roddy P, Bielawski A, Hannun YA. The structural requirements for ceramide activation of serine-threonine protein phosphatases. Journal of Lipid Research 2004; 45: 496-506.

210. Deng X, Gao F, May WS. Protein phosphatase 2A inactivates Bcl2's anti-apoptotic function by dephosphorylation and up-regulation of Bcl2-p53 binding. Blood 2009; 113: 422-428.

211. Mao Z, Sun W, Xu R, Novgorodov S, Szulc ZM, Bielawski J, Obeid LM, Mao C. Alkaline ceramidase 2 (ACER2) and its product dihydrosphingosine mediate the cytotoxicity of N-(4-hydroxyphenyl)retinamide in tumor cells. Journal of Biological Chemistry 2010; 285(38): 29078-29090.

212. Gottesman MM. Mechanisms of cancer drug resistance. Annu Rev Med 2002; 12: 5929-5931.

213. Baselga J, *et al*. Lapatinib with trastuzumab for Her 2-positive early breast cancer (NeoALTTO): A randomized, open-label, multi centre, phase 3 trial. The Lancet Oncology 2012; 50140-6736(11): 61847-61853.

214. Kane RC, Farrell AT, Saber H, Tang S, Williams G, Jee JM, Liang C, Booth B, Chidambaram N, Morse D, Sridhara R, Garvey P, Justice R, Pazdur R. Sorafenib for the treatment of advanced renal cell carcinoma. Clinical Cancer Research 2006; 12: 7271-7278.

215. Zhang G, Park MA, Mitchell C, Hamed H, Rahmani M, Martin AP, Cruiel DT, Yacoub A, Graf M, Lee R, Roberts JD, Fisher PB, Grant S, Dent P. Vorinostat and sorafenib synergistically kill tumor cells via FLIP suppression and CD95 activation. Clinical Cancer Research 2008; 14(17): 5385-5399.

216. Gao N, Dai Y, Rahmani M, Dent P, Grant S. Contribution of disruption of the nuclear factor-κB pathway to induction of apoptosis in human leukemia cells by histone deacetylase inhibitors and flavopiridol. Molecular Pharmacology 2004; 66(4): 956-963.

217. Mitchell C, Park MA, Zhang G, Yacoub A, Cruiel DT, Fisher PB, Roberts JD, Grant S, Dent P. Extrinsic pathway- and cathepsin-dependent induction of mitochondrial dysfunction are essential for synergistic flavorpiridol and vorinostat lethality in breast cancer cells. Molecular Cancer Therapeutics 2007; 6: 3103-3112.

218. Farber S. Some observations on the effect of folic acid antagonists on acute leukemia and other forms of incurable cancer. Blood 1949; 4(2): 160-167.

219. Werkheiser WC. The biochemical, cellular, and pharmacological action and effects of the folic acid antagonists. Cancer Research 1963; 23: 1277-1285.

220. Pui CH, Evans WE. Treatment of acute lymphoblastic leukemia. N Engl J Med 2006; 354(2): 166-178.

221. H RH Jr., Auerbach R, Maibach H, Weinstein G, Lebwhol M. Methotrexate in psoriasis: Concensus conference. J Am Acad Dermatol 1998; 38(3): 478-485.

222. Rosenblatt DS, Whitehead VM, Vera N, Pottier A, Dupont M, Vuchich MJ. Prolonged inhibition of DNA synthesis associated with the accumulation of methotrexate. Biochem Biophys Res Commun 1973; 52(1): 27-34.

223. Thompson CA. FDA approves pralatrexate for treatment of rare lymphoma. Am J Health Syst Pharm 2009; 66(21): 1890.

224. Ray MS, Muggia FM, Leichman CG, *et al*. Phase I study of (6R)-5,10-dideazatetrahydrofolate: A folate antimetabolite inhibitory to de novo purine synthesis. Natl Cancer Inst 1993; 85(14): 1154-1159.

225. Alati T, Worzalla JF, Shih C, *et al*. Augmentation of the therapeutic utility of lomotrexol-(6-R)-5,10-dideazatetrahydrofolate- by oral folic acid. Cancer Research 1996; 56(10): 1154-1159.

226. Taylor EC, Kuhnt D, Shih C, *et al*. A dideazatetrahydrofolate analog lacking a chiral center at C-6,N-[4[2-(2-amino-3,4-dihydro-4-oxo-7H-pyrrolo[2,3-d]pyrimindin-5-yl)ethyl]benzoyl]-L-glutamic acid, is an inhibitor of thymidylate synthase. J Med Chem 1992; 35(23): 4450-4454.

227. Adjei AA. Pemetrexed: a novel antifolate agent enters clinical practice. Exp Rev Anticancer Ther 2004; 4(4): 511-522.

228. Ciuleanu T, Brodwicz T, Zielinski C, et al. Maintenance pemetrexed plus best supportive care versus placebo plus best supportive care for non-small-cell lung cancer: A randomized, double-blind, phase 3 study. Lancet 2009; 374(9699): 1432-1440.

229. Altima. Lilly USA, LLC. 2012. Eli Lilly and Company. 23 Jan. 2012 <www.altima.com>.

230. Zhao R, Goldman ID. Enter Altima: A new generation antifolate. The Oncologist 2004; 9(3): 242-244.

231. Adjei AA. Pemetrexed (Altima®): a novel multi-targeted antifolate agent. Exp Rev Anticancer Ther 2003; 3(2): 145-156.

232. Rollins KD, Lindley C. Pemetrexed: a multi-targeted antifolate. Clinical Therapeutics 2005; 27(9): 1343-1382.

233. Hanna N, Shepherd FA, Fossella FV, *et al*. Randomized phase III clinical trial of pemetrexed vs docetaxel in patients with non-small-cell lung cancer previously treated with chemotherapy. Journal of Clinical Oncology 2004; 22(9): 1589-1597.

234. Fossella FV, Gatzemeler U. Phase I trials of pemetrexed. Semin Oncol 2002; 29(2 Suppl. 5): 8-16.

235. Chattopadhyay S, Moran RG, Goldman ID. Pemetrexed: biochemical and cellular pharmacology, mechanisms, and clinical applications. Molecular Cancer Therapeutics 2007; 6: 404-417.

236. Morotti M, Valenzano Menada M, Venturini P, Mammoliti S, Ferrero S. Pemetrexed disodium in ovarian cancer treatment. Exp Opin Investig Drugs 2012; 21(4): 437-449.

237. Sorensen JB. Pharmacokinetic evaluation of pemetrexed. Exp Opin Drug Metab Toxicol 2011; 7(7): 919-928.

238. Hanauske AR, Chen V, Paoletti P, Niyikiza C. Pemetrexed disodium: A novel antifolate clinically active against multiple solid tumors. The Oncologist 2001; 6: 363-373.

239. Theti DS, Jackman AL. The role of alpha-folate receptor-mediated transport into the antitumor activity of antifolate drugs. Clinical Cancer Research 2004; 10(3): 1080-1089.

240. Hardy LW, Finer-Moore JS, Montfort WR, Jones MO, Santi DV, Stroud RM. Atomic structure of thymidylate synthetase: target for rational drug design. Science 1987; 235(4787): 448-455.

241. Richardson CC, Inman RB, Kornberg A. Enzymic synthesis of deoxyribonucleic acid. 18. The repair of partially single-stranded DNA templates by DNA polymerase. J Mol Biol 1964; 9: 46-69.

242. Takezawa K, Okamoto I, Okamoto W, Takeda M, Sakai K, Tsukioka S, Kuwata K, Yamaguchi H, Nishio K, Nakagawa K. Thymidylate synthase as a determinant of pemetrexed sensitivity in non-small cell lung cancer. British Journal of Cancer 2011; 104: 1594-1601.

243. Rothbart SR, Racenelli AC, Moran RG. Pemetrexed indirectly activates the metabolic kinase AMPK in human carcinomas. Cancer Research 2010; 70: 10299-10309.

244. Racenelli AC, Rothbart SR, Heyer CI, Moran RG. Therapeutics by cytotoxic metabolite accumulation: pemetrexed causes ZMP accumulation, AMPK activation, and mammalian target of rapamycin inhibition. Cancer Research 2009; 69: 5467-5474.

245. Hendricksen K, Moonen PMJ, Vander Heiden AG, Molkenboer-Kuenen J, Hulsbergen-van de kaa CA, Witjes JA. Potential and toxicity of intravesical pemetrexed: a preclinical study in pigs. Clinical Cancer Research 2006; 12: 2597-2601.

246. Shen X, DeNittus A, Waner-Wasik M, Axelrod R, Gilman P, Meyer T, Treat J, Curran WJ, Machtay M. Phase I study of “dose-dense” pemetrexed plus carboplatin/ radiotherapy for locally advanced non-small cell lung carcinoma. Radiotion Oncology 2011; 6: 17.

247. Moran RG, Mulkins M, Heideberger C. Role of Thymidylate Synthetase activity in development of methotrexate cytotoxicity. PNAS 1979; 76(11):5924-5928.

248. Jung CH, Jun CB, Ro SH, Kim YM, Otto NM, Cao J, Kundu M, Kim DH. ULK-Atg13-FIP200 complexes mediate mTOR signaling to the autophagy machinery. Mol Biol Cell 2009; 20(7): 1992-2003.

249. Park MA, Reinhnr R, Haussinger D, Voelkel-Johnson C, Orgetmen B, Yacoub A, Grant S, Dent P. Sorafenib activates CD95 and promotes autophagy and cell death via Src-family kinases in gastrointestinal tumor cells. Molecular Cancer Therapy 2010. 9(8): 2220-2231.

250. National Cancer Institute. 2012. National Institutes of Health.10 Jul. 2012 <http://www.cancer.gov/clinicaltrials/search/results?protocolsearchid=6383246>.

251. Tyer R, Fetterly G, Lugade A, Thanavala Y. Sorafenib: a clinical and pharmacologic review. Exp Opin Pharmacother 2010; 11(11): 1943-1955.

252. Wilhelm S, Carter C, Lynch M, Lowinger T, Duman J, Smith RA, Schwartz B, Simantov R, Kelley S. Discovery and development of sorafenib: a multi-kinase inhibitor for treating cancer. Nat Rev Drug Discov 2006; 5(10): 835-844.

253. Park MA, Reinher R, Haussinger D, Voelkel-Johnson C, Ogretmen B, Yacoub A, Grant S, Dent P. Sorafenib activates CD95 and promotes autophagy and cell death via Src family kinases in gastrointestinal tumor cells. Molecular Cancer Therapeutics 2010; 9: 2220-2231.

254. Rose A, Grandoch M, vom Dorp F, Rubben H, Rosenkranz A, Fischer JW. Stimulatory effects of the multikinase inhibitor sorafenib on human bladder cancer cells. British Journal of Pharmacology 2010; 160: 1690-1698.

255. Yacoub A, Hamed HA, Allegood J, Mitchell C, Spiegel S, Lesniak MS, Ogretmen B, Dash R, Sarkar D, Broaddus WC, Grant S, Curiel DT, Fisher PB, Dent P. PERK-dependent regulation of ceramide synthase 6 and thioredoxin play a key role in MDA-7/IL-24-induced killing of primary human glioma multiforme cells. Cancer Research 2010; 70(3): 1120-1129.

256. Walker T, Mitchell C, Park MA, Yacoub A, Graf M, Rahmani M, Houghton PJ, Voelkel-Johnson C, Grant S, Dent P. Sorafenib and vorinostat kill colon cancer cells by CD95-dependent and –independent mechanisms. Molecular Pharmacology 2009; 76(2): 342-355.

257. Martin AP, Park MA, Mitchell C, Walker T, Rahmani M, Thorburn A, Haussinger D, Reinehr R, Grant S, Dent P. Bcl-2 family member enhance p inhibitor and sorafenib lethality via autophagy and overcome blockade of extrinsic pathway to facilitate killing. Molecular Pharmacology 2009; 76(2): 327-341.

258. Sauane M, Su ZZ, Dash R, Liu X, Norris JS, Sarkar D, Lee SR, Allegood JC, Dent P, Spiegel S, Fisher PB. Ceramide plays a prominent role in MDA-7/IL-24-induced cancer-specific apoptosis. J Cell Physiol 2010; 222(3): 546-555.

259. Yu C, Bruzek LM, Meng XM, Gores GJ, Carter CA, Kaufmann SH, Adjei AA. The role of Mcl-1 downregulation in the proapoptotic activity of the multikinase inhibitor BAY 43-9006. Oncogene 2005; 24(46): 6861-6864.

260. Lin L, Cao Y, Chen C, Zhang X, McNabola A, Wilkie D, Wilhelm S, Lynch M, Carter C. Sorafenib blocks the Raf/MEK/ERK pathway, inhibits tumor angiogenesis, and induces tumor cell apoptosis in hepatocellular carcinoma model PLC/PRF/5. Cancer Research 2006; 66: 11851-11858.

261. Takezawa K, Okamoto I, Yonesaka K, Hatashita E, Yamada Y, Fukouka M, Nakagawa K. Sorafenib inhibits non-small cell lung cancer growth by targeting B-RAF and K-RAS wild-type cells and C-RAF in K-RAS mutant cells. Cancer Research 2009; 69(16): 6515-6521.

262. Dhomen M, Marais R. BRAF signaling and targeted therapies in melanoma. Hematol Oncol Clin North Am 2009; 23(3): 529-545.

263. Grandinetti CA, Goldspiel BR. Sorafenib and sunitinib: novel targeted therapies for renal cell cancer. Pharmacotherapy 2007; 27(8); 1125-1144.

264. Moreno-Aspitia A. Clinical review of sorafenib in breast cancer. Future Oncology 2010; 6(5): 655-663.

265. Wilhelm S, Chien DS. BAY 43-9006: preclinical data. Curr Pharm Des 2002; 8(25): 2255-2257.

266. Kane RC, Farrell AT, Saber H, Tang S, Williams G, Jee JM, Liang C, Booth B, Chidambarum N, Morse D, Sridhara R, Garvey P, Justice R, Padzur P. Sorafenib for the treatment of advanced renal cell carcinoma. Clinical Cancer Research 200; 12(24): 7271-7178.

267. Escudier B, Eisen T, Stadler WM, Szczylik C, Oudard S, Siebels M, Negrier S, Cheveau C, Solska E, Desai AA, Rolland F, Demkow T, Hutson TE, Gore M, Freeman S, Schwartz B, Shan M, Simantov R, Bukowksi RM. Sorafenib in advanced clear-cell renal-cell carcinoma. New Engl J Med 2007; 356(2): 125-134.

268. Simpson D, Keating GM. Sorafenib: in hepatocellular carcinoma. Drugs 2008; 68(2): 251-258.

269. Llovet JM, Ricci S, Mazzaferro V, *et al*. Sorafenib in advanced hepatocellular carcinoma. N Engl J Med 2008; 359(4): 378-390.

270. Zhang Z, Zhou X, Shen H, Wang D, Wang Y. Phosphorylated ERK is a potential predictor of sensitivity to sorafenib when treating hepatocellular carcinoma. BMC Med 2009; 7:41.

271. Chen J, Fujii K, Zhang L, Roberts T, Fu H. Raf-1 promotes cell survival by antagonizing apoptosis signal-regulating kinase 1 through a MEK-Erk-independent mechanism. PNAS 2001; 98: 7783-7788.

272. Cheng EH, Sheiko TV, Fisher JK, Craigen WJ, Korsmeyer SJ. VDAC2 inhibits BAK activation and mitochondrial apoptosis. Science 2003; 301: 513-517.

273. Salomoni P, Wasik MA, Riedel RF, Reiss K, Choi JK, Skorski T, Calabretta B. Expression of constitutively active Raf-1 in the mitochondria restores antiapoptotic and leukemogenic

potential of a transformation-deficient BCR/ABL mutant. Journal of Experimental Medicine 1998; 187(12): 1995-2007.

274. Hindley A, Kolch W. Extracellular signal regulated kinase (ERK)/ Mitogen activated protein kinase (MAPK)-independent functions of Raf kinases. Journal of Cell Science 2002; 115: 1575-1581.

275. Amault JP, Mateus C, Escucher B, Tomasic G, Wechcler J, Hollville E, Soria JC, Malka D, Sarasin A, Larcher M, Andree J, Kamsu-Kom N, Boussemart L, Lacroix L, Spatz A, Eggermont AM, Druilenec S, Vagner S, Eychene A, Dumaz N, Robert C. Skin tumors induced by sorafenib: paradoxical RAS-RAF pathway activation and oncogenic mutations of HRAS, TP53, and TGFBR1. Clinical Cancer Research 2011; 1(1): 263-272.

276. Spirilli C, Morell CM, Locatelli L, Okolicsanyi S, Ferroro C, Kim AK, Fabris L, Fiorotto R, Strazzabosco M. Cyclic AMP/PKA-dependent paradoxical activation of Raf/MEK/Erk signaling in polycistin-2 defective mice treated with sorafenib. Hepatology 2012. [Epub ahead of print]

277. Poulikakos PI, Zhang C, Bollag G, Shokat M, Rosen N. RAF inhibitors transactivate RAF dimers and ERK signaling in cells with wild-type BRAF. Nature 2010; 464(7287): 427-430.

278. Nguyen TK, Jordan N, Friedberg J, Fisher RI, Dent P, Grant S. Inhibition of MEK/ERK1/2 sensitizes lymphoma cells to sorafenib-induced apoptosis. Leukemia Research 2010; 34(3): 379-386.

279. Haussinger D, Reinehr R, Grant S, Dent P. BCL-2 family inhibitors enhance histone deacetylase inhibitors and sorafenib lethality via autophagy and overcome blockade of the extrinsic pathway to facilitate killing. Molecular Pharmacology 2009; 76(2): 327-341.

280. Rahmani M, Davis EM, Baner C, Dent P, Grant S. Apoptosis induced by the kinase inhibitor BAY 43-9006 in human leukemia cells involves down-regulation of Mcl-1 through inhibition of translation. Journal of Biological Chemistry 2005; 280(42): 35217-35227.

281. Rahmani M, Nguyen TK, Dent P, Grant S. The multikinase inihibitor sorafenib induces apoptosis in highly imatinib mesylate-resistant bcr/abl+ human leukemia cells in association with signal transducer and activator of transcription 5 inhibition and myeloid cell leukemia-1 down-regulation. Molecular Pharmacology 2007; 72(3): 788-795.

282. Zhang W, Konoplera M, Ruvolo VR, McQueen T, Evans RL, Bornmann WG, McCubrey J, Cortes J, Andreeff M. Sorafenib induces apoptosis of AML cells via Bim-mediated activation of the intrinsic apoptotic pathway. Leukemia 2008; 22(4): 808-818.

283. Fectean JF, Bhareti IS, O'hayre M, Handel TM, Kipps TJ, Messmer D. Sorafenib-induced apoptosis of chronic lymphocytic leukemia cells is associated with downregulation of RAF and myeloid cell leukemia sequence 1 (Mcl-1). Molecular Medicine 2012; 18(1): 19-28.

284. Vatsyayan R, Singhal J, Nagaprashantha LD, Awasthi S, Singhal SS. Nutlin-3 enhances sorafenib efficacy in renal cell carcinoma. Molecular Carcinogenesis 2011. [Epub ahead of print].

285. Roskos R Jr. Sunitinib: A VEGF and PDGF receptor protein kinase and angiogenesis inhibitor. Biochemical and Biophysical Research Communications 2007; 356: 323-328.

286. Park MA, Reinher R, Haussinger D, Voelkel-Johnson C, Ogretmen B, Yacoub A, Grant S, Dent P. Sorafenib activates CD95 and promotes autophagy and cell death via Src family kinases in gastrointestinal tumor cells. Molecular Cancer Therapeutics 2010; 9(8): 2220-2231.

287. Masson K, Ronnstrand L. Oncogenic signaling from the hemapoietic growth factor receptors c-kit and FLT-3. Cell Signaling 2009; 21(12): 1717-1726.

288. Reilly JT. FLT-3 and its role in the pathogenesis of acute myeloid leukemia. Leuk Lymphoma 2003; 44(1): 1-7.

289. Borthakur G, Kantarjian H, Ravandi F, Zhang W, Konopleva M, Wright JJ, Fader IS, Verstovsek S, Mathews S, Andreeff M, Cortes JE. Phase I study of sorafenib in patients with refractory or relapsed acute leukemias. Hematologica 2011; 96(1): 62-68.

290. Zhang W, Konopleva M, Shiy X, McQueen T, Harris D, Ling X, Estrov Z, Quintas-Cardama A, Small D, Cortes J, Andreeff M. Mutant FLT-3: a direct target of sorafenib in acute myelonomous leukemia. J Natl Cancer Inst 2008; 100(3): 184-198.

291. Martinelli E, Troiani T, Morgillo F, Rodolico G, Vitagliano D, Morelli MP, Tuccillio C, Vecchione L, Capasso A, Orditura M, DeVita F. Synergistic antitumor activity of sorafenib in combination with epidermal growth factor receptor inhibitors in colorectal and lung cancer cells. Clinical Cancer Research 2010; 16(20): 4990-5001.

292. Nagai K, Arao T, Furuta K, Sakai K, Kudo K, Kaneda H, Tamura D, Aomatsu K, Kimura H, Fujita Y, Matsumoto K, Saijo N, Kudo M, Nishio K. Sorafenib inhibits the hepatocyte growth factor-mediated epithelial mesenchymal transition in hepatocellular carcinoma. Molecular Cancer Therapeutics 2011; 10(1): 169-177.

293. Switzer CH, Cheng RYS, Vitek TM, Christensen DH, Wink DA, Vitek MP. Targetting SET/I2PP2A oncoprotein functions as a multi-pathway strategy for cancer therapy. Oncogene 2011; 30: 2504-2513.

294. Ogretmen B, Hannun YA Biologically active sphingolipids in cancer pathogenesis and treatment. Nature Reviews in Cancer 2004; 4: 604-616.

295. Kharaziha P, Rodriguez P, Li Q, Rundqvist H, Bjorklund A-C, Augsten M, Ullen A, Egevad L, Wiklund P, Nilsson S, Kroemer G, Grander D, Panaretakis T. Targeting of distinct signaling cascades and cancer-associated fibroblasts define the efficacy of sorafenib against prostate cancer cells. Cell Death and Disease 2012; 3: e262.

296. Martin AP, Mitchell C, Rahmani M, Nephew KP, Grant S, Dent P. Inhibition of Mcl-1 enhances lapatinib toxicity and overcomes lapatinib resistance via Bak-dependent autophagy. Cancer Biology and Therapy 2009; 8: 2084-2096.

297. Ramakrichnan V, Timm M, Hang JL, Halling T, Wellick LE, Witzig TE, Rajkumar SV, Adjei AA, Kumar S. Sorafenib, a multikinase inhibitor, is effective in vitro against non-Hodgkin lymphoma and synergizes with the mTOR inhibitor rapamycin. American Journal of Hematology 2011; 87(3): 277-283.

298. Fan M, Yan PS, Hartman-Frey C, Chen L, Paik H, Oyer SL, Salisbury JD, Cheng AS, Li L, Abbosh PH, Huang TH, Nephew KP. Diverse gene expression and DNA methylation profiles correlate with differential adaptation of breast cancer cells to the antiestrogens tamoxifen and fulvestrant. Cancer Research 2006; 66(24): 11954-11966.

299. Howell A, Bergh J. Insights into the place of fulvestrant for the treatment of advanced endocrine responsive breast cancer. Journal of Clinical Oncology 2010; 28(30): 4548-4550.

300. Sutherland RL. Endocrine resistance of breast cancer: new roles for ErbB3 and ErbB4. Breast Cancer Research 2011; 13(3): 106.

301. Soule HDm, Vazquez J, Long A, Albert S, Brennan M. A human cell line from a pleural effusion derived from a breast carcinoma. J Natl Cancer Inst 1973; 51(5): 1409-1416.

302. Liu H, Ching D, Weichel AK, Osipo C, Wing LK, Chen B, Louis TE, Jordan VC. Cooperative effect of gefitinib and fumitremorgin C on cell growth and chemosensitivity in estrogen receptor α-negative fulvestrant-resistant MCF7 cells. Intl J Oncol 2006; 29: 1237-1246.

303. Wadsworth VK, Patel S, Kravchuk O, Chen G, Mathew R, Jin S, White E. Autophagy mitigates metabolic stress and genome damage in mammary tumorigenesis. Genes Dev 2007; 21(13): 1621-1635.

304. Qu X, Yu J, Bhagat G, Furuya N, Hibshoosh H, Troxel A, Rosen J, Eskelinen EL, Mizushima N, Ohsumi Y, Cattoretti G, Levine B. Promotion of tumorigenesis by heterozygous disruption of the beclin1 autophagy gene. J Clin Invest 2003; 112(12): 1809-1820.

305. Invitrogen. 2012. Life Tehcnologies Corporation. 10 Jul. 2012 < https://es-cl.invitrogen.com/site/mx/es/home/References/Molecular-Probes-The-Handbook/Probes-for-Organelles/Probes-for-Lysosomes-Peroxisomes-and-Yeast-Vacuoles.html#head3>.

306. Scherz-Shouval R, Elazar Z. ROS, mitochondria and the regulation of autophagy. Trends in Cell Biology 2007; 17(9): 422-427.

307. Kubota C, Toril S, Hou N, Saito N, Yoshimoto Y, Imai H, Takeuchi J. Constitutive reactive oxygen species generation from autophagosome/ lysosome in neuronal oxidative toxicity. Journal of Biological Chemistry 2009; 285(1): 667-674.

308. Chen Y, McMillan-Ward E, Kong J, Israel S, Gibson SB. Mitochondrial electron transport chain inhibitors of complexes I and II induce autophagic cell death mediated by reactive oxygen species. Journal of Cell Science 2007; 120: 4155-4166.

309. Yeatman TJ. A renaissance for Src. Nature Reviews on Cancer 2004; 4: 470-480.

310. Marshall CJ. Specificity of receptor tyrosine kinase signaling: transient versus sustained extracellular signal related kinase activation. Cell 1995; 80: 179-185.

311. Kalev P, Sablina AA. Protein phosphatase 2A as a potential target for anticancer therapy. Med Chem 2011; 11: 38-46.

312. Widau RC, Jin Y, Dixon SA, Wadzinski BE, Gallagher PJ. Journal of Biological Chemistry 2010; 285(18): 13827-13838.

313. Li M, Damuni Z. Two potent protein phosphatase 2A-specific inhibitor proteins. Methods in Molecular Biology 1998; 93: 59-66.

314. Carlson SG, Eng E, Kim EG, Perlman EJ, Copeland TD, Ballermann BJ. Expression of SET, an inhibitor of protein phosphatase 2A, in renal development and Wilm's tumor. J Am Soc Nephrol 1998; 9: 1873-1880.

315. Li M, Makkinje A, Damuni Z. The myeloid-leukemia associated SET is a potent inhibitor of protein phosphatase 2A. Journal of Biological Chemistry 1996; 271: 11059-11062.

316. Wu WK, Cho CH, Lee CW, Wu YC, Yu L, Li ZJ, Wong CC, Li HT, Zhang L, Ren SX, Che CT, Wu K, Kan D, Yu J, Sung JJ. Macroautophagy and ERK phosphorylation counteract the anti-proliferative effect of proteosome inhibitor in gastric cancer cells. Autophagy 2010; 6: 228-238.

317. Aoki H, Takada Y, Kondo S, Sawaya R, Aggarwal BB, Kondo Y. Evidence that curcumin suppresses the growth of malignant gliomas in vitro and in vivo through induction of autophagy: role of Akt and extracellular signal-regulated kinase signaling pathways. Molecular Pharmacology 2007; 72: 29-39.

318. Park MA, Yacoub A, Rahmani M, Zhang G, Hart L, Hagan MP, Calderwood SK, Sherman MY, Koumenis C, Spiegel S, Chen CS, Graf M, Curiel DT, Fisher PB, Grant S, Dent P. OSU-03012 stimulates PKR-like endoplasmic reticulum-dependent increases in 70 kDa heat shock protein expression, attenuating its lethal actions in transformed cells. Molecular Pharmacology 2008; 73(4): 1168-1184.

319. Kaushik S, Cuervo Am. Methods to monitor chaperone-mediated autophagy. Methods Enzymology 2009; 452: 297-324.

320. Grinberg M, Sarig R, Zaltsman Y, Frumkin D, Grammatikakis N, Reuvany E, Gross A. tBid homooligerimizes in the mitochondrial membrane to induce apoptosis. Journal of Biological Chemistry 2002; 277: 12237-12245.

321. Schmid K, Bago-Horvath Z, Berger W, Haitel A, Cejka D, Werzowa J, Filipits M, Herberger N, Hayden H, Sieghart W. Dual inhibition of EGFR and mTOR pathways in small cell lung cancer. British Journal of Cancer 2010; 103: 622-628.

322. Li X, Fan Z. The epidermal growth factor receptor antibody cetuximab induces autophagy in cancer cells by down-regulating HIF-1alpha and Bcl-2 and activating the beclin1/hVps34 complex. Cancer Research 2010; 70: 5942-5952.

323. Muthuswamy SK, Siegel PM, Dankort DK, Webster MA, Muller WJ. Mammary tumors expressing the neu proto-oncogene possess elevated c-Src tyrosine kinase activity. Molecular and Cellular Biology 1994; 14(1): 735-743.

324. Belches AP, Haskell MD, Parsons SJ. c-Src tyrosine kinase in EGF-induced mitogenesis. Frontiers in Bioscience 1997; 2: d501-d518.

325. Pettus BJ, Chalfant CE, Hannun YA. Sphingolipids in inflammation: roles and implications. Curr Mol Med 2004; 4(4): 405-418.

326. Pettus BJ, Chalfant CE, Hannun YA. Ceramide in apoptosis: an overview and current prospectives. Biochim Biophys Acta 2002; 1585(2-3): 114-125.

327. Bareford MD, Hamed HA, Allegood J, Cruickshanks N, Poklevic A, Park MA, Ogretmen B, Spiegel S, Grant S, Dent P. Sorafenib and pemetrexed toxicity in cancer cells is mediated via SRC-ERK signaling. Cancer Biology and Therapy 2012; 13(9). [Epub ahead of print].

328. Karahatay S, Thomas K, Koybasi S, Senkal CE, Elojeimy S, Liu X, Bielawski J, Day TA, Sinha D, Norris JS, Hannun YA, Ogretmen B. Clinical relevance of ceramide metabolism in the pathogenesis of human head and neck squamous cell carcinoma (HNSCC): Attenuation of C18-ceramide in HNSCC tumor correlates with lymphovascular invasion and nodal metastasis. Cancer Letters 2007; 256(1): 101-111.

329. Yano M, Kishida E, Muneyuki Y, Masuzawa Y. Quantitative analysis of ceramide molecular species by high performance liquid chromatography. Journal of Lipid Research 1998; 39: 2091-2098.

Curriculum Vitae

M. Danielle Bareford

701 St. James St. Apt #103
Richmond, VA 23220
Phone: 804-840-1214
Email: s2mdbare@vcu.edu

Education

2006-2012	*Ph.D. Biochemistry and Molecular Biology* School of Medicine, Virginia Commonwealth University Richmond, VA
1999-2004	*B.S. Forensic Science- Biology Track* Minors- Biology, Chemistry Virginia Commonwealth University Richmond, VA

Research Experience

2010-2012 *Doctoral Research* (Advisor: Paul Dent, Ph.D.)
Department of Biochemistry and Molecular Biology
Virginia Commonwealth University, Richmond, VA

- *Dissertation*: Sorafenib enhances pemetrexed cytotoxicity through an autophagy-dependent mechanism in cancer cells.
- Determined the role of autophagy in pemetrexed-treated cancer cells, as well as the combined effects of pemetrexed and sorafenib in these tumor types (NSCLC, hepatoma, glioma, mammary carcinoma).
- Investigated the mechanism by which pemetrexed and sorafenib interact to induce a toxic form of autophagy in breast cancer cells.
- Identified roles for PDGFRβ, c-Src, MEK/Erk1/2, PP2A, I2PP2A/SET, and LASS-6 in the toxic interactions of pemetrexed and sorafenib in breast cancer cells.

2006-2010 *Doctoral Research* (Advisor: William A. Barton Ph.D.)
Department of Biochemistry and Molecular Biology
Virginia Commonwealth University, Richmond, VA

- Engineered *Escherichia coli* biotin ligase and Cysteinyl tRNA Synthetase variants using random mutagenesis and structure-based engineering techniques to promote enzymatic activity with novel

substrates in order to site-specifically label a protein of interest with useful chemical moieties.
- Developed yeast surface display, mRNA display, and ribosome display techniques to be utilized for high-throughput screening of mutant enzyme libraries in order to identify unique enzyme variants exhibiting a desired phenotype.
- Purification of proteins in bacterial and mammalian cell systems for use in a variety of *in vitro* assays, as well as structural characterization.

2005-2006

Research Assistant/ Lab Manager (PI: Sumitra Deb, Ph.D.)
Department of Biochemistry and Molecular Biology
Virginia Commonwealth University, Richmond, VA
- Characterized the signaling pathways regulated by p53 which mediate cell growth and survival.
- Analyzed the effects of various chemotherapeutic drug treatments on H1299 NSCLC cells stably expressing wild-type p53 or one of several catalytically and/or transcriptionally inactive p53 mutants in order to identify the signaling pathways regulated by each variant which alter drug sensitivity.

2004-2006

Adjunct Faculty, Department of Biology
Virginia Commonwealth University, Richmond, VA
- Instructed 2-10 sections of introductory biology laboratory per semester to undergraduate students.
- Prepared weekly lectures covering the material relevant for each lesson; as well as weekly exams and homework assignments to assess the students' knowledge of material covered the week prior.
- Trained students on proper laboratory safety and a variety of basic laboratory techniques.
- Evaluated student performances and assigned final semester grades.

Honors and Awards

2004

2004 Outstanding Graduating Senior- Forensic Science
School of Humanities and Life Sciences, Virginia Commonwealth University, Richmond, VA

2000

Phi Eta Sigma National Honor Society
Virginia Commonwealth University, Richmond, VA

Publications

Bareford MD, Hamed HA, Allegood J, Cruickshanks N, Poklepovic A, Park MA, Ogretmen B, Spiegel S, Grant S, Dent P. Sorefenib and Pemetrexed toxicity is mediated via SRC-ERK signaling. Cancer Biol Ther 2012; 13(9). [Epub ahead of print]

Cruickshanks N, Hamed HA, **Bareford MD**, Poklepovic A, Fisher PB, Grant S, Dent P. Lapatinib and Obatoclax kill tumor cells through blockade of ERBB1/3/4 and through inhibition of BCL-XL and MCL-1. Mol Pharmacol 2012; 81(5): 748-758.

Bareford MD, Hamed HA, Tang Y, Cruickshanks N, Burow ME, Fisher PB, Moran RG, Newphew KP, Grant S, Dent P. Sorafenib enhances pemetrexed cytotoxicity through an autophagy-dependent mechanism in cancer cells. Autophagy 2011; 7(10): 1261-1262.

Mitchell C, Hamed HA, Cruickshanks N, Tang Y, **Bareford MD**, Hubbard N, Tye G, Yaboub A, Dai Y, Grant S, Dent P. Simultaneous exposure of transformed cells to SRC family inhibitors and CHK1 inhibitors causes cell death. Cancer Biol Ther 2011; 12(3): 215-228.

Bareford MD, Park MA, Yacoub A, Hamed HA, Tang Y, Cruickshanks N, Eulitt P, Hubbard N, Tye G, Burow ME, Fisher PB, Moran RG, Newphew KP, Grant S, Dent P. Sorafenib enhances pemetrexed cytotoxicity through an autophagy-dependent mechanism in cancer cells. Cancer Research 2011; 71(14): 4955-4967.

Mitchell C, Yacoub A, Hamed HA, Martin AP, **Bareford MD**, Eulitt P, Yang C, Nephew KP, Dent P. Inhibition of MCL-1 in breast cancer cells promotes cell death in vitro and in vivo. Cancer Biol Ther 2010; 10(9): 903-917.

Presentations

2011	American Association for Cancer Research Annual Meeting 2011 Orlando, Florida (poster) Title: A serotype 5/3 adenovirus expressing MDA-7/IL-24 infects renal carcinoma cells and promotes toxicity of agents that increase ROS and ceramide levels
2008	25th Annual Daniel T. Watts Research Symposium Virginia Commonwealth University, Richmond, VA (poster) Title: *In vitro* selection of a ribozyme for site-specific incorporation of p-azidophenylalanine using ribosome display

Student Membership

2010-present	American Association for Cancer Research, member